Design of Tudor Arches
with
Structural Glued Laminated Timber

American Institute of Timber Construction
7012 South Revere Parkway Suite 140, Centennial, CO 80112
Phone: 303/792-9559 Fax: 303/792-0669
www.aitc-glulam.org

CONTENTS

Chapter 1
Structural Glued Laminated Timber Arches

Structural glued laminated timber (glulam) has many advantages over traditional sawn members or other engineered wood products including its ability to be manufactured in a variety of shapes from straight beams and columns to graceful curved members. Glulam can be manufactured with constant cross section along the length or with taper to meet architectural requirements. The glulam arch fully takes advantage of the unique properties of laminated timber construction.

Since their U.S. debut in 1934, in a school gymnasium in Peshtigo, Wisconsin, glulam arches have been successfully used in a variety of structures including churches, schools, warehouses, barns, aircraft hangars, and others. Several of the early U.S. glulam arch structures, including the original gymnasium are still in use today (A.J. Rhude 1996).

Glulam arches continue to be popular for use in large open structures such as churches and gymnasiums because of their excellent structural performance, inherent fire resistance, and aesthetic appeal. Laminated timber arches are also used for vehicle and pedestrian bridges.

Figure 1.1 illustrates a number of common arch configurations. Arches may be of either two- or three-hinged design. The AITC Timber Construction Manual (TCM) indicates that Tudor arches can generally be used economically for spans of up to 120 feet and that parabolic and radial arches can be used economically for spans of up to 250 feet (AITC 2004, p. 6).

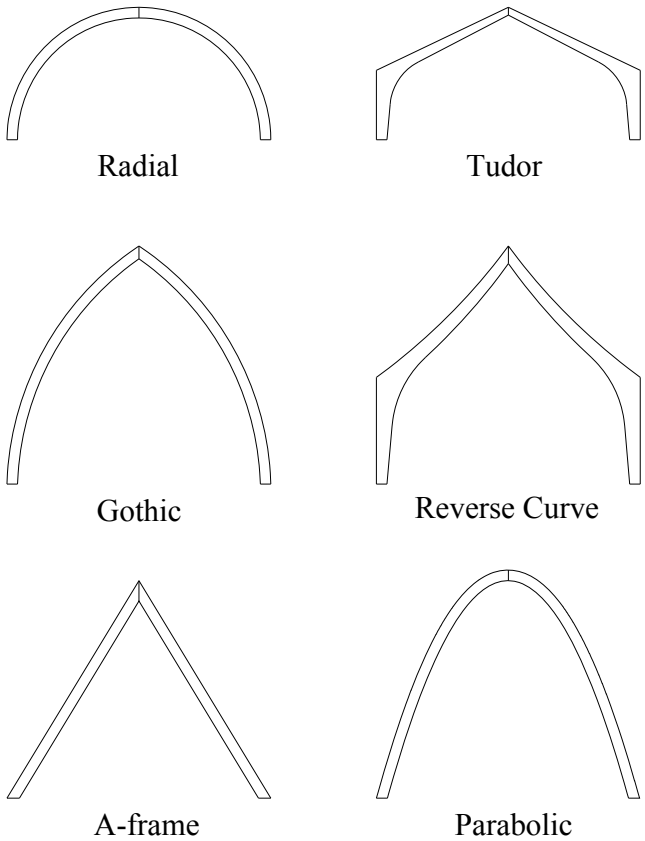

Figure 1.1. *Common arch configurations.*

The most common arch configuration in use today is the three-hinged Tudor arch. It provides a vertical wall frame and sloping roof that are commonly used for modern structures. Its appearance is also pleasing to most people. Because of its popularity, the three-hinged Tudor arch is the focus of this technical note, however, the same principles can be used to design other types of glulam arches.

Arch Design

The procedures presented in this document can be used to design tudor arches, however, other suitable methods may exist. Alternate methods, which have been validated through tests, extensive experience, or analyses based on recognized theory, can also be used. Manufacturers of structural glued laminated timber arches and engineering firms specializing in laminated timber design may have proprietary methods for design. Finite element modeling or other numerical methods may be used to compute member forces and deflections under load.

Aesthetic Considerations

Because structural glued laminated timber arches are typically exposed to view, the aesthetic appeal of the arch is an important design consideration in addition to its structural performance. The building designer and owner should verify that the final geometry meets the aesthetic requirements and any other architectural requirements for the design. Because of the numerous material and geometric parameters involved in arch design, multiple geometries can be utilized to meet the same structural requirements.

Dimensional Considerations

The length of arch segments is generally limited by transportation and erection constraints. Properly designed moment splices may be used in long span arches to facilitate shipping (AITC 2004, pps. 280-288).

Arches can pose significant challenges in shipping, particularly with tall wall heights and roofs with low pitch. Critical shipping dimensions are shown in **Figure 1.2**. To facilitate shipping, it may be necessary to design and manufacture the arch halves with moment splices occurring in the arms (**Figure 1.3**). These are typically placed at inflection points, or other locations with low bending moments. The arch can also be designed and manufactured with a detached haunch to reduce its overall width for shipping (**Figure 1.4**). Shipping widths of up to 12 ft can typically be accommodated. Wider loads may be possible depending on the distance from the manufacturing plant to the jobsite and the route the shipment will follow. Glulam manufacturers can often provide guidance regarding maximum shipping dimensions for various localities.

For arches with deep haunches, manufacturing constraints may also dictate the use of a detached haunch (**Figure 1.4**) to facilitate passing the arch through a surface planer. Glulam manufacturers should be contacted early in the design process to determine their maximum recommended haunch depths.

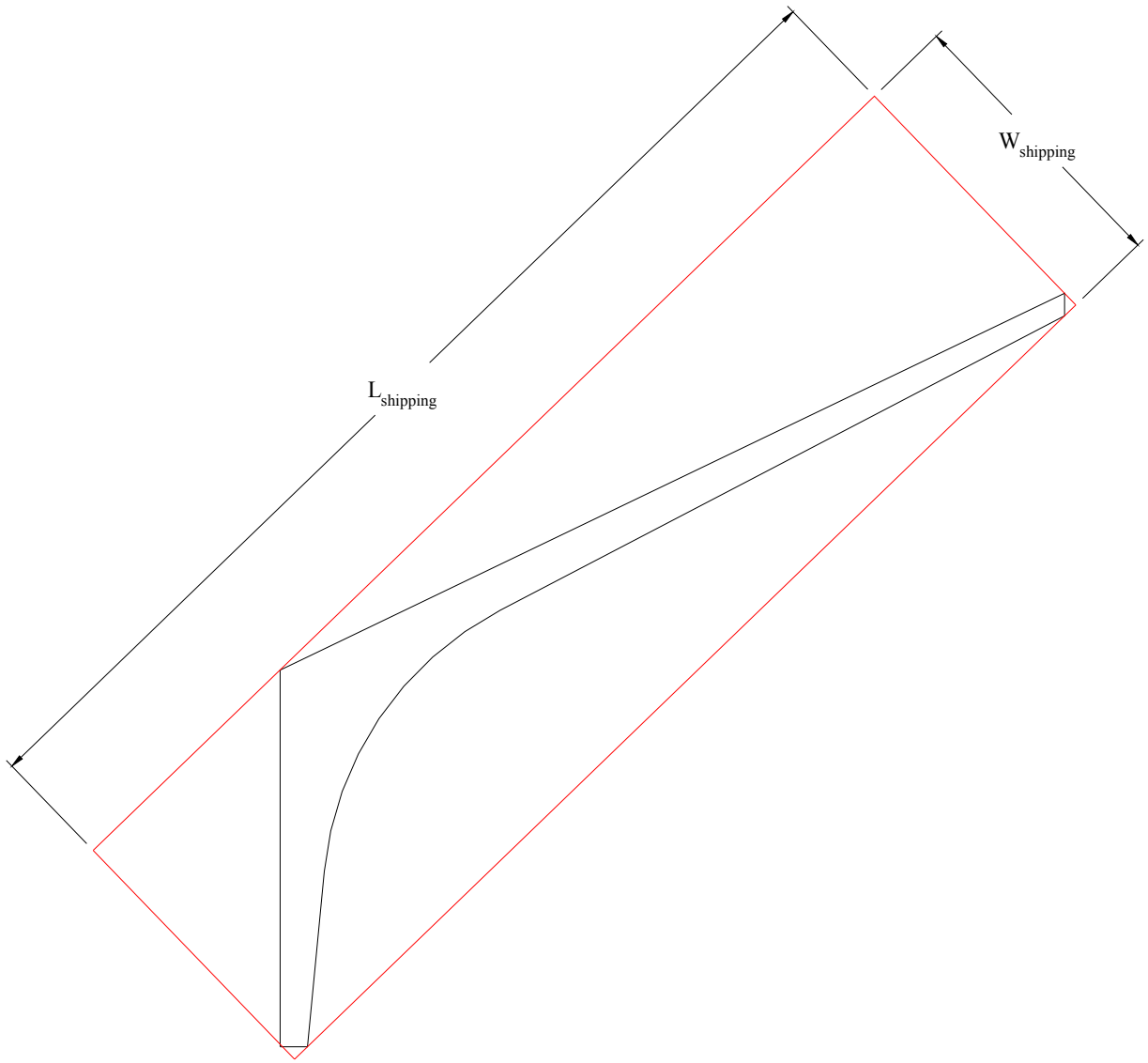

Figure 1.2 *Critical Shipping Dimensions*

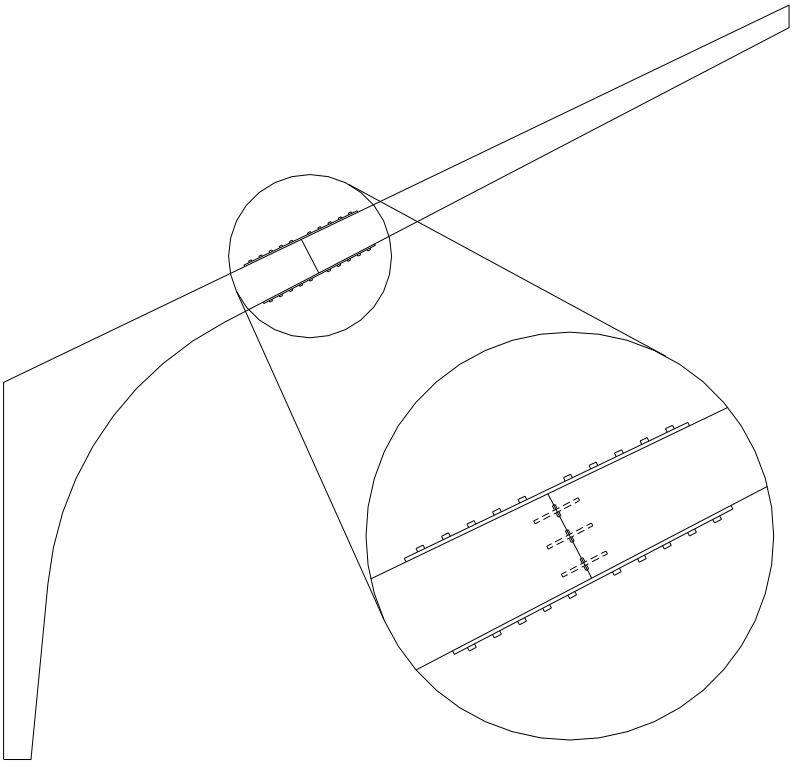

Figure 1.3 *Arch with Moment Splice in Arm (Schematic, some details omitted)*

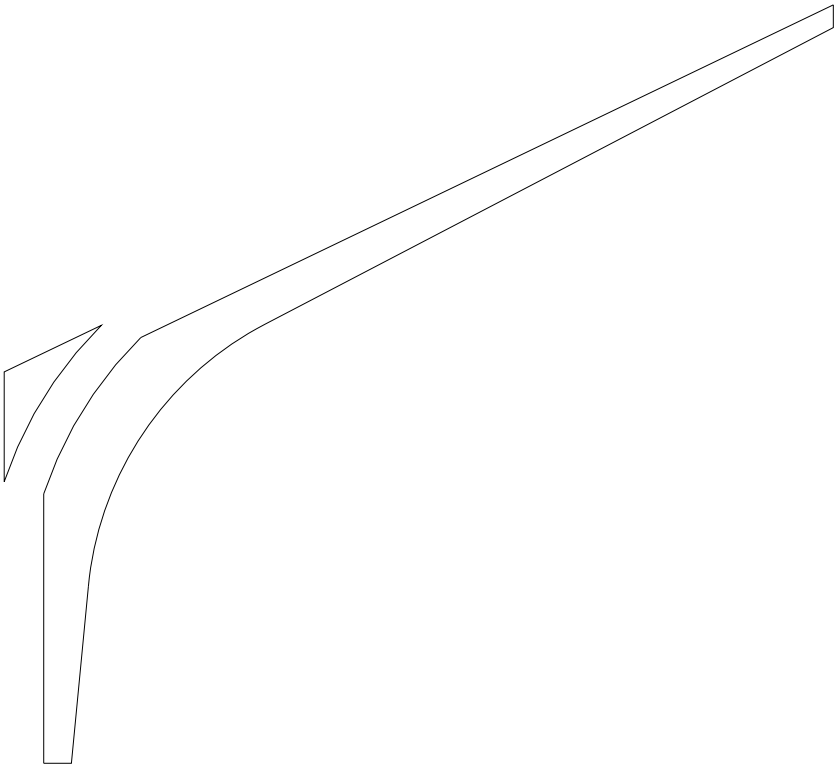

Figure 1.4 *Arch with Detached Haunch*

Structural Design

The design of arches is an iterative process. Experience will lead to less design iterations. Design checks must be made at several sections along the arch. Because the number of calculations required is large, the use of a spreadsheet or structural analysis software is recommended for arch design and analysis.

The basic design procedure includes the following steps:

1. *Determine all applicable loads and load combinations.* Roof and wall loads can typically be assumed to be uniform if decking is applied directly to the arch (or if purlins are closely spaced) or they may be concentrated at purlin points. Appropriate loads and load combinations can be obtained from the applicable building code or from the building official having jurisdiction.

2. *Determine a trial geometry.* The outside geometry (wall heights, peak height, outside span) of the arch is typically dictated by architectural constraints of the building. To complete a trial geometry, the designer must choose a width, end depths, a radius, and angles of taper for the wall leg and roof arm. Critical geometric features of a Tudor arch are shown in **Figure 1.5**.

   The base and crown sections of the arch must be adequately sized to resist the reaction loads at those locations and to accommodate the required fasteners. Typical connection details are shown in AITC 104 (AITC 2003). All other sections must be sized to resist bending moment, axial forces, and shear forces and the combined effect of these as appropriate.

3. *Divide the arch into segments, locate sections of interest, and calculate their section properties*. Because of the complex geometry of the arch and the variability of loading conditions, deflections are typically estimated using the principle of virtual work (programmed into a spreadsheet) or using structural analysis software. Additionally, the critical cross section for stress analysis will not be obvious. Therefore, several sections along the length of the arch, taken perpendicular to the laminations, should be chosen for evaluation. To minimize calculations, the same sections chosen for analysis of stresses can be used for virtual work calculations.

4. *Determine forces and moments with corresponding stresses on each section.* The bending moment, shear force, and axial force must be determined for each section of interest. These forces and moments can be determined using free-body diagrams at the sections of interest or structural analysis software. The resulting stresses can be calculated for each section.

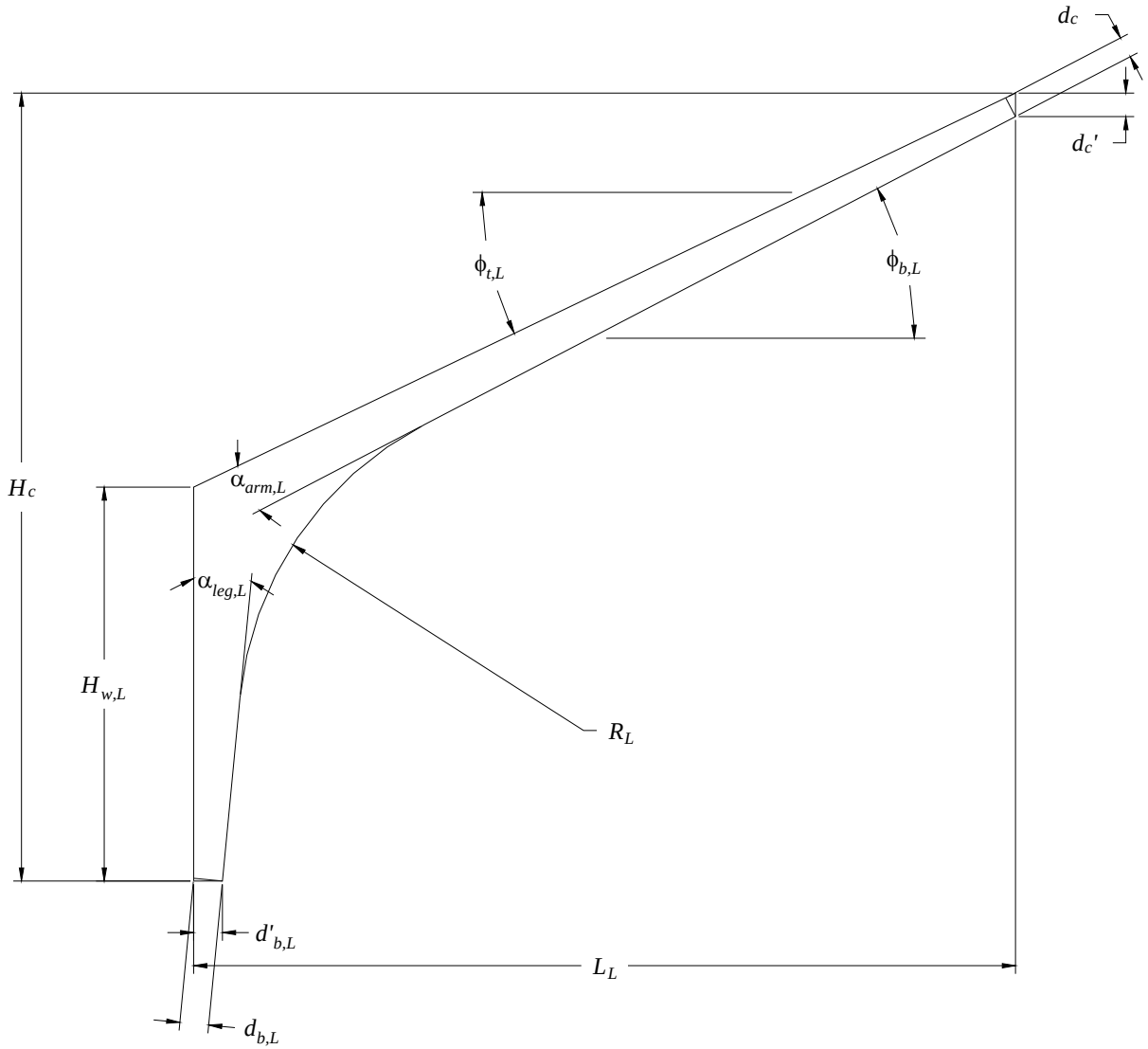

Figure 1.5. *Arch geometry. (Only left half shown for clarity.)*

5. *Determine the adjusted design values (allowable stresses) for each section.* Allowable stresses in compression, bending, and shear, must be determined for each of the sections chosen for evaluation. Reference design values must be adjusted by all appropriate adjustment factors specified in the National Design Specification® (NDS®) for Wood Construction.

   In addition to the factors described in the NDS®, the stress interaction factor, C_I, described in the AITC Timber Construction Manual (TCM) (5th ed. p. 108) should be applied for sections taken through the straight-tapered segments of the arch. For arches with taper sawn on the outer faces, it is also appropriate to reduce the flexural design value to account for the loss of high grade laminations due to the tapered cut (Appendix A).

Out-of-plane buckling of arches should be considered between points of lateral support through application of the column stability factor, C_P. In-plane buckling of the straight segments of the arch should also be considered through application of the column stability factor, C_P. These segments can be analyzed as tapered columns modeling the large end as fixed and the small end as pinned for the arch legs and modeling both ends as pinned for the arch arms (assumes inflection point is near upper tangent point). The column length for the arm is approximated as the distance from the upper tangent point to the peak, and the column length for the leg is approximated as the distance from the lower tangent to the base.

It is not necessary to evaluate in-plane buckling in the curved segment of Tudor arches, because secondary moments due to the eccentricity caused by buckling will generally be small compared to the bending moment caused by the curved shape. Therefore, for in-plane buckling in the curved segment, the column stability factor can be taken equal to unity ($C_P = 1.0$).

6. *Evaluate combined stresses on each section.* Arches simultaneously resist both axial and flexural stresses, so stress interactions must be considered. The combined effect of axial and flexural stresses at each section must satisfy the NDS® interaction inequalities. Combined flexure and compression are usually critical, however, for some loadings, flexure and axial tension may be developed.

Furthermore, the abrupt change in section at the haunch of a Tudor arch causes stress concentrations that can be accounted for by multiplying the stresses calculated by the flexure formula for that segment by the following factor:

$$K_{\theta,haunch} = 1 + 2.7 \tan\left(\frac{180^\circ - \theta}{2}\right)$$

where: θ = the included angle between the outer faces of the wall leg and roof arm

The factor, $K_{\theta,haunch}$, should be applied to the stresses calculated by the flexure formula prior to checking the section for combined stress interaction. However, when using structural analysis software, it may be more convenient to reduce the allowable stress by dividing by $K_{\theta,haunch}$, rather than increasing the flexure formula stress by multiplying by the factor.

7. Evaluate radial stresses in the curved segment. Loads that result in an increase in the radius of curvature cause radial tension stresses in the curved segment of the arch. Loads causing a decreased radius of curvature result in radial compression stresses. These stresses may be calculated using the following equation.

$$f_r = K_r \frac{6M}{bd_{haunch}^2}$$

where: $K_r = 0.29\left(\frac{d_c}{R_m}\right)^2 + 0.32 \tan^{1.2}\left(\frac{180^\circ - \theta}{2}\right)$

9. *Use the principal of virtual work (or structural analysis software) to calculate arch deflections for each load combination.* Because of the complex and varied geometry of Tudor arches, deflections are generally determined using approximate analysis methods, such as by using the principle of virtual work. By using the same sections chosen for stress calculations, the number of calculations can be reduced. Deflections should be checked against applicable limits. In the absence of specified deflection limits, it is recommended that the limits of Table 1.1 be applied.

Table 1.1. *Recommended Deflection Limits for Tudor Arches.*

	Haunch (Horizontal)	Arch Arm	Crown (Vertical)
With Brittle Finishes	$\frac{H_w}{120}$	$\frac{\ell_{arm}}{360}$	$\frac{L_L + L_R}{360}$
With Flexible Finishes	$\frac{H_w}{60}$	$\frac{\ell_{arm}}{180}$	$\frac{L_L + L_R}{180}$

10. *Design and detail connections.* Shear plates are typically used to transfer the vertical reaction forces at the peak connection. Bolts with steel side plates are used to transfer tension forces between members at the peak. The base connection typically consists of a bearing seat to resist outward thrust, with a bolt to resist inward thrust and uplift.

11. *Iterate until an acceptable design is obtained.* Because it is unlikely that an optimum design will be obtained on the first try, iteration will typically be necessary.

Conclusion

This chapter has provided an overview of the arch design process. Chapter 2 describes a simplified method for preliminary arch design. Chapter 3 presents a simplified, approximate method for modeling Tudor arches for use in structural analysis software. Chapter 4 discusses a rigorous analysis method that can be programmed into a spreadsheet, and should be considered when three-hinged Tudor arches will be designed regularly. Chapter 5 addresses the analysis of system effects of using a structural diaphragm and shear walls with Tudor arches for simple rectangular structures. Chapter 6 covers the design of arches to resist seismic loads. Chapter 7 discusses the requirements for specifying a Tudor arch once the design is complete.

Works Cited

AITC. 2004. Timber Construction Manual. John Wiley & Sons, Inc. Hoboken, New Jersey.

AITC. 2003. Typical Construction Details. AITC 104-2003. American Institute of Timber Construction. Centennial, Colorado.

Rhude, A. J. 1996. Structural Glued Laminated Timber: History of Its Origins and Early Development. Forest Prod. J. 46(1):15-22.

Chapter 2
Preliminary Tudor Arch Design

Because arch design can be quite complex and involved, many designers may choose to have the arches engineered by the structural glued laminated timber manufacturer or an engineer specializing in custom glulam structures. However, a method of approximating the geometry of an arch is useful to both the architect and engineer for preliminary design purposes. This allows the designer to visualize the appearance of the arches in the structure and illustrate this for his client. It also gives the final designer a starting point for his structural analysis.

This chapter presents one method of developing a symmetric arch geometry. **This method involves multiple approximations and should not be used for the final design**, but should give a reasonable approximation of an efficient arch geometry for preliminary purposes. The final arch geometry must be evaluated by a qualified engineer to ensure that it is adequate for all anticipated loads.

Nomenclature

A	distance from the haunch to the approximate tangent points
b	arch width
C_D	load duration factor
C_I	stress interaction factor for tapered members
C_M	wet-service factor
C_t	temperature factor
C_V	volume factor
C_x	horizontal reaction force at arch peak connection
C_y	vertical reaction force at arch peak connection
C_Δ	geometry factor
$C_{\Delta,u}$	geometry factor for unloaded edge distance
D	dead load
d_b	depth at arch base measured perpendicular to laminations
d_b'	depth at arch base measured horizontally
d_c	depth at arch peak measured perpendicular to laminations
d_c'	depth at arch peak measured vertically
d_{LT}	depth at section through lower tangent point
d_{UT}	depth at section through upper tangent point
d_x	depth at section through point x
E_C	minimum shear plate end distance for parallel-to-grain loads for a geometry factor of C_Δ = 1.0 or 0.83

E_D minimum shear plate loaded edge distance for perpendicular-to-grain loads for a geometry factor of C_Δ = 1.0 or 0.83

E_α loaded edge distance for shear plate connection

E_{α,C_Δ} shear plate loaded edge distance corresponding to a geometry factor, C_Δ

$E_{\alpha,1.0}$ required shear plate loaded edge distance for a geometry factor, $C_\Delta = 1.0$

$E_{\alpha,0.83}$ required shear plate loaded edge distance for a geometry factor, $C_\Delta = 0.83$

F_{bx} reference design stress in bending

F_{vx} reference design stress in shear

H_w height of wall

k_1 factor for proportioning unbalanced snow load

k_2 factor for proportioning unbalanced snow load

L_L span of left arch half

L_R span of right arch half

N reference capacity for single shear plate in sloped end grain

$n_{\min}$ minimum number of shear plates required to transfer vertical reaction force at peak

n_x number of rows of shear plates

n_y number of shear plates per row

P parallel-to-grain reference capacity for single shear plate

Q_{90} perpendicular-to-grain reference capacity for single shear plate in end grain

R radius of curvature

$R_{x,L}$ horizontal reaction at base of left arch half

$R_{x,R}$ horizontal reaction at base of right arch half

$R_{y,L}$ vertical reaction at base of left arch half

$R_{y,R}$ horizontal reaction at base of right arch half

S snow load

S_C minimum shear plate spacing parallel to grain for parallel-to-grain loads for a geometry factor of C_Δ = 1.0

S_D minimum shear plate spacing perpendicular to grain for perpendicular-to-grain loads for a geometry factor of C_Δ = 1.0

S_α spacing for shear plate connection

S_{α,C_Δ} shear plate spacing corresponding to a geometry factor, C_Δ

$S_{\alpha,1.0}$ required shear plate spacing for a geometry factor, $C_\Delta = 1.0$

$S_{\alpha,0.5}$ required shear plate spacing for a geometry factor, $C_\Delta = 0.5$

x horizontal distance to critical section for flexure in arch arm (estimated)

x_2 horizontally projected distance from haunch to approximate upper tangent point

y_1 vertical distance from base to approximate lower tangent point

y_2 vertically projected distance from base to approximate upper tangent point

α_{arm} taper angle in arch arm

α_{leg} taper angle in arch leg

ω_D uniformly distributed dead load

ω_S uniformly distributed snow load

ϕ roof slope

Procedure

The arch geometry will be established based on the D + S loading. (For areas without snow load, roof live load can be substituted). The required depths in the arch leg are determined based on the balanced snow loading or the unbalanced loading, whichever results in larger base reaction forces. The depths in the arch arm are controlled by the unbalanced snow loading. The following steps are used to establish the geometry:

1. *Choose angles of taper, radius of curvature, wall height, peak height, span, and arch width (Figure 1.2).* The outside arch geometry (wall height, peak height, and span) will generally be dictated by the building dimensions. The angles of taper should generally be less than 3° for the arch arm and less than 5° for the arch leg (steeper tapers can be used if they are properly accounted for in design). The radius of curvature of the inside face is commonly chosen as 7 ft 0 in. for Southern Pine and 9 ft 4 in. for other softwood species. The arch width is often chosen so that it exceeds the minimum requirements for Heavy Timber Construction in addition to structural requirements.

2. *Choose material properties (species, design stresses: F_{bx}, F_{vx}).* For Douglas fir arches, common properties are: F_{bx} = 2400 psi and F_{vx} = 190 psi. For Southern Pine arches, common properties are: F_{bx} = 2400 psi and F_{vx} = 215 psi.

3. *Locate approximate tangent points (**Figure 2.1**).*

$$A = R\tan\left(\frac{90-\phi}{2}\right) \quad [2\text{-}1]$$

$$x_2 = A\cos(\phi) \quad [2\text{-}2]$$

$$y_2 = H_w + A\sin(\phi) \quad [2\text{-}3]$$

$$y_1 = H_w - A \quad [2\text{-}4]$$

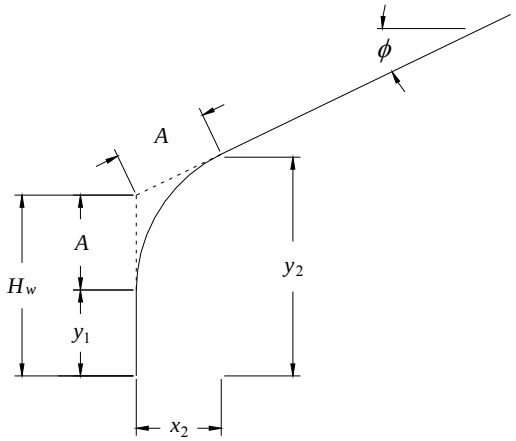

Figure 2.1. *Location of approximate tangent points.*

4. *Calculate the reactions and pin forces for balanced (**Figure 2.2**) and unbalanced (**Figure 2.3**) snow loads.* These forces are calculated based on the outside geometry of the arch, because the actual centerline of the members is not known. This produces a reasonably accurate estimate of the forces.

Balanced Snow Load (Figure 2.2)

$$R_{y,R} = R_{y,L} = \left(\omega_D + \omega_S\right) L_L^2 \qquad [2\text{-}5]$$

$$R_{x,R} = R_{x,L} = \frac{1}{H_c}\left[R_{y,L} L_L - \frac{\left(\omega_D + \omega_S\right) L_L^2}{2} \right] \qquad [2\text{-}6]$$

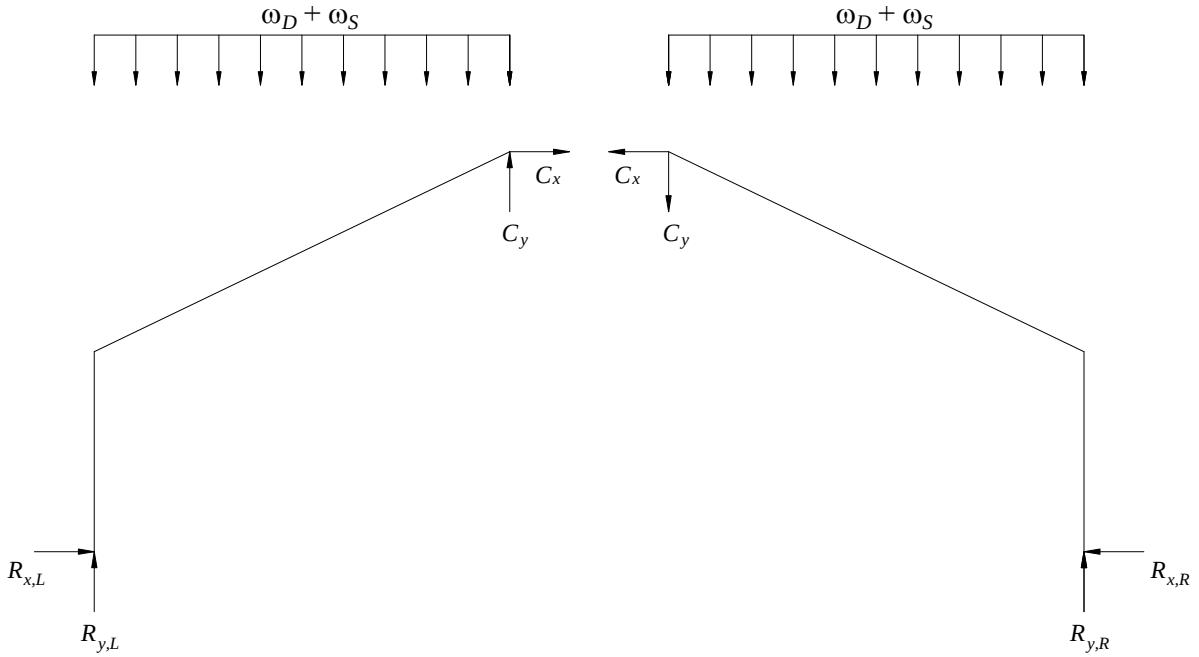

Figure 2.2. *Dead load plus balanced snow load.*

Unbalanced Snow Load (Figure 2.3)

$$R_{y,L} = \frac{\left(k_1\omega_S + \omega_D\right)\left(3L_L\right) + \left(k_2\omega_S + \omega_D\right)\left(L_L\right)}{4} \quad [2\text{-}7]$$

$$C_y = \left(k_1\omega_D + \omega_S\right)L_L - R_{y,L} \quad [2\text{-}8]$$

$$R_{x,L} = \frac{R_{y,L}L_L + \left(k_1\omega_S + \omega_D\right)\frac{L_L^2}{2}}{H_c} \quad [2\text{-}9]$$

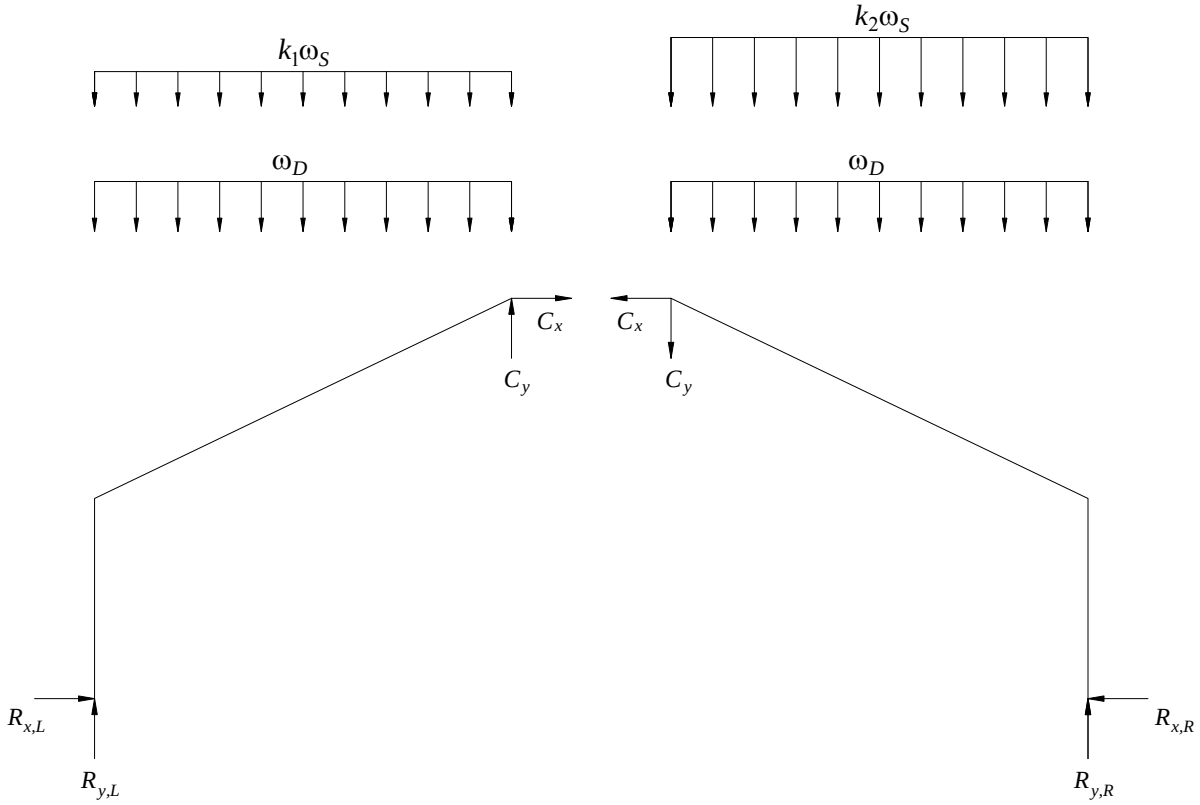

Figure 2.3. *Dead load plus unbalanced snow load (simplified).*

5. *Estimate the required depth at the lower tangent point, d_{LT}.* The minimum depth at the lower tangent point is estimated based on the bending moment created by the horizontal reaction (from the balanced snow load or unbalanced snow load, whichever gives larger reaction) applied at a distance, y_1, from the approximate tangent point. The depth should be increased approximately 5% over that calculated based on moment alone to account for compression-flexure interaction.

$$d_{LT} > 1.05\sqrt{\frac{6y_1 R_{x,L}}{bF_{bx}C_D C_I C_V C_M C_t}} \qquad [2\text{-}10]$$

C_D is 1.15 for snow loading (1.25 for roof live load). C_I is calculated based on the chosen material properties and leg taper angle. A rough estimate of the volume factor, C_V, at the tangent point can be obtained from one of the following expressions: $C_V \approx$ 0.95-0.0015*(L_L) for southern pine or $C_V \approx$ 0.90-0.0025*(L_L) for other species, where L_L is expressed in units of feet.

The depth at the lower tangent point should not be greater than 6 times the width for arches braced against lateral buckling by decking or closely spaced girts or purlins and should not be greater than 5 times the width for arches without such lateral bracing. If the required depth calculated by Equation [2-10] is not within these limitations, the width must be increased.

6. *Estimate the required depth at the base.* The minimum depth at the base is estimated based on the horizontal reaction force and is also determined based on the estimated tangent point depth and the amount of taper chosen for the leg. The greater depth from these two calculations should be chosen. Generally the base depth is also chosen to be a minimum of 1.5 times the arch width. The base depth may also be chosen based on the minimum size required for Heavy Timber Construction.

   Required base depth for shear:

$$d'_b > \frac{3R_x}{2bF_{vx}C_D C_M C_t} \qquad [2\text{-}11]$$

   Required base depth to get the required lower tangent depth with chosen leg taper angle:

$$d'_b > d_{LT} - y_1 \tan\alpha_{leg} \qquad [2\text{-}12]$$

   Occasionally, the required depth at the base for shear may be greater than the depth required at the tangent point. In such cases, the base depth required for shear should be chosen and the leg taper angle should be set to zero to avoid excessive depth at the tangent point.

   The base depth should generally not be chosen as less than 1.5 times the arch width. If this criterion governs the selection of the depth, the leg taper angle can be reduced to avoid excessive depth at the lower tangent point.

7. *Estimate the required depth at the crown.* The minimum depth at the crown is estimated based on the shear plate connector requirements to resist the vertical shear force at the crown due to unbalanced snow loading and based on flexure in the loaded arm due to unbalanced snow load.

Required crown depth based on shear plate capacity:

- *Calculate reference capacity for a single shear plate in sloped end grain using Hankinson's formula for the chosen roof slope and arm taper*.

$$N = \frac{PQ_{90}}{P\sin^2\left(90^\circ - \phi - \alpha_{arm}\right) + Q_{90}\cos^2\left(90^\circ - \phi - \alpha_{arm}\right)} \qquad [2\text{-}13]$$

- *Adjust the capacity for load duration and apply the geometry factor for reduced unloaded edge distance*. Shear plate design values are tabulated for unloaded edge distances of 1.75 in. and 2.75 in. for 2-5/8 in. and 4 in. shear plates, respectively. For narrower edge distances typical of standard glulam arches, a reduction in capacity is required. Geometry factors for reduced unloaded edge distance are shown in Table 2.1 for standard arch widths. The effect of group action will generally be small and can be ignored at this point.

Table 2.1. *Geometry Factors, $C_{\Delta,u}$, for shear plate capacity based on arch width.*

Arch width ***b*** **(in.)**	**Geometry Factors, $C_{\Delta,u}$**	
	2-5/8 in. Connectors	4 in. Connectors
3	0.88	--
3-1/8	0.91	--
5	1.0	0.93
5-1/8	1.0	0.95
5-1/2 or wider	1.0	1.0

$$N^* = NC_D C_M C_t C_{\Delta,u} \qquad [2\text{-}14]$$

- *Determine the minimum number of connectors, n_{min}, to transfer the load by dividing the vertical crown reaction force by the partially adjusted capacity of an individual connector (round up to nearest whole number).*

$$n_{\min} = \frac{\left|C_y\right|}{N^*} \qquad [2\text{-}15]$$

- *Determine the number of rows of connectors, n_x,*. Table 2.2 gives the maximum number of rows of connectors based on arch width. (Rows are oriented vertically)

Table 2.2. *Maximum number of rows of connectors based on arch width*

Arch width ***b*** **(in.)**	**Maximum rows of connectors,** n_x	
	2-5/8 in. Connectors	4 in. Connectors
3, 3-1/8, 3-1/2	1	--
5, 5-1/8, 5-1/2	1	1
6-3/4	1	1
8-1/2, 8-3/4	2	1
10-1/2, 10-3/4	3	2

- *Calculate the required number of connectors per row,* n_y.

$$n_y = \frac{n_{\min}}{n_x} \qquad [2\text{-}16]$$

Except for very shallow members, a minimum of two shear plates is generally required per row to prevent significant reductions in member shear capacity due to notch effects (NDS 3.4.3.3).

- *Determine the geometry factor for optimal spacing and edge distance:*

$$0.5 \le C_\Delta = \frac{|C_y|}{nN^*} \le C_{\Delta,u} \qquad [2\text{-}17]$$

- *Determine the required spacing for the cases of* C_Δ = 0.5 and C_Δ = 1.0.

The required spacing for C_Δ = 1.0 is determined based on the angle of the connector with respect to the grain of the member using the following equation (adapted from Equation 5.14 from the 5th edition TCM):

$$S_\alpha = \frac{S_C S_D}{\sqrt{S_C^2 \sin^2\left(90 - \phi - \alpha_{arm}\right) + S_D^2 \cos^2\left(90 - \phi - \alpha_{arm}\right)}} \qquad [2\text{-}18]$$

where: S_α = Required spacing of connectors
S_C = 6.75 in. for 2-5/8 in. shear plates
= 9 in. for 4 in. shear plates
S_D = 4.25 in. for 2-5/8 in. shear plates
= 6 in. for 4 in. shear plates

The required minimum spacing for C_Δ = 0.5 is 3.5 in. for 2-5/8 in. shear plates and is 5.0 in. for 4 in. shear plates.

- *Calculate the required loaded edge distance for* $C_\Delta = 0.83$ and $C_\Delta = 1.0$.

$$E_\alpha = \frac{E_C E_D}{\sqrt{E_C^2 \sin^2\left(90 - \phi - \alpha_{arm}\right) + E_D^2 \cos^2\left(90 - \phi - \alpha_{arm}\right)}} \qquad [2\text{-}19]$$

E_α = Required loaded edge distance

E_C = 5.5 in. for 2-5/8 in. shear plates and $C_\Delta = 1.0$
= 4.25 in. for 2-5/8 in. shear plates and $C_\Delta = 0.83$
= 7 in. for 4 in. shear plates and $C_\Delta = 1.0$
= 5.4 in. for 4 in. shear plates and $C_\Delta = 0.83$

E_D = 2.75 in. for 2-5/8 in. shear plates and $C_\Delta = 1.0$
= 1.5 in. for 2-5/8 in. shear plates and $C_\Delta = 0.83$
= 3.75 in. for 4 in. shear plates and $C_\Delta = 1.0$
= 2.5 in. for 4 in. shear plates and $C_\Delta = 0.83$

- *Determine the required spacing and loaded edge distance corresponding to the optimal geometry factor using linear interpolation.* If the optimal geometry factor is less than 0.83, use the minimum edge distance determined for $C_\Delta = 0.83$.

$$S_{\alpha,C_\Delta} = \left(\frac{C_\Delta - 0.5}{1 - 0.5}\right)\left(S_{\alpha,1.0} - S_{\alpha,0.5}\right) + S_{\alpha,0.5} \qquad [2\text{-}20]$$

$$E_{\alpha,C_\Delta} = \left(\frac{C_\Delta - 0.83}{1 - 0.83}\right)\left(E_{\alpha,1.0} - E_{\alpha,0.83}\right) + E_{\alpha,0.83} \qquad [2\text{-}21]$$

Choose spacing, *S*, and end distance, *E*, equal to or greater than those calculated. The chosen spacing and end distance should be rounded up to the nearest 1/16 in. or other practical unit of measure to facilitate fabrication.

- *Calculate the required depth based on connector spacing and edge distance:*

$$d_c' \geq d_{c\ shear\ plates}' = \left(n_y - 1\right)S_\alpha + 2E_\alpha \qquad [2\text{-}22]$$

Required crown depth based on flexure in the arm and chosen arm taper angle:

Estimating that the point of inflection occurs near the upper tangent point of the loaded arch for the unbalanced snow loading and that the crown depth is approximated by the depth required for the shear plates, the location of the critical section in the upper arm of the loaded arch (measured from the crown) can be determined from the following relationship, which was derived for this case from

equation 4.32 of the AITC Timber Construction Manual (5th edition) (*x* is measured horizontally from the crown):

$$x \approx \frac{\cos(\phi)(L_R - x_2)\left(\frac{d_c'}{\cos(\alpha_{arm})}\right)}{2\left(d_c'\frac{\cos(\phi)}{\cos(\alpha_{arm})}\right)+\frac{(L_R - x_2)}{\cos(\phi)}\tan\alpha_{arm}} \qquad [2\text{-}23]$$

The required depth at that section can be approximated as:

$$d_x > \sqrt{\frac{3(\omega_S + \omega_D)(L_R - x_2)x\left(1-\frac{x}{L_R - x_2}\right)}{bF_{bx}C_DC_IC_MC_t}} \qquad [2\text{-}24]$$

For tapered arms, the reference flexural stress, F_{bx}, used in [2-24] should be reduced to account for the loss of high strength material at the surface due to tapering, unless the arch is laid up with a uniform-grade lay-up or the high grade material is maintained throughout the length of the arch (Appendix A). Either of these options may increase the cost of the arch. For standard arches with tapered arms, a 10% reduction is suitable for preliminary design purposes.

The corresponding depth at the crown can be estimated as:

$$d_c > d_x - \left(\frac{x}{\cos\phi}\right)\tan\alpha_{arm} \qquad [2\text{-}25]$$

$$d_c' = \frac{d_c\cos(\alpha_{arm})}{\cos\phi_t} \qquad [2\text{-}26]$$

The greater depth from connector requirements or from arm flexure is chosen as the minimum depth of the arch at the crown.

With the preceding steps completed, a trial arch geometry is defined. The trial geometry should be further adjusted to ensure that the upper and lower tangent point depths are within approximately 10% of each other. The trial arch should be drawn to scale and the geometry should be adjusted if necessary for aesthetic considerations.

At this point, the preliminary design of the arch is completed. The final design must include a thorough analysis of the arch subject to all applicable loads and load combinations by the procedures discussed in Chapters 3-5. An example including the preliminary design procedure described in this chapter follows.

Example 2-1: Design of Tudor Arch

Given: A building with outside dimension of 50 ft by 60 ft is to be constructed using Southern Pine Tudor arches spaced at 15 ft.

The arches will be subject to normal temperatures and dry-use conditions.

The arches will be symmetric with a maximum roof height of 24 ft. and a wall height of 12 ft as shown in Figure E4.1.

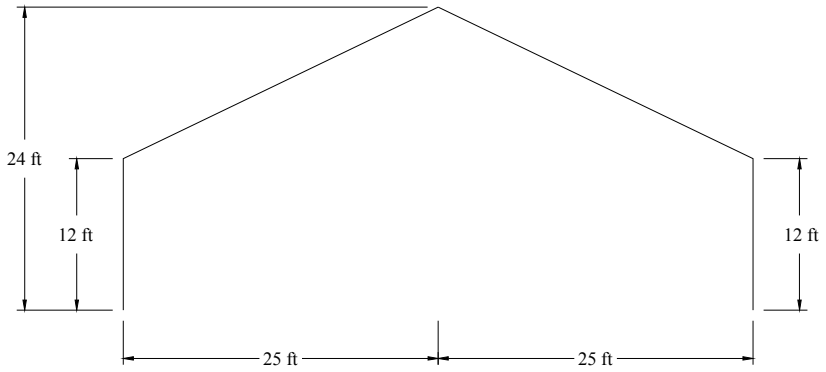

Figure E2.1. *Outside geometry of arch.*

The curved portion of the arches will have a radius of 10.5 ft at the inside face and a lamination thickness of ¾ in.

The arch has continuous lateral bracing along the wall and roof.

The building has no shear walls at the ends, so the arches will be assumed to support all vertical and lateral loads acting parallel to the planes of the arches.

Material Properties: $\mathbf{F_{bx}^{+}}$ = 2000 psi
$\mathbf{F_{vx}}$ = 215 psi

Loads: the loads have been determined as shown in Figures E2.2 through E2.4. The wall dead loads are assumed to act at the outer face of the arch.

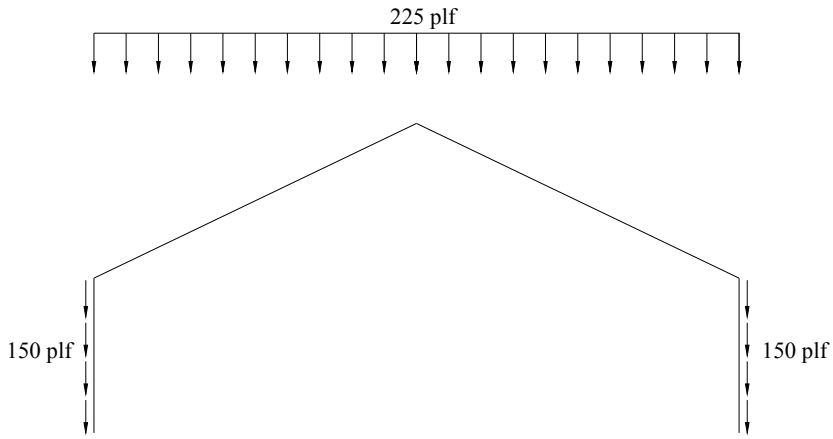

Figure E2.2. *Dead loads.*

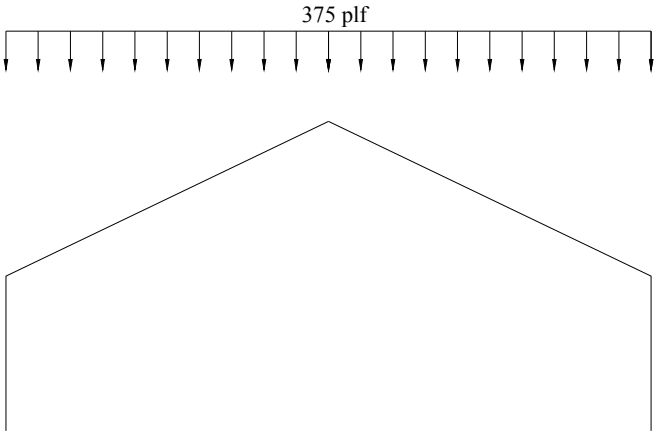

Figure E2.3. *Balanced snow load.*

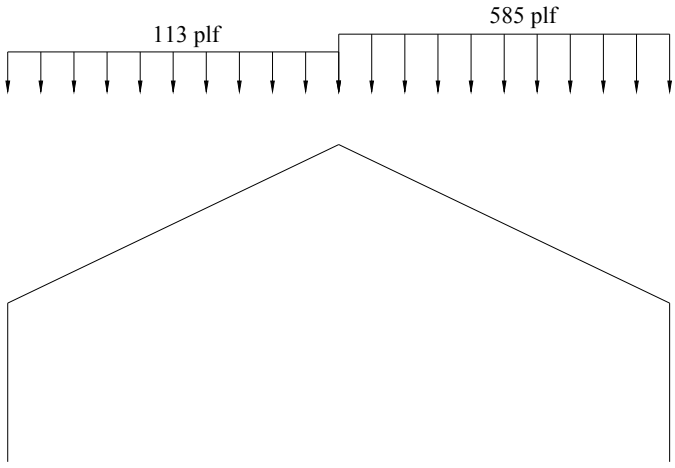

Figure E2.4. *Unbalanced snow load.*

Wanted: Perform preliminary design of a Tudor arch with a width of 6.75 in. based on the dead plus snow load combinations:

(1) D + S (balanced snow)
(2) D + S (unbalanced snow)

For final design, additional load combinations will need to be considered.

Solution:

The required depth at the lower tangent is commonly governed by the balanced snow loading. The depths in the arch arm are commonly controlled by the unbalanced snow loading.

Approximate reaction forces (using the outside arch geometry) for each considered snow load combination are included in Table E2.1.

Table E2.1. *Approximate reactions for* **D + S** *load combinations.*

Load	$R_{y,L}$	$R_{x,L}$	C_y	C_x	$R_{y,R}$	$R_{x,R}$
D+S (Balanced)	16800	7810	0	-7810	16800	7810
D+ S (Unbalanced)	13200	7470	-2950	-7470	19100	7470

Estimating the required depth at the crown based on connection requirements

The minimum depth at the crown will be estimated based on the vertical reaction force at the peak connection due to unbalanced snow loading and the number of shear plates required to transfer the load.

For 4 inch shear plates in Southern Pine:

$$P = 4360 \text{ lb}$$
$$Q = 3040 \text{ lb}$$
$$Q_{90} = 0.6Q = 0.6\left(3040 \text{ lb}\right) = 1824 \text{ lb}$$

The shear plates will be loaded at an angle to the grain of $90° - \phi - \alpha_{arm}$.

$$\phi = \arctan\left(\frac{12 \text{ ft}}{25 \text{ ft}}\right) = 25.64°$$
$$\alpha_{arm} = 2.5°$$
$$90° - \phi - \alpha_{arm} = 90° - 25.64° - 2.5° = 61.86°$$

Hankinson's formula can be used to determine the reference capacity for a single shear plate loaded at an angle to the grain of $90° - \phi - \alpha_{arm}$.

$$N = \frac{PQ_{90}}{P\sin^2\left(90° - \phi - \alpha_{arm}\right) + Q_{90}\cos^2\left(90° - \phi - \alpha_{arm}\right)}$$

$$N = \frac{\left(4360 \text{ lb}\right)\left(1824 \text{ lb}\right)}{\left(4360 \text{ lb}\right)\sin^2\left(61.86°\right) + \left(1824 \text{ lb}\right)\cos^2\left(61.86°\right)}$$

$$N = 2095 \text{ lb}$$

The partially adjusted capacity (dry-use, normal temperatures, snow load) for a single shear plate is:

$$N^* = NC_D C_{\Delta,u} = \left(2095 \text{ lb}\right)\left(1.15\right)\left(1.0\right) = 2410 \text{ lb}$$

Based on the vertical reaction at the crown of $C_y = -2950$ lb, a minimum of two shear plates will be required:

$$n_{\min} = \frac{\left|C_y\right|}{N^*} = \frac{2950 \text{ lb}}{2410 \text{ lb}} = 1.22 \qquad \therefore \text{Use two shear plates}$$

The geometry factor for optimal spacing and edge distance is:

$$0.83 \le C_\Delta = \frac{\left|C_y\right|}{nN^*} \le C_{\Delta,\text{unloaded edge distance}}$$

$$C_\Delta = \frac{\left|C_y\right|}{nN} = \frac{2950 \text{ lb}}{2\left(2410 \text{ lb}\right)} = 0.612 \ge 0.5 \qquad \therefore C_\Delta = 0.61$$

The required spacing between shear plates for $C_\Delta = 1.0$ is calculated as:

$$S_{\alpha,1.0} = \frac{S_C S_D}{\sqrt{S_C^2\sin^2\left(90^\circ - \phi - \alpha_{arm}\right) + S_D^2\cos^2\left(90^\circ - \phi - \alpha_{arm}\right)}}$$

$$S_{\alpha,1.0} = \frac{\left(9 \text{ in}\right)\left(6 \text{ in}\right)}{\sqrt{\left(9 \text{ in}\right)^2\sin^2\left(61.86^\circ\right) + \left(6 \text{ in}\right)^2\cos^2\left(61.86^\circ\right)}}$$

$$S_{\alpha,1.0} = 6.41 \text{ in}$$

The required spacing between shear plates for $C_\Delta = 0.5$ for 4 in. shear plates is:

$$S_{\alpha,0.5} = 5.0 \text{ in}$$

The required spacing between shear plates for $C_\Delta = 0.61$ is determined by linear interpolation:

$$S_{\alpha,0.61} = \left(\frac{C_\Delta - 0.5}{1-0.5}\right)\left(S_{\alpha,1.0} - S_{\alpha,0.5}\right) + S_{\alpha,0.5}$$

$$S_{\alpha,0.61} = \left(\frac{0.61-0.5}{1-0.5}\right)\left(6.41\text{ in} - 5.0\text{ in}\right) + 5.0\text{ in}$$

$$S_{\alpha,0.61} = 5.3\text{ in} \qquad \therefore \text{Choose } S_\alpha = 5.5\text{ in}$$

The actual geometry factor based on the spacing of 5.5 in. is:

$$C_\Delta = \left(\frac{S_\alpha - S_{\alpha,0.5}}{S_{\alpha,1.0} - S_{\alpha,0.5}}\right)\left(1.0-0.5\right) + 0.5 = \left(\frac{5.5-5.0}{6.41-5.0}\right)\left(1.0-0.5\right) + 0.5 = 0.68$$

The minimum loaded edge distance for $C_\Delta = 0.83$ is calculated as:

$$E_\alpha = \frac{E_C E_D}{\sqrt{E_C^2 \sin^2\left(90^\circ - \phi_t - \alpha_{arm}\right) + E_D^2 \cos^2\left(90^\circ - \phi_t - \alpha_{arm}\right)}}$$

$$E_{\alpha,0.83} = \frac{\left(5.4\text{ in}\right)\left(2.5\text{ in}\right)}{\sqrt{\left(5.4\text{ in}\right)^2 \sin^2\left(61.86^\circ\right) + \left(2.5\text{ in}\right)^2 \cos^2\left(61.86^\circ\right)}}$$

$$E_{\alpha,0.83} = 2.75\text{ in} \qquad \therefore \text{Choose } E_\alpha = 2.75\text{ in}$$

The minimum vertical depth at the crown to accommodate the two 4 in. shear plates is:

$$d_c' = S_\alpha + 2E_\alpha = 5.5\text{ in} + 2\left(2.75\text{ in}\right) = 11.0\text{ in}$$

The depth measured perpendicular to the laminations at the crown is:

$$d_c = \frac{d_c' \cos\phi}{\cos\alpha_{arm}} = \frac{\left(11.0\text{ in}\right)\cos\left(25.6^\circ\right)}{\cos\left(2.5^\circ\right)} = 9.9\text{ in}$$

A depth, d_c', of 11.0 inches is sufficient to accommodate the use of two 4 in. shear plates. The geometry factor will be the lesser of that determined for spacing and edge distance, $C_\Delta = 0.68$. The adjusted capacity (dry-use, normal temperatures, snow load) of the connection is:

$$N' = 2\left(P_{90^\circ-\phi-\alpha} C_D C_\Delta C_g\right) = 2\left(2095\text{ lb}\right)\left(1.15\right)\left(0.68\right)\left(1.0\right)$$

$$N' = 3280\text{ lb} \geq C_y = 2950\text{ lb} \qquad \therefore \text{OK}$$

Estimating the required depth at the crown based on flexure in the arm

The location of the upper tangent point of the loaded arch half can be approximated by:

$$x_2 = A\cos(\phi) = (79.3\text{ in})\cos(25.64^\circ) = 71.5\text{ in}$$

Estimating that the point of inflection will occur near the upper tangent point of the loaded arch for the unbalanced snow loading and that the crown depth is approximately equal to the depth required to accommodate the shear plates at the crown, the location of the critical section in the upper arm of the loaded arch (measured from the crown) can be determined from the following relationship, which was derived for this case from equation 4.32 of the AITC Timber Construction Manual (5th edition):

$$x \approx \frac{\cos(\phi)(L_R - x_2)\left(\frac{d_c'}{\cos(\alpha_{arm})}\right)}{2\left(d_c'\frac{\cos(\phi)}{\cos(\alpha_{arm})}\right) + \frac{(L_R - x_2)}{\cos(\phi)}\tan\alpha_{arm}}$$

$$x \approx \frac{\cos(25.64^\circ)(300\text{ in} - 71.5\text{ in})\left(\frac{12.5\text{ in}}{\cos(2.5^\circ)}\right)}{2\left(12.5\text{ in}\frac{\cos(25.64^\circ)}{\cos(2.5^\circ)}\right) + \frac{(300\text{ in} - 71.5\text{ in})}{\cos(25.64^\circ)}\tan(2.5^\circ)}$$

$$x \approx 76.7\text{ in}$$

The required depth at that section can be approximated as:

$$d_x > \sqrt{\frac{3\omega_{y,R}(L_R - x_2)x\left(1 - \frac{x}{L_R - x_2}\right)}{bF_{bx}C_DC_I}}$$

$$d_x > \sqrt{\frac{3(67.5\text{ lb/in})(300\text{ in} - 71.5\text{ in})(76.7\text{ in})\left(1 - \frac{76.7\text{ in}}{300\text{ in} - 71.5\text{ in}}\right)}{(6.75\text{ in})(2000\text{ psi})(0.9)(1.15)(0.926)}} = 13.5\text{ in}$$

The corresponding depth at the crown can be estimated as:

$$d_c \approx d_x - \left(\frac{x}{\cos\phi}\right)\tan\alpha_{arm} = 13.5 \text{ in} - \left(\frac{76.7 \text{ in}}{\cos\left(25.6^\circ\right)}\right)\tan\left(2.5^\circ\right) = 9.8 \text{ in}$$

$$d_c' = \frac{d_c\cos\left(\alpha_{arm}\right)}{\cos\phi} = \frac{9.8\cos\left(2.5^\circ\right)}{\cos\left(25.6^\circ\right)} = 10.9 \text{ in}$$

A trial depth, d_c', of 11.0 inches will be chosen (controlled by connector design). The depth of the crown (measured perpendicular to the laminations) is $d_c = 9.9$ inches as previously calculated.

Estimating the depth at the upper tangent based on chosen crown depth and taper angle

The depth of the upper tangent can be estimated as:

$$d_{UT} \approx d_c + \left(\frac{L_R - x_2}{\cos\phi}\right)\tan\alpha_{arm} = 9.9 \text{ in} + \left(\frac{300 \text{ in} - 71.5 \text{ in}}{\cos\left(25.6^\circ\right)}\right)\tan\left(2.5^\circ\right) = 21.0 \text{ in}$$

Estimating the required depth of the lower tangent point

The minimum depth at the lower tangent point will be estimated based on the moment created by the horizontal reaction applied at a distance, $y_{1,L}$, from the approximate tangent point. The leg taper is chosen as 4° for the determination of C_I. The volume factor will be estimated as 0.95.

$$A = R\tan\left(\frac{90^\circ - \phi}{2}\right) = \left(126 \text{ in}\right)\left(\tan\left(\frac{90^\circ - 25.64^\circ}{2}\right)\right) = 79.28 \text{ in}$$

$$y_1 = H_w - A = 144 \text{ in} - 79.28 \text{ in} = 64.72 \text{ in}$$

$$d_{LT} > \sqrt{\frac{6y_1R_{x,L}}{bF_{bx}C_DC_IC_V}} = \sqrt{\frac{6\left(64.72 \text{ in}\right)\left(7812.5 \text{ lb}\right)}{\left(6.75 \text{ in}\right)\left(2000 \text{ psi}\right)\left(1.15\right)\left(0.83\right)\left(0.95\right)}}$$

$$d_{LT} > 15.74 \text{ in}$$

The trial depth should be a minimum of 5% larger than calculated based on flexure alone, to accommodate the interaction of compression and bending stresses. Additionally, it is recommended that the upper and lower tangent point depths be within approximately 10% of each other. To satisfy both objectives, a trial depth of 19 in. will be chosen.

Estimating the required depth at the base

The minimum depth at the base will be estimated based on the horizontal shear reaction and also determined based on the estimated tangent point depth and the amount of taper chosen.

$$d_b' > \frac{3R_{x,L}}{2bF_{vx}C_D} = \frac{3\left(7812.5 \text{ lb}\right)}{2\left(6.75 \text{ in}\right)\left(215 \text{ psi}\right)\left(1.15\right)} = 7.022 \text{ in}$$

$$d_b' > d_{LT} - y_1 \tan\alpha_{leg} = 19 \text{ in} - \left(64.7 \text{ in}\right)\tan\left(4^\circ\right) = 14.5 \text{ in}$$

A trial depth of 14.5 inches will be chosen for the base.

Results:

$b = 6.75$ in
$H_{w,L} = H_{w,R} = 144 \text{ in} = 12 \text{ ft}$
$H_c = 288 \text{ in} = 24 \text{ ft}$
$d_{b,L}' = d_{b,R}' = 14.5 \text{ in}$
$d_c' = 11.0 \text{ in}$
$R_L = R_R = 126 \text{ in} = 10.5 \text{ ft}$
$\alpha_{leg,L} = \alpha_{leg,R} = 4^\circ$
$\alpha_{arm,L} = \alpha_{arm,R} = 2.5^\circ$

A drawing of the trial arch is shown in Figure E2.5. The appearance is determined to be acceptable. The preliminary design is complete.

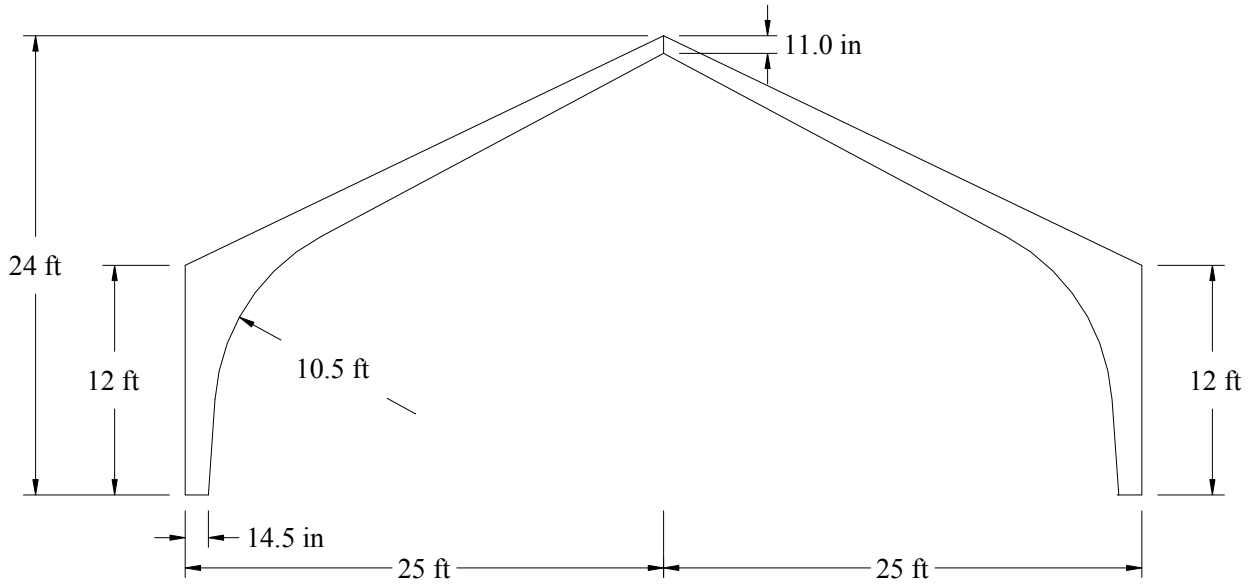

Figure E2.5. *Trial arch with α_{arm} = 2.5° and α_{leg} = 4°.*

Chapter 3
Arch Design Using Structural Analysis Software

The complexity of Tudor arch geometry and loading makes analysis and design cumbersome without the use of a spreadsheet or structural analysis software. Chapter 4 presents the formulas necessary to create a spreadsheet for the analysis of Tudor arches. This chapter presents procedures for designing a Tudor arch using structural design software, including assumptions that can be made to reasonably approximate the shape of arches as a series of linear elements.

Nomenclature

a	coefficient for calculation of effective column depth
A_L	distance from the haunch to the approximate tangent points on the left arch half
A_R	distance from the haunch to the approximate tangent points on the right arch half
b	arch width
C_c	curvature factor
C_D	load duration factor
C_I	stress interaction factor for tapered members
C_L	beam stability factor
C_M	wet-service factor
C_P	column stability factor
C_t	temperature factor
C_V	volume factor
d	section depth
d_{LD}	depth of section through lower discontinuity
d_{UD}	depth of section through upper discontinuity
$d_{\min}$	depth of smaller end of tapered column
$d_{\max}$	depth of larger end of tapered column
d_P	effective depth for tapered column buckling calculations
E_x	reference modulus of elasticity
E'_x	adjusted modulus of elasticity
f_{bx}	bending stress due to applied loads
F_{bx}	reference design stress in bending
F'_{bx}	adjusted design stress in bending
F^*_{bx}	reference design stress in bending adjusted by all applicable factors except C_L
F^{**}_{bx}	reference design stress in bending adjusted by all applicable factors except C_V
f_c	compression stress parallel-to-grain due to applied loads
F_c	reference design stress in compression parallel-to-grain
F'_c	adjusted design stress in compression parallel-to-grain

F_{cE} Euler buckling stress

f_r radial stress due to applied loads

F'_r adjusted radial design stress, either tension or compression

F_{rc} reference design stress in radial compression

F'_{rc} adjusted design stress in radial compression

F_{rt} reference design stress in radial tension

F'_{rt} adjusted design stress in radial tension

f_t tension stress parallel-to-grain due to applied loads

F_t reference design stress in tension parallel-to-grain

F'_t adjusted design stress in tension parallel-to-grain

F_{vx} reference design stress in shear

F'_{vx} adjusted design stress in shear

H_c height of arch at peak

$H_{w,L}$ height of wall for left arch half

$H_{w,R}$ height of wall for right arch half

K_r radial stress shape factor

$K_{r,h}$ radial stress shape factor at the haunch

$K_{r,LD}$ radial stress shape factor at the lower discontinuity

$K_{r,UD}$ radial stress shape factor at the upper discontinuity

K_θ bending stress shape factor

$K_{\theta,h}$ bending stress shape factor at the haunch

$K_{\theta,LD}$ bending stress shape factor at the lower discontinuity

$K_{\theta,UD}$ bending stress shape factor at the upper discontinuity

$\ell_{e,arm,L}$ effective length for column buckling calculations for left arch arm

$\ell_{e,arm,R}$ effective length for column buckling calculations for right arch arm

$\ell_{e,leg,L}$ effective length for column buckling calculations for left arch leg

$\ell_{e,leg,R}$ effective length for column buckling calculations for right arch leg

L_L span of left arch half

L_R span of right arch half

M bending moment on a section

P_{cx} horizontal point load applied at crown of arch

P_{cy} vertical point load applied at crown of arch

R_L radius of curvature for left arch half

R_m radius of curvature measured to the mid-depth of arch

$R_{m,LD}$ radius of curvature measured to the mid-depth of arch at lower discontinuity

$R_{m,UD}$ radius of curvature measured to the mid-depth of arch at the upper discontinuity

R_R radius of curvature for right arch half

$R_{x,L}$ horizontal reaction force at left base

$R_{x,R}$ horizontal reaction force at right base

$R_{y,L}$ vertical reaction force at left base

$R_{y,R}$ vertical reaction force at right base

V shear force on section

$x_{2,L}$ horizontally projected distance from haunch to approximate upper tangent point for left arch half

$x_{2,R}$ horizontally projected distance from haunch to approximate upper tangent point for right arch half

$y_{1,L}$ vertical distance from base to approximate lower tangent point for left arch half

$y_{1,R}$ vertical distance from base to approximate lower tangent point for right arch half

$y_{2,L}$ vertically projected distance from base to approximate upper tangent point for left arch half

$y_{2,R}$ vertically projected distance from base to approximate upper tangent point for right arch half

β_{LD} angle between horizontal line and line from center of curvature through lower discontinuity

β_{UD} angle between horizontal line and line from center of curvature through lower discontinuity

ϕ roof slope

ϕ_L roof slope on left arch half

ϕ_R roof slope on right arch half

θ included angle between arch leg and arm

θ_L included angle between leg and arm of left arch half

θ_R included angle between leg and arm of right arch half

$\omega_{rx,L}$ horizontal distributed load on roof arm of left arch half

$\omega_{rx,R}$ horizontal distributed load on roof arm of right arch half

$\omega_{ry,L}$ vertical distributed load on roof arm of left arch half

$\omega_{ry,R}$ vertical distributed load on roof arm of right arch half

$\omega_{wx,L}$ horizontal distributed load on wall leg of left arch half

$\omega_{wx,R}$ horizontal distributed load on wall leg of right arch half

$\omega_{wy,L}$ vertical distributed load on wall leg of left arch half

$\omega_{wy,R}$ vertical distributed load on wall leg of right arch half

Procedure

1. *Determine applicable loads and load combinations.* Roof and wall loads can typically be assumed to be uniform if decking is applied directly to the arch (or if purlins are closely spaced) or they may be concentrated at purlin points. Appropriate loads and load combinations can be obtained from the applicable building code or from the building official having jurisdiction. **Figure 3.1** illustrates a general loading for consideration.

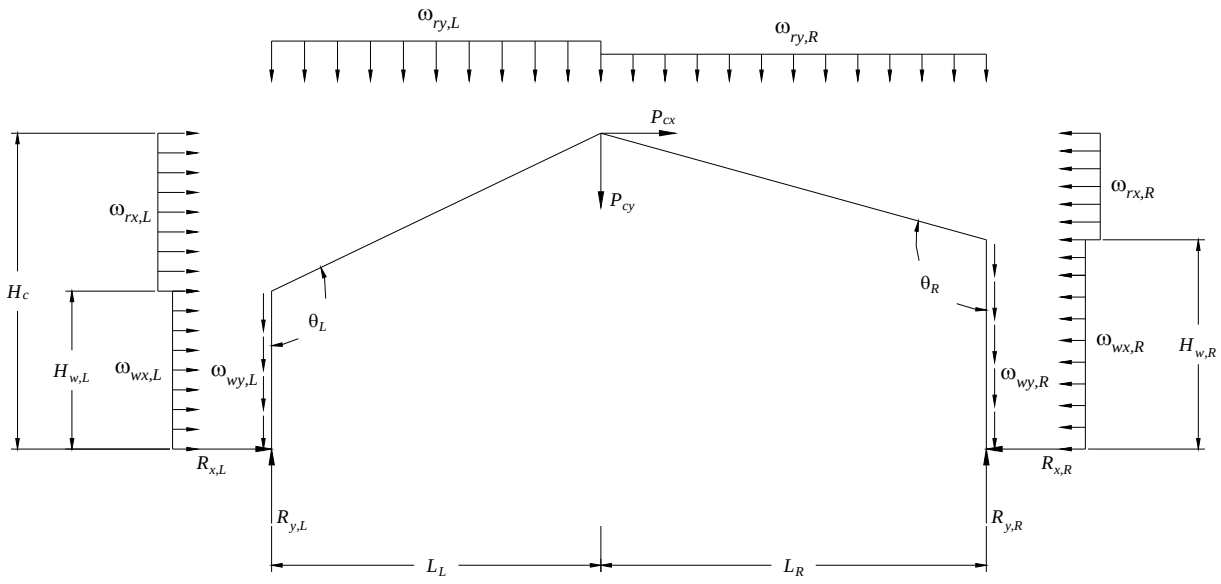

Figure 3.1. *Arch loading diagram.*

2. *Model the arch as linear elements* by connecting the outside faces of each arch half with a circular arc having a radius equal to the radius used for the inside face of the arch. Equations 3-1 through 3-8 can be used to locate the tangent points as shown in **Figure 3.2**.

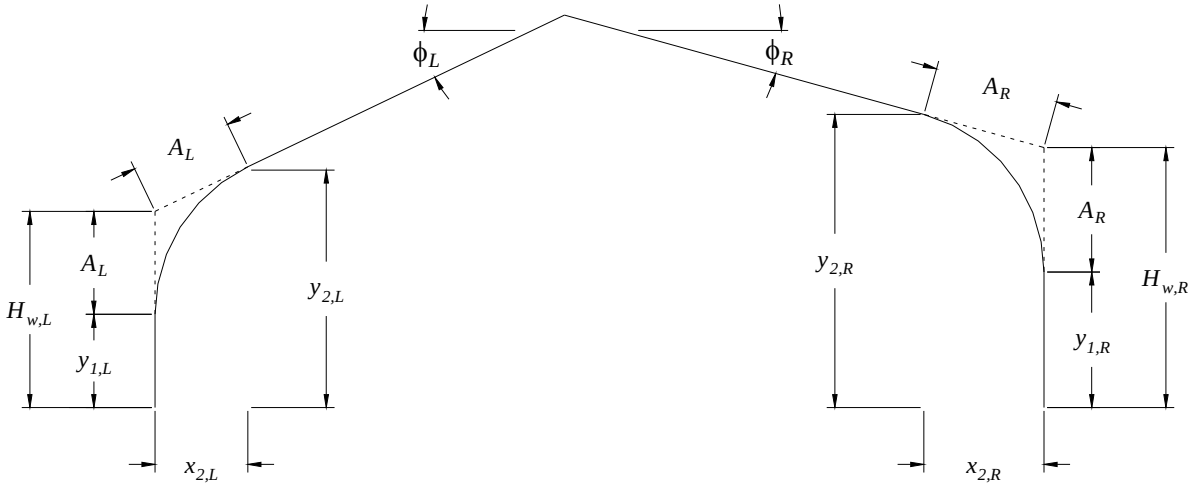

Figure 3.2. *Simplified arch model with locations of tangent points.*

$$A_L = R_L \tan\left(\frac{90-\phi_L}{2}\right) \quad [3\text{-}1]$$

$$x_{2,L} = A_L \cos(\phi_L) \quad [3\text{-}2]$$

$$y_{2,L} = H_{w,L} + A_L \sin(\phi_L) \quad [3\text{-}3]$$

$$y_{1,L} = H_{w,L} - A_L \quad [3\text{-}4]$$

$$A_R = R_R \tan\left(\frac{90-\phi_R}{2}\right) \quad [3\text{-}5]$$

$$x_{2,R} = A_R \cos(\phi_R) \quad [3\text{-}6]$$

$$y_{2,R} = H_{w,R} + A_R \sin(\phi_R) \quad [3\text{-}7]$$

$$y_{1,R} = H_{w,R} - A_R \quad [3\text{-}8]$$

3. *Divide the arch into segments for analysis.* Each arch leg, arm, and curved portion should be broken into multiple segments.

4. *Determine the forces and moments on each segment.* Each applicable load combination should be used in the calculation of forces and moments.

5. *Determine adjusted design values for each segment.* Estimate geometry-dependent adjustment factors, such as C_P, C_L, C_V, and C_I. For tapered sections outside of the tangent points, where high-grade material on the face is removed, exposing lower grades toward the core, a reduction in the reference flexural design value is appropriate (Appendix A).

$$F'_{bx} = F_{bx} C_D C_M C_t \left(C_L \text{ or } C_V\right) C_I C_c \quad [3\text{-}9]$$

$$F'_{vx} = F_{vx} C_D C_M C_t \quad [3\text{-}10]$$

$$F'_c = F_c C_D C_M C_t C_P \quad [3\text{-}11]$$

$$F'_t = F_t C_D C_M C_t \quad [3\text{-}12]$$

$$F'_{rt} = F_{rt} C_D C_M C_t \quad [3\text{-}13]$$

$$F'_{rc} = F_{rc} C_D C_M C_t \quad [3\text{-}14]$$

$$E'_x = E_x C_M C_t \quad [3\text{-}15]$$

6. *Establish a trial geometry.* Calculate the required depths at the arch bases and crown using shear stresses and any connection requirements. Calculate the required depths at the tangent points based on flexural requirements. Establish a trial geometry that satisfies these depth requirements, keeping in mind that the interaction equations for bending and axial loads must also be satisfied. The angle of taper on the arch legs should generally not exceed 5° and the angle of taper on arch arms should generally not exceed 3° (steeper tapers can be used if they are properly accounted for in design).

7. *Calculate geometry dependent adjustment factors.* The calculated factors should be compared to the estimated factors, and the geometry should be adjusted as necessary.

   The straight arm and leg portions should be evaluated for in plane buckling as tapered columns, modeling the large end as fixed and the small end as pinned for the arch legs, and modeling both ends as pinned for the arch arms (assumes that the inflection point is near the upper tangent point).

   Representative depths, d_P, for the column stability calculations can be calculated using the following equation (NDS 3.7.2).

$$d_P = d_{\min} + \left(d_{\max} - d_{\min}\right)\left[a - 0.15\left(1 - \frac{d_{\min}}{d_{\max}}\right)\right] \qquad [3\text{-}16]$$

   where: a = 0.70 for the arch leg
   = 0.50 for the arch arm

   Effective lengths for the column stability calculations for in-plane buckling can be estimated as:

$$\ell_{e,leg,L} = 0.7 y_{1,L} \qquad [3\text{-}17]$$

$$\ell_{e,arm,L} = \frac{L_L - x_{2,L}}{\cos\phi_L} \qquad [3\text{-}18]$$

$$\ell_{e,leg,R} = 0.7 y_{1,R} \qquad [3\text{-}19]$$

$$\ell_{e,arm,R} = \frac{L_R - x_{2,R}}{\cos\phi_R} \qquad [3\text{-}20]$$

8. *Evaluate combined stresses on each section.* Arches act as combined axial and flexural members, so stress interactions must be considered. The combined effect of axial compressive stresses and flexural stresses at each section must satisfy the following inequality:

$$\left[\frac{f_c}{F_c'}\right]^2 + \left[\frac{f_{bx}}{F_{bx}'\left[1 - \left(f_c / F_{cE}\right)\right]}\right] \le 1.0 \qquad [3\text{-}21]$$

   The following inequalities must be satisfied for sections stressed in combined bending and tension:

$$\frac{f_t}{F_t'} + \frac{f_{bx}}{F_{bx}^*} \le 1.0 \qquad [3\text{-}22]$$

$$\frac{f_{bx} - f_t}{F_{bx}^{**}} \leq 1.0 \qquad [3\text{-}23]$$

The abrupt change in section at the haunch causes a redistribution of flexure stresses that is accounted for by multiplying the bending stress, f_{bx}, calculated using the flexure formula by an empirical bending stress shape factor, K_θ. (To facilitate the use of structural analysis software, it may be more convenient to reduce the allowable stress by dividing by K_θ, rather than adjusting the applied flexure stress.) For the section through the haunch, this factor can be calculated using the following equation:

$$K_{\theta,h} = 1 + 2.7 \tan\left(\frac{180^\circ - \theta}{2}\right) \qquad [3\text{-}24]$$

Linear interpolation between a value of $K_{\theta,h}$ at the haunch and a value of $1/C_I$ at the tangent points can be used to estimate factors for the sections located between the section through the haunch and sections through the tangent points.

If a detached haunch is used, two points of discontinuity will be created on the back face of the arch. At the lower point of discontinuity, the bending stress shape factor, K_θ, can be calculated using Equation [3-25]. At the upper point of discontinuity K_θ can be calculated using Equation [3-26].

$$K_{\theta,LD} = 1 + 2.7 \tan\left(\frac{\beta_{LD}}{2}\right) \qquad [3\text{-}25]$$

$$K_{\theta,UD} = 1 + 2.7 \tan\left(\frac{90^\circ - \phi - \beta_{UD}}{2}\right) \qquad [3\text{-}26]$$

For sections between the points of discontinuity and the tangent points, K_θ can be determined by interpolation. Between the two points of discontinuity, interpolation can be used to calculate K_θ for intermediate sections or the larger value can be used.

Shear stresses on each section must satisfy the following inequality.

$$F'_{vx} \geq \frac{3V}{2bd} \qquad [3\text{-}27]$$

Evaluate radial stresses in the curved segment. Loads that result in an increase in the radius of curvature cause radial tension stresses in the curved segment(s). Loads causing a decreased radius of curvature result in radial compression stresses. These stresses must satisfy the following inequality:

$$F_r' \geq f_r = K_r \frac{6M}{bd^2} \qquad [3\text{-}28]$$

The radial stress shape factor at the haunch can be calculated as:

$$K_{r,h} = 0.29\left(\frac{d_c}{R_m}\right)^2 + 0.32\tan^{1.2}\left(\frac{180^\circ - \theta}{2}\right) = 0.29\left(\frac{d_c}{R_m}\right)^2 + 0.32\tan^{1.2}\left(\frac{90^\circ - \phi}{2}\right) \qquad [3\text{-}29]$$

Linear interpolation between a value of $K_{r,h}$ at the haunch and a value of 0 at the tangent points can be used to estimate factors for the sections between the section through the haunch and sections through the tangent points.

For arches with detached haunches, K_r can be calculated for the section through the lower point of discontinuity using Equation [3-30] and can be calculated for the section through the upper point of discontinuity using Equation [3-31]. Interpolation can be used to estimate factors for sections between the tangent points.

$$K_{r,LD} = 0.29\left(\frac{d_{LD}}{R_{m,LD}}\right)^2 + 0.32\tan^{1.2}\left(\frac{\beta_{LD}}{2}\right) \qquad [3\text{-}30]$$

$$K_{r,UD} = 0.29\left(\frac{d_{UD}}{R_{m,UD}}\right)^2 + 0.32\tan^{1.2}\left(\frac{90^\circ - \phi_t - \beta_{UD}}{2}\right) \qquad [3\text{-}31]$$

9. *Check deflections against any applicable limits.* Typically, horizontal deflections should be checked at the haunch and vertical deflections checked at the peak. Deflection in the arch arms should also be checked. In addition to deflections from applied loads, shrinkage of the laminations as the arch seasons in service will cause changes to the shape of the arch that should be considered. A calculation method to estimate displacements caused by changes in moisture content is presented in the next chapter.

   In lieu of specified deflection limits, the limits of **Table 1.1** are recommended for arches.

10. *Design and detail connections.* Shear plates are typically used to transfer the vertical reaction forces at the peak connection. Bolts with steel side plates are used to transfer tension forces between members at the peak. The base connection typically consists of a bearing seat to resist outward thrust, with a bolt to resist inward thrust and uplift.

11. *Iterate as necessary until a final design is established.*

Conclusion

This chapter presented a simplified arch geometry for use with structural analysis software. The results of the analysis using the simplified geometry are approximate, but will be generally close enough for design applications. Modeling with structural analysis software is particularly useful for the design of arches in three-dimensional structural systems. For simple three-hinged tudor arches, development of a spreadsheet to automate the procedures of the next chapter is recommended.

Chapter 4
Arch Design Using a Spreadsheet

The procedure presented in this chapter precisely defines the arch geometry. Sections through the arch are taken perpendicular to the laminations. The approximations and simplifying assumptions used in the previous chapter have not been applied. A designer who expects to design arches on a regular or repeated basis should consider developing a spreadsheet to apply this method.

Nomenclature

a_L	length of a line from left base to crown
a_R	length of a line from right base to crown
C_c	curvature factor
C_D	load duration factor
C_I	stress interaction factor for tapered members
C_L	beam stability factor
C_M	wet-service factor
C_P	column stability factor
C_t	temperature factor
C_V	volume factor
C_x	horizontal component of pin force at arch crown
C_y	vertical component of pin force at arch crown
D	dead load
b	arch width
d	depth of section of interest, measured perpendicular to the laminations
d_b	depth at arch base, measured perpendicular to the laminations
d'_b	depth at arch base, measured horizontally
$d_{b,L}$	depth at left arch base, measured perpendicular to the laminations
$d'_{b,L}$	depth at left arch base, measured horizontally
$d_{b,R}$	depth at right arch base, measured perpendicular to the laminations
$d'_{b,R}$	depth at right arch base, measured horizontally
d_c	depth of arch half at crown, measured perpendicular to the laminations
d'_c	depth at arch crown, measured vertically
$d_{c\,e}$	effective depth for notch effect calculations, measured perpendicular to the laminations
$d'_{c\,e}$	depth of member at peak after subtraction of effective notch, measured vertically
$d_{c,L}$	depth of left arch half at crown, measured perpendicular to the laminations

$d_{c,R}$ depth of right arch half at crown, measured perpendicular to the laminations

$d_{haunch,L}$ depth of section through haunch in left arch half

$d_{haunch,R}$ depth of section through haunch in right arch half

d_L depth of section of interest on left arch half

d_{LD} depth of section through the lower discontinuity

$d_{LT,L}$ depth of section through lower tangent point of left arch half

$d_{LT,R}$ depth of section through lower tangent point of right arch half

$d_{\max,L}$ maximum depth of left arch half when haunch is detached

$d_{\max,R}$ maximum depth of right arch half when haunch is detached

d_R depth of section of interest on right arch half

d_{UD} depth of section through the upper discontinuity

$d_{UT,L}$ depth of section through upper tangent point of left arch half

$d_{UT,R}$ depth of section through upper tangent point of right arch half

E_x reference modulus of elasticity

E'_x adjusted modulus of elasticity

$E_{x\min}$ modulus of elasticity for buckling about the x-axis

$E_{y\min}$ modulus of elasticity for buckling about the y-axis

f_{bx} bending stress due to applied loads

F_{bx} reference design stress in bending

F^{+}_{bx} reference design stress for positive bending (inside face of arch in tension)

F^{-}_{bx} reference design stress for negative bending (outside face of arch in tension)

F'_{bx} adjusted design stress in bending

F^{*}_{bx} reference design stress in bending adjusted by all applicable factors except C_L

F^{**}_{bx} reference design stress in bending adjusted by all applicable factors except C_V

f_c compression stress parallel-to-grain due to applied loads

F_c reference design stress in compression parallel-to-grain

F'_c adjusted design stress in compression parallel-to-grain

F_{cE} Euler buckling stress

f_r radial stress due to applied loads

F'_r adjusted radial design stress, either tension or compression

F_{rc} reference design stress in radial compression

F'_{rc}	adjusted design stress in radial compression
F_{rt}	reference design stress in radial tension
F'_{rt}	adjusted design stress in radial tension
f_t	tension stress parallel-to-grain due to applied loads
F_t	reference design stress in tension parallel-to-grain
F'_t	adjusted design stress in tension parallel-to-grain
F_{vx}	reference design stress in shear
F'_{vx}	adjusted design stress in shear
H_c	overall height of arch
$H_{w,L}$	wall height on left arch half
$H_{w,R}$	wall height on right arch half
I	moment of inertia of section of interest
K_r	radial stress shape factor
$K_{r,haunch}$	radial stress shape factor at haunch
$K_{r,LD}$	radial stress shape factor at the lower discontinuity
$K_{r,UD}$	radial stress shape factor at the upper discontinuity
K_θ	bending stress shape factor
$K_{\theta,arm}$	bending stress shape factor for curved section above haunch
$K_{\theta,haunch}$	bending stress shape factor at haunch
$K_{\theta,LD}$	bending stress shape factor at the lower discontinuity
$K_{\theta,leg}$	bending stress shape factor for curved section below haunch
$K_{\theta,UD}$	bending stress shape factor at the upper discontinuity
L_L	outside span of left arch half
L_R	outside span of right arch half
m_1	moment on section of interest due to virtual load P_1
m_2	moment on section of interest due to virtual load P_2
m_3	moment on section of interest due to virtual load P_3
m_4	moment on section of interest due to virtual load P_4
m_5	moment on section of interest due to virtual load P_5
m_6	moment on section of interest due to virtual load P_6
M	moment on section of interest caused by applied loads
$MC_{in-service}$	expected equilibrium moisture content of the arch
N	reference capacity for single shear plate in sloped end grain
n	number of shear plates connector units at peak connection
P	normal force on section of interest caused by applied loads
P	parallel-to-grain reference capacity for single shear plate

P_{cx} horizontal point load applied at crown of arch

P_{cy} vertical point load applied at crown of arch

P_1 virtual point load applied vertically at crown

P_2 virtual point load applied horizontally at crown

P_3 virtual point load applied horizontally at left haunch

P_4 virtual load applied horizontally at right haunch

P_5 virtual load applied perpendicular to right arm

P_6 virtual load applied perpendicular to left arm

Q_{90} perpendicular-to-grain reference capacity for single shear plate in end grain

R_L radius of curvature of left arch half

R_m radius of curvature measured to the mid-depth of arch

$R_{m,LD}$ radius of curvature measured to the mid-depth of arch at lower discontinuity

$R_{m,UD}$ radius of curvature measured to the mid-depth of arch at the upper discontinuity

R_R radius of curvature of right arch half

$R_{x,L}$ horizontal reaction force at left base

$R_{x,R}$ horizontal reaction force at right base

$R_{y,L}$ vertical reaction force at left base

$R_{y,R}$ vertical reaction force at right base

s length of segment for virtual work calculation

S snow load

V shear force on section of interest caused by applied loads

V_r' member shear capacity accounting for notch effect

W wind load

x x-coordinate chosen for analysis

x_c x-coordinate of crown

$x_{centerline,L}$ x-coordinate of center of section through $\left(x_{inner,L}, y_{inner,L}\right)$

$x_{centerline,R}$ x-coordinate of center of section through $\left(x_{inner,R}, y_{inner,R}\right)$

$x_{inner,haunch,L}$ x-coordinate of inner edge of a section through the left haunch

$x_{inner,haunch,R}$ x-coordinate of inner edge of a section through the right haunch

$x_{inner,L}$ x-coordinate at any point along inner face of left arch half

$x_{inner,R}$ x-coordinate at any point along inner face of right arch half

$x_{LT,L}$ x-coordinate of lower tangent point on left arch half

$x_{LT,R}$ x-coordinate of lower tangent point on right arch half

$x_{outer,L}$	x-coordinate of outer edge of section through $\left(x_{inner,L}, y_{inner,L}\right)$
$x_{outer,R}$	x-coordinate of outer edge of section through $\left(x_{inner,R}, y_{inner,R}\right)$
$x_{P_5,centerline}$	x-coordinate of load P_5 applied at the centerline of the member
$x_{P_6,centerline}$	x-coordinate of load P_6 applied at the centerline of the member
$x_{UD,L}$	x-coordinate of upper discontinuity on left arch half
$x_{UD,R}$	x-coordinate of upper discontinuity on right arch half
$x_{UT,L}$	x-coordinate of upper tangent point on left arch half
$x_{UT,R}$	x-coordinate of upper tangent point on right arch half
$x_{wall,L}$	x-coordinate of vertical load due to left wall
$x_{wall,R}$	x-coordinate of vertical load due to right wall
$x_{0,L}$	x-coordinate of the center of curvature of left arch half
$x_{0,R}$	x-coordinate of the center of curvature of right arch half
y_c	y-coordinate of crown
$y_{centerline,L}$	y-coordinate of center of section through $\left(x_{inner,L}, y_{inner,L}\right)$
$y_{centerline,R}$	y-coordinate of center of section through $\left(x_{inner,R}, y_{inner,R}\right)$
$y_{inner,haunch,L}$	y-coordinate of inner edge of a section through the left haunch
$y_{inner,haunch,R}$	y-coordinate of inner edge of a section through the right haunch
$y_{inner,L}$	y-coordinate at any point along inner face of left arch half
$y_{inner,R}$	y-coordinate at any point along inner face of right arch half
$y_{LT,L}$	y-coordinate of lower tangent point on left arch half
$y_{LT,R}$	x-coordinate of lower tangent point on right arch half
$y_{outer,L}$	y-coordinate of outer edge of section through $\left(x_{inner,L}, y_{inner,L}\right)$
$y_{outer,R}$	y-coordinate of outer edge of section through $\left(x_{inner,R}, y_{inner,R}\right)$
$y_{P_5,centerline}$	y-coordinate of load P_5 applied at the centerline of the member
$y_{P_6,centerline}$	y-coordinate of load P_6 applied at the centerline of the member
$y_{UT,L}$	y-coordinate of upper tangent point on left arch half
$y_{UT,R}$	y-coordinate of upper tangent point on right arch half
$y_{0,L}$	y-coordinate of the center of curvature of left arch half
$y_{0,R}$	y-coordinate of the center of curvature of right arch half
α_{arm}	angle of taper of arch arm
$\alpha_{arm,L}$	angle of taper of arm of left arch half
$\alpha_{arm,R}$	angle of taper of arm of right arch half
α_{leg}	angle of taper of arch leg

$\alpha_{leg,L}$ angle of taper of leg of left arch half

$\alpha_{leg,R}$ angle of taper of leg of right arch half

$\beta_{haunch,L}$ angle between horizontal line and line from center of curvature through haunch for left arch half

$\beta_{haunch,R}$ angle between horizontal line and line from center of curvature through haunch for right arch half

β_L angle between horizontal line and section of interest on left arch half

$\beta_{LD,L}$ angle between horizontal line and lower discontinuity on left arch half

$\beta_{LD,R}$ angle between horizontal line and lower discontinuity on right arch half

$\beta_{LT,L}$ angle between horizontal line and line from center of curvature through lower tangent point for left arch half

$\beta_{LT,R}$ angle between horizontal line and line from center of curvature through lower tangent point for right arch half

β_R angle between horizontal line and section of interest on right arch half

$\beta_{UD,L}$ angle between horizontal line and upper discontinuity on left arch half

$\beta_{UD,R}$ angle between horizontal line and upper discontinuity on right arch half

$\beta_{UT,L}$ angle between horizontal line and line from center of curvature through upper tangent point for left arch half

$\beta_{UT,R}$ angle between horizontal line and line from center of curvature through upper tangent point for right arch half

Δ_1, Δ_{cy} vertical displacement at peak

Δ_2, Δ_{cx} horizontal displacement at peak

$\Delta_3, \Delta_{x,L}$ horizontal displacement at left haunch

$\Delta_4, \Delta_{x,R}$ horizontal displacement at right haunch

$\Delta_5, \Delta_{arm,L}$ displacement of left arch arm

$\Delta_6, \Delta_{arm,R}$ displacement of right arch arm

$\Delta\eta$ change in angle η due to moisture content changes

$\Delta\eta_L$ change in angle η_L due to moisture content changes

$\Delta\eta_R$ change in angle η_R due to moisture content changes

Δx_c horizontal displacement of crown due to moisture content changes

$\Delta x_{haunch,L}$ horizontal displacement of haunch due to moisture content changes

$\Delta x_{haunch,R}$ horizontal displacement of haunch due to moisture content changes

Δy_c vertical displacement of crown due to moisture content changes

ϕ_t angle of roof slope

$\phi_{t,L}$ angle of roof slope of left arch half

$\phi_{t,R}$ angle of roof slope of right arch half

ϕ_b	angle of soffit slope
$\phi_{b,L}$	angle of soffit slope on left arch half
$\phi_{b,R}$	angle of soffit slope on right arch half
γ	angle between horizontal line and line from base to crown
γ_L	angle between horizontal line and line from left base to crown
γ_R	angle between horizontal line and line from right base to crown
η	angle between vertical line and arch roof
η_L	angle between vertical line and roof of left arch half
η_R	angle between vertical line and roof of right arch half
θ	included angle between the outer faces of the arch leg and arm
θ_L	included angle between the outer faces of the left arch leg and arm
θ_R	included angle between the outer faces of the right arch leg and arm
$\omega_{rx,L}$	horizontal distributed load on roof arm of left arch half
$\omega_{rx,R}$	horizontal distributed load on roof arm of right arch half
$\omega_{ry,L}$	vertical distributed load on roof arm of left arch half
$\omega_{ry,R}$	vertical distributed load on roof arm of right arch half
$\omega_{wx,L}$	horizontal distributed load on wall leg of left arch half
$\omega_{wx,R}$	horizontal distributed load on wall leg of right arch half
$\omega_{wy,L}$	vertical distributed load on wall leg of left arch half
$\omega_{wy,R}$	vertical distributed load on wall leg of right arch half
ξ_L	angle used in calculation of ψ_L
ξ_R	angle used in calculation of ψ_R
ψ	angle of rotation of arch leg due to moisture content changes
ψ_L	angle of rotation of left arch leg due to moisture content changes
ψ_R	angle of rotation of right arch leg due to moisture content changes

Procedure

The analysis procedure includes the following steps:

1. ***Determine all applicable loads and load combinations.*** Roof and wall loads can typically be assumed to be uniform if decking is applied directly to the arch (or if purlins are closely spaced) or they may be concentrated at purlin points. Appropriate loads and load combinations can be obtained from the applicable building code or from the building official having jurisdiction.

2. ***Define the arch geometry*** (**Figure 4.1**). The outside geometry (wall heights, peak height, outside span) of the arch is typically dictated by architectural constraints of the building.

To complete a trial geometry, the designer must choose a width, end depths, a radius, and angles of taper for the wall leg and roof arm.

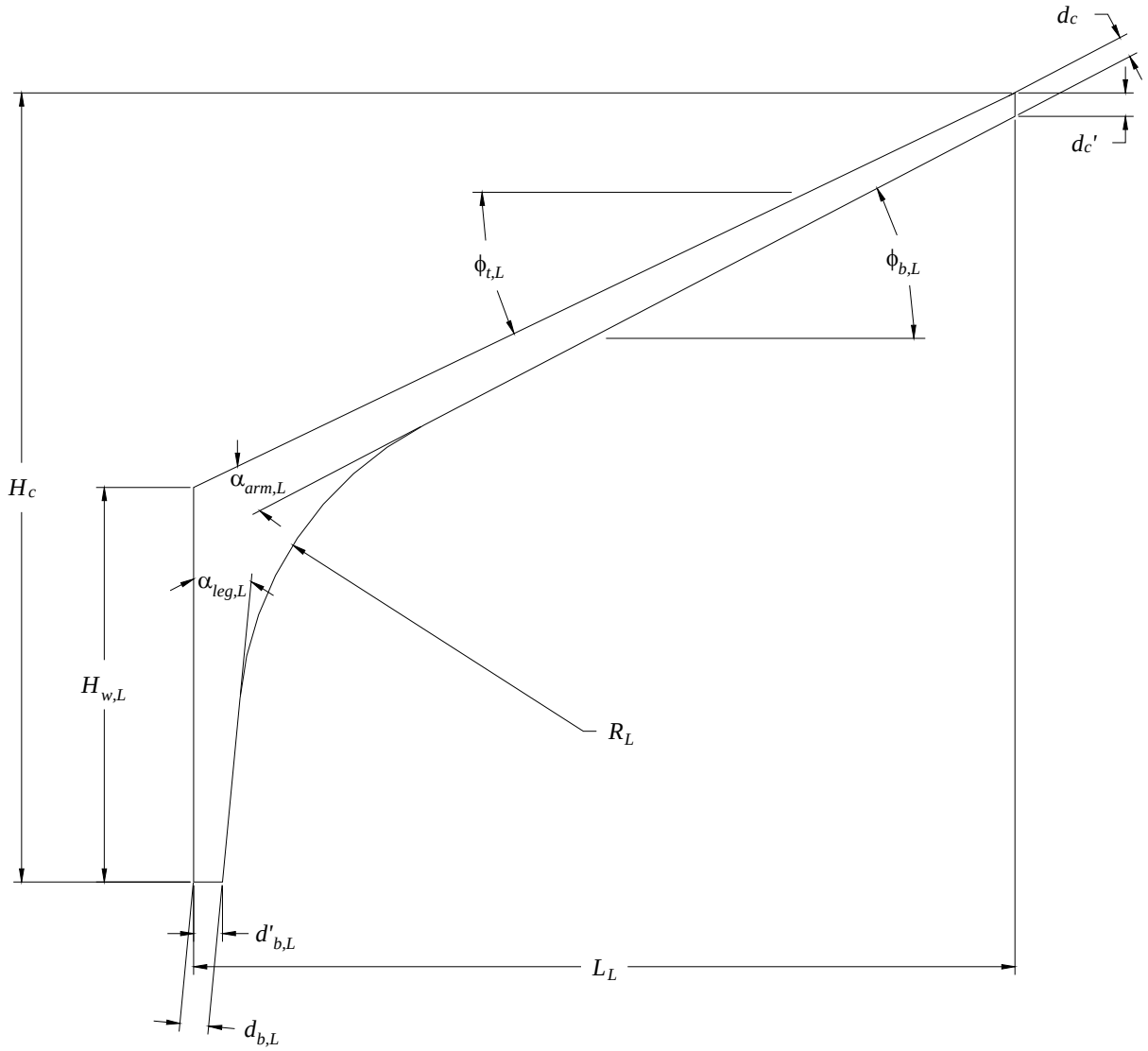

Figure 4.1. *Arch geometry. (Only left half shown for clarity.)*

2.1. *Choose the angles of taper for the wall legs, $\alpha_{leg,L}$ and , $\alpha_{leg,R}$, and the angles of taper for the roof arms, $\alpha_{arm,L}$ and $\alpha_{arm,R}$.* (Taper in the wall legs should generally not exceed 5° and taper in the roof arms should generally not exceed 3°, however, steeper tapers can be used if they are properly accounted for in design.)

2.2. *Calculate the angles of the roof slopes, $\phi_{t,L}$ and $\phi_{t,R}$, and the angles of the soffit slopes, $\phi_{b,L}$ and $\phi_{b,R}$.*

For the left arch half:

$$\phi_{t,L} = \arctan\left(\frac{H_c - H_{w,L}}{L_L}\right) \quad [4\text{-}1]$$

$$\phi_{b,L} = \phi_{t,L} + \alpha_{arm,L} \quad [4\text{-}2]$$

For the right arch half:

$$\phi_{t,R} = \arctan\left(\frac{H_c - H_{w,R}}{L_R}\right) \quad [4\text{-}3]$$

$$\phi_{b,R} = \phi_{t,R} + \alpha_{arm,R} \quad [4\text{-}4]$$

2.3. *Determine the end dimensions for each arch half.*

It is convenient to choose the end depths based on the depth of the cuts at the ends. However stresses should be checked based on the depths of sections taken perpendicular to the laminations. The following equations relate the depths measured perpendicular to the laminations to the depths of the end cuts.

The depth at the base, d_b, measured perpendicular to the laminations, is calculated as:

$$d_b = \frac{d_b'}{\cos\alpha_{leg}} \quad [4\text{-}5]$$

The depth at the crown, d_c, measured perpendicular to the laminations, is calculated as:

$$d_c = \frac{d_c' \cos\phi_t}{\cos\left(\alpha_{arm}\right)} \quad [4\text{-}6]$$

2.4. *Choose the radius of curvature for each arch half.* The inside radius for the curved portion of the arch half should be a minimum of 100 times the lamination thickness for Southern Pine and hardwood species and 125 times the lamination thickness for other softwood species to enable bending of the laminations to the required curvature. Using standard lamination thicknesses, minimum radii are:

7 ft 0 in. for Southern Pine and hardwood species
9 ft 4 in. for other softwood species

Tighter curves require the laminations to be planed to a thinner dimension and are significantly more expensive.

2.5. *Locate the centers of curvature.* Cartesian coordinates with the origin at a point on the floor under the arch crown are used to locate the centers of curvature (**Figure 4.2**). These coordinates are used in subsequent calculations. These values can be determined using the following equations.

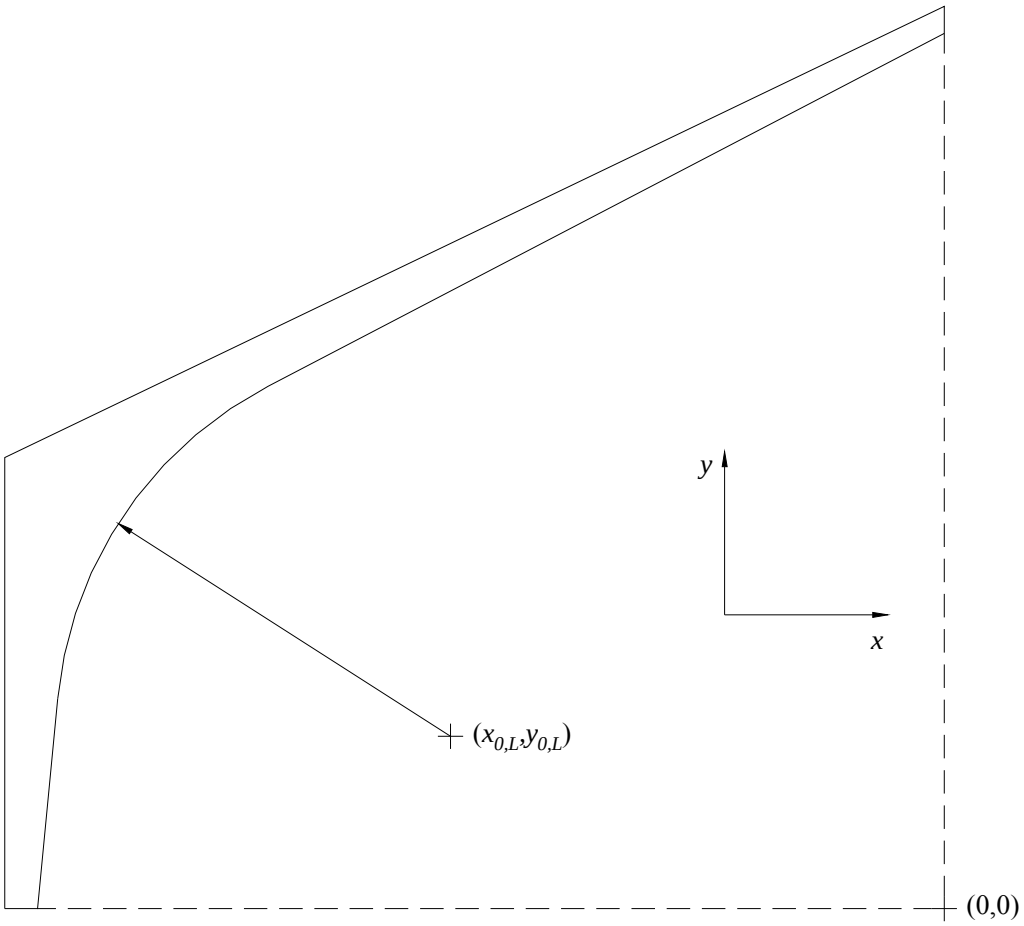

Figure 4.2. *Coordinate system and center of curvature for left arch half.*

For the left arch half:

$$x_{0,L} = \begin{cases} \dfrac{H_c - d_c' + R_L\left(\dfrac{1}{\sin\alpha_{leg,L}} - \dfrac{1}{\cos\phi_{b,L}}\right) - \left(L_L - d'_{b,L}\right)\cot\alpha_{leg,L}}{\cot\alpha_{leg,L} - \tan\phi_{b,L}} & \text{for: } \alpha_{leg,L} > 0 \\ -L_L + d'_{b,L} + R_L & \text{for: } \alpha_{leg,L} = 0 \end{cases} \quad [4\text{-}7]$$

$$y_{0,L} = \cot\alpha_{leg,L}\left(x_{0,L} + L_L - d'_{b,L}\right) - \frac{R_L}{\sin\alpha_{leg,L}}$$

or [4-8]

$$y_{0,L} = x_{0,L}\tan\phi_{b,L} + H_c - d_c' - \frac{R_L}{\cos\phi_{b,L}}$$

For the right arch half:

$$x_{0,R} = \begin{cases} \dfrac{H_c - d_c' + R_R\left(\dfrac{1}{\sin\alpha_{leg,R}} - \dfrac{1}{\cos\phi_{b,R}}\right) - \left(L_R - d'_{b,R}\right)\cot\alpha_{leg,R}}{\tan\phi_{b,R} - \cot\alpha_{leg,R}} & \text{for: } \alpha_{leg,R} > 0 \\ L_R - d'_{b,R} - R_R & \text{for: } \alpha_{leg,R} = 0 \end{cases} \quad [4\text{-}9]$$

$$y_{0,R} = \cot\alpha_{leg,R}\left(L_R - x_{0,R} - d'_{b,R}\right) - \frac{R_R}{\sin\alpha_{leg,R}}$$

or [4-10]

$$y_{0,R} = -x_{0,R}\tan\phi_{b,R} + H_c - d_c' - \frac{R_R}{\cos\phi_{b,R}}$$

3. ***Draw the arch to scale and verify that its appearance is satisfactory.*** Adjust the trial geometry until a satisfactory shape is obtained.

4. ***Divide the arch into segments, locate sections of interest, and calculate their section properties.*** Because of the complex geometry of the arch and the variability of loading conditions, deflections are typically estimated using the principle of virtual work. Additionally, the critical cross section for stress analysis will not be obvious. Therefore, several sections, taken perpendicular to the laminations, should be chosen for evaluation along the length of the arch. To reduce calculations, the same sections chosen for analysis of stresses can be used for virtual work calculations.

4.1. *Locate the sections through the haunches and determine their depths.* The sections through the haunches are located at angles of $\beta_{haunch,L}$ and $\beta_{haunch,R}$ on radial lines from the respective centers of curvature (**Figure 4.3**).

For the left arch half:

$$\beta_{haunch,L} = \arctan\left(\frac{H_{w,L} - y_{0,L}}{L_L + x_{0,L}}\right) \quad [4\text{-}11]$$

$$x_{inner,\,haunch,L} = x_{0,L} - R_L\cos\beta_{haunch,L} \quad [4\text{-}12]$$

$$y_{inner,\,haunch,L} = y_{0,L} + R_L\sin\beta_{haunch,L} \quad [4\text{-}13]$$

$$d_{haunch,L} = \frac{L_L + x_{0,L}}{\cos\beta_{haunch,L}} - R_L \quad [4\text{-}14]$$

For the right arch half:

$$\beta_{haunch,R} = \arctan\left(\frac{H_{w,R} - y_{0,R}}{L_R - x_{0,R}}\right) \quad [4\text{-}15]$$

$$x_{inner,\,haunch,R} = x_{0,R} + R_R \cos\beta_{haunch,R} \quad [4\text{-}16]$$

$$y_{inner,\,haunch,R} = y_{0,R} + R_R \sin\beta_{haunch,R} \quad [4\text{-}17]$$

$$d_{haunch,R} = \frac{L_R - x_{0,R}}{\cos\beta_{haunch,R}} - R_R \quad [4\text{-}18]$$

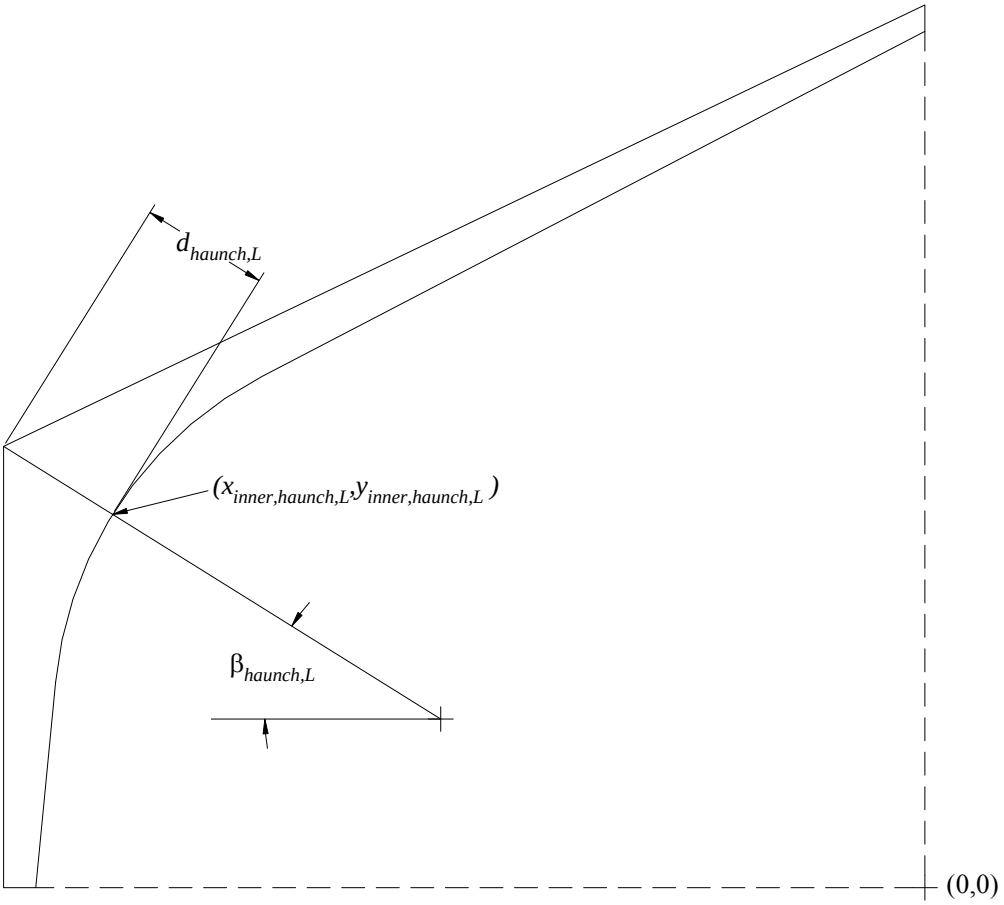

Figure 4.3. *Haunch location.*

4.2. *Locate the upper and lower tangent points for each arch half and determine the depths at those locations* (**Figure 4.4**). For stability considerations, the tangent point depths should not exceed six times the width if the arch is laterally braced by decking fastened directly to the arch or by girts or purlins placed at frequent intervals. When such lateral bracing is lacking, the depths at the tangent points should not exceed five times the width. If the depths at the tangent points are excessive, the geometry should be revised so that the depths are within the prescribed limits. Adjustments may need to be made to the arch width, angles of taper and/or the radius.

For the left arch half:

$$x_{LT,L} = x_{0,L} - R_L \cos\alpha_{leg,L} \quad [4\text{-}19]$$

$$y_{LT,L} = y_{0,L} + R_L \sin\alpha_{leg,L} \quad [4\text{-}20]$$

$$x_{UT,L} = x_{0,L} - R_L \sin\phi_{b,L} \quad [4\text{-}21]$$

$$y_{UT,L} = y_{0,L} + R_L \cos\phi_{b,L} \quad [4\text{-}22]$$

The angles between a horizontal line and the radial lines to the tangent points are:

$$\beta_{LT,L} = \alpha_{leg,L} \quad [4\text{-}23]$$

$$\beta_{UT,L} = 90^\circ - \phi_{b,L} \quad [4\text{-}24]$$

The tangent point depths are determined from the following equations:

$$d_{LT,L} = \frac{L_L + x_{LT,L}}{\cos\beta_{LT,L}} = \frac{L_L + x_{LT,L}}{\cos\alpha_{leg,L}} \quad [4\text{-}25]$$

$$d_{UT,L} = \frac{\left[\left(L_L + x_{UT,L}\right)\tan\phi_{t,L} + H_{w,L} - y_{UT,L}\right]\cos\phi_{t,L}}{\cos\left(90^\circ - \beta_{UT,L} - \phi_{t,L}\right)} \quad [4\text{-}26]$$

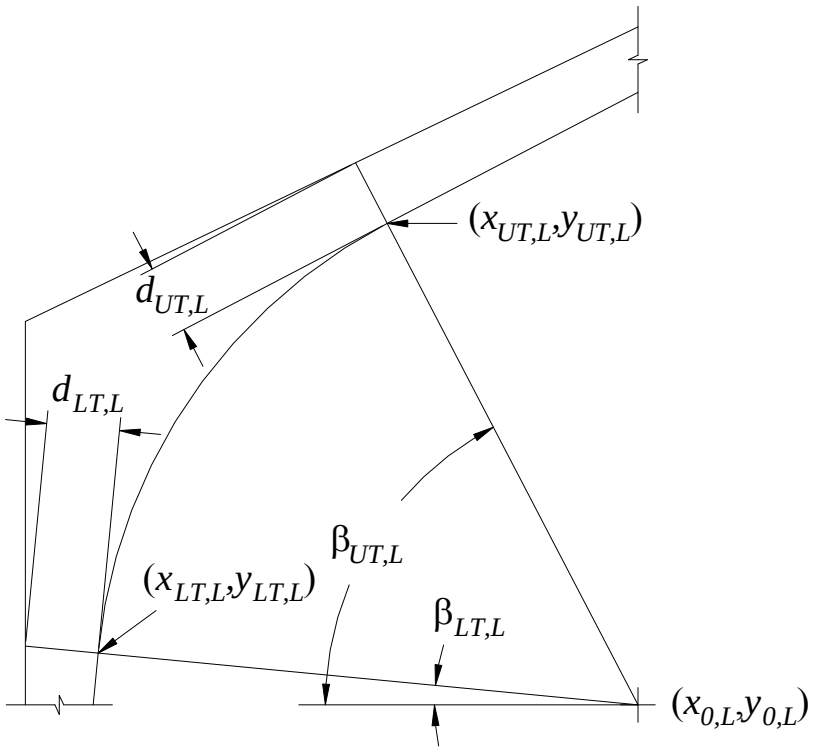

Figure 4.4. *Tangent point locations (only left arch half shown for clarity).*

For the right arch half:

$$x_{LT,R} = x_{0,R} + R_R \cos\alpha_{leg,R} \quad [4\text{-}27]$$

$$y_{LT,R} = y_{0,R} + R_R \sin\alpha_{leg,R} \quad [4\text{-}28]$$

$$x_{UT,R} = x_{0,R} + R_R \sin\phi_{b,R} \quad [4\text{-}29]$$

$$y_{UT,R} = y_{0,R} + R_R \cos\phi_{b,R} \quad [4\text{-}30]$$

The angles between a horizontal line and the radial lines to the tangent points are:

$$\beta_{LT,R} = \alpha_{leg,R} \quad [4\text{-}31]$$

$$\beta_{UT,R} = 90^\circ - \phi_{b,R} \quad [4\text{-}32]$$

The tangent point depths are determined from the following equations:

$$d_{LT,R} = \frac{L_R - x_{LT,R}}{\cos\beta_{LT,R}} = \frac{L_R - x_{LT,R}}{\cos\alpha_{leg,R}} \quad [4\text{-}33]$$

$$d_{UT,R} = \frac{\left[\left(L_R - x_{UT,R}\right)\tan\phi_{t,R} + H_{w,R} - y_{UT,R}\right]\cos\phi_{t,R}}{\cos\left(90^\circ - \beta_{UT,R} - \phi_{t,R}\right)} \quad [4\text{-}34]$$

4.3. *If arches will be manufactured with detached haunches, choose the maximum depths, $d_{max,L}$ and $d_{max,R}$, through the curved segments and locate the points of discontinuity on the back of each arch half. The depth through the curved segment must be chosen such that it is equal to or larger than both the upper and lower tangent point depths.*

For the left arch half:

The angle between a horizontal line and a radial line to the lower point of discontinuity is:

$$\beta_{LD,L} = \cos^{-1}\left(\frac{L_L + x_{0,L}}{R_L + d_{\max,L}}\right) \quad [4\text{-}35]$$

The x-coordinate of the upper point of discontinuity is:

$$x_{UD,L} = \frac{-\left[\tan\phi_{t,L}\left(H_c - y_{0,L}\right) - x_{0,L}\right]}{\left(\frac{1}{\cos^2\phi_{t,L}}\right)} - \frac{\sqrt{\left[\tan\phi_{t,L}\left(H_c - y_{0,L}\right) - x_{0,L}\right]^2 - \left[\frac{1}{\cos^2\phi_{t,L}}\right]\left[x_{0,L}^2 + \left(H_c - y_{0,L}\right)^2 - \left(R_L + d_{\max,L}\right)^2\right]}}{\left(\frac{1}{\cos^2\phi_{t,L}}\right)} \quad [4\text{-}36]$$

The angle between a horizontal line and a radial line to the upper point of discontinuity is:

$$\beta_{UD,L} = \cos^{-1}\left(\frac{x_{0,L} - x_{UD,L}}{R_L + d_{\max,L}}\right) \quad [4\text{-}37]$$

For the right arch half:

The angle between a horizontal line and a radial line to the lower point of discontinuity is:

$$\beta_{LD,R} = \cos^{-1}\left(\frac{L_R - x_{0,L}}{R_R + d_{\max,R}}\right) \quad [4\text{-}38]$$

The x-coordinate of the upper point of discontinuity is:

$$x_{UD,R} = \frac{\left[\tan\phi_{t,R}\left(H_c - y_{0,R}\right) + x_{0,R}\right]}{\left(\frac{1}{\cos^2\phi_{t,R}}\right)} + \frac{\sqrt{\left[\tan\phi_{t,R}\left(H_c - y_{0,R}\right) - x_{0,R}\right]^2 - \left[\frac{1}{\cos^2\phi_{t,R}}\right]\left[x_{0,R}^2 + \left(H_c - y_{0,R}\right)^2 - \left(R_R + d_{\max,R}\right)^2\right]}}{\left(\frac{1}{\cos^2\phi_{t,R}}\right)} \quad [4\text{-}39]$$

The angle between a horizontal line and a radial line to the upper point of discontinuity is:

$$\beta_{UD,R} = \cos^{-1}\left(\frac{x_{UD,R} - x_{0,R}}{R_R + d_{\max,R}}\right) \quad [4\text{-}40]$$

4.4. *Locate points along the inside face of the arch corresponding to sections of interest using the following equations:*

Left arch half, below lower tangent:

$$y_{inner,L} = \frac{\left(x + L_L - d'_{b,L}\right)}{\tan\alpha_{leg,L}} \quad \text{for: } \left(-L_L + d'_{b,L}\right) \le x \le x_{LT,L} \text{ and } \alpha_{leg,L} > 0 \quad [4\text{-}41]$$

Left arch half, in curved segment:

$$x_{inner,L} = x_{0,L} - R_L \cos\beta_L \quad \text{for: } \beta_{UT,L} \le \beta_L \le \alpha_{leg,L} \quad [4\text{-}42]$$

$$y_{inner,L} = y_{0,L} + R_L \sin\beta_L \quad \text{for: } \beta_{UT,L} \le \beta_L \le \alpha_{leg,L} \quad [4\text{-}43]$$

Left arch half, above upper tangent:

$$y_{inner,L} = x\tan\phi_{b,L} + H_c - d'_c \quad \text{for: } x_{UT,L} \le x \le 0 \quad [4\text{-}44]$$

Right arch half, above upper tangent:

$$y_{inner,R} = -x\tan\phi_{b,R} + H_c - d'_c \quad \text{for: } 0 \le x \le x_{UT,R} \quad [4\text{-}45]$$

Right arch half, in curved segment:

$$x_{inner,R} = x_{0,R} + R_R \cos\beta_R \quad \text{for: } \alpha_{leg,R} \le \beta_R \le \beta_{UT,R} \quad [4\text{-}46]$$

$$y_{inner,R} = y_{0,R} + R_R \sin\beta_R \quad \text{for: } \alpha_{leg,R} \le \beta_R \le \beta_{UT,R} \quad [4\text{-}47]$$

Right arch half, below lower tangent:

$$y_{inner,R} = \frac{\left(L_R - d'_{b,R} - x\right)}{\tan\alpha_{leg,R}} \quad \text{for: } x_{LT,R} \le x \le \left(L_R - d'_{b,R}\right) \text{ and } \alpha_{leg,R} > 0 \quad [4\text{-}48]$$

4.5. *With sections of interest in the arch identified and located, determine the depth at each section (taken perpendicular to the laminations) and determine the coordinates of the outer face and centerline of each section. For arches with detached haunches, maximum depth limits,* $d_{L,\max}$ and $d_{R,\max}$, *chosen by the designer, establish the depth through the curved segments.*

The **depth** (perpendicular to the laminations) in the **left arch half**, at any section **below the haunch** is given by:

$$d_L = \frac{L_L + x_{inner,L}}{\cos \beta_L} \le d_{\max,L} \qquad [4\text{-}49]$$

(for points below the lower tangent, $\beta_L = \alpha_{leg,L}$)

The **depth** (perpendicular to the laminations) in the **left arch half**, at any section **above the haunch** is given by:

$$d_L = \frac{\left[\left(L_L + x_{inner,L}\right)\tan \phi_{t,L} + H_{w,L} - y_{inner,L}\right]\cos \phi_{t,L}}{\cos\left(90^\circ - \beta_L - \phi_{t,L}\right)} \le d_{\max,L} \qquad [4\text{-}50]$$

(for points above upper tangent, $\beta_L = 90^\circ - \phi_{b,L}$)

The coordinates of the **outer face** of any section in the **left arch half** are given by:

$$x_{outer,L} = x_{inner,L} - d_L \cos \beta_L \qquad [4\text{-}51]$$

$$y_{outer,L} = y_{inner,L} + d_L \sin \beta_L \qquad [4\text{-}52]$$

The coordinates of the **centerline** of any section in the **left arch half** are given by:

$$x_{centerline,L} = x_{inner,L} - \frac{d_L \cos \beta_L}{2} \qquad [4\text{-}53]$$

$$y_{centerline,L} = y_{inner,L} + \frac{d_L \sin \beta_L}{2} \qquad [4\text{-}54]$$

The **depth** (perpendicular to the laminations) in the **right arch half**, at any section **above the haunch** is given by:

$$d_R = \frac{\left[\left(L_R - x_{inner,R}\right)\tan \phi_{t,R} + H_{w,R} - y_{inner,R}\right]\cos \phi_{t,R}}{\cos\left(90^\circ - \beta_R - \phi_{t,R}\right)} \le d_{\max,R} \qquad [4\text{-}55]$$

(for points above upper tangent, $\beta_R = 90^\circ - \phi_{b,R}$)

The **depth** (perpendicular to the laminations) in the **right arch half**, at any section **below the haunch** is given by:

$$d_R = \frac{L_R - x_{inner,R}}{\cos\beta_R} \le d_{\max,R} \qquad [4\text{-}56]$$

(for points below the lower tangent, $\beta_R = \alpha_{leg,R}$)

The coordinates of the **outer face** of any section in the **right arch half** are given by:

$$x_{outer,R} = x_{inner,R} + d_R \cos\beta_R \qquad [4\text{-}57]$$

$$y_{outer,R} = y_{inner,R} + d_R \sin\beta_R \qquad [4\text{-}58]$$

The coordinates of the **centerline** of any section in the **right arch half** are given by:

$$x_{centerline,R} = x_{inner,R} + \frac{d_R \cos\beta_R}{2} \qquad [4\text{-}59]$$

$$y_{centerline,R} = y_{inner,R} + \frac{d_R \sin\beta_R}{2} \qquad [4\text{-}60]$$

4.6. *Calculate the moment of inertia and section modulus for each section.*

5. ***Calculate the base reactions and forces at the peak connection.*** Distributed loads are assumed to act on the outer faces of the arch, and base reactions and peak connection forces act at the arch centerline. **Figures 4.5 and 4.6** show the free-body diagrams used for determination of the base reactions and peak connection forces. The resulting equations follow.

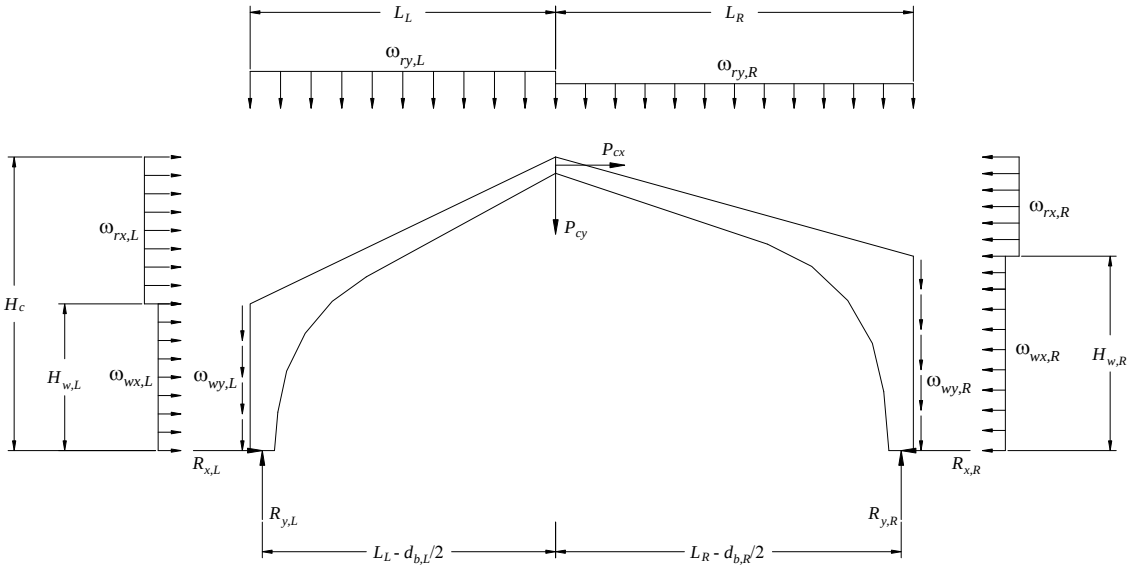

Figure 4.5. *Free body diagram of arch.*

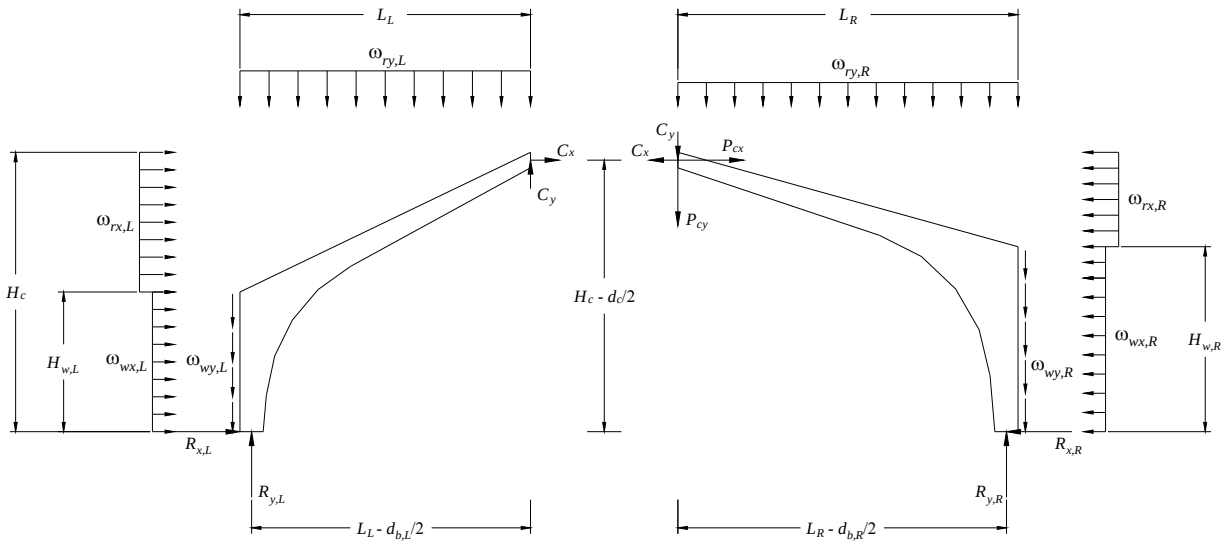

Figure 4.6. *Free body diagram of arch separated at crown connection.*

$$R_{y,L} = \frac{1}{\left(L_L - \frac{d'_{b,L}}{2} + L_R - \frac{d'_{b,R}}{2}\right)} \left[\begin{array}{l} \frac{\omega_{wx,R} H_{w,R}^2}{2} + \frac{\omega_{rx,R}\left(H_c^2 - H_{w,R}^2\right)}{2} + \frac{\omega_{ry,R} L_R \left(L_R - d'_{b,R}\right)}{2} \\ + \frac{\omega_{ry,L} L_L \left(L_L + 2L_R - d'_{b,R}\right)}{2} - \frac{\omega_{rx,L}\left(H_c^2 - H_{w,L}^2\right)}{2} - \frac{\omega_{wx,L} H_{w,L}^2}{2} \\ + P_{cy}\left(L_R - \frac{d'_{b,R}}{2}\right) - P_{cx}\left(H_c - \frac{d'_c}{2}\right) + \omega_{wy,L} H_{w,L}\left(L_R - \frac{d'_{b,R}}{2} - x_{wall,L}\right) \\ - \omega_{wy,R} H_{w,R}\left(x_{wall,R} - L_R + \frac{d'_{b,R}}{2}\right) \end{array} \right]$$

[4-61]

$$R_{y,R} = \frac{1}{\left(L_L - \frac{d'_{b,L}}{2} + L_R - \frac{d'_{b,R}}{2}\right)} \left[\begin{array}{l} \frac{\omega_{wx,L} H_{w,L}^2}{2} + \frac{\omega_{rx,L}\left(H_c^2 - H_{w,L}^2\right)}{2} + \frac{\omega_{ry,L} L_L \left(L_L - d'_{b,L}\right)}{2} \\ + \frac{\omega_{ry,R} L_R \left(L_R + 2L_L - d'_{b,L}\right)}{2} - \frac{\omega_{rx,R}\left(H_c^2 - H_{w,R}^2\right)}{2} - \frac{\omega_{wx,R} H_{w,R}^2}{2} \\ + P_{cy}\left(L_L - \frac{d'_{b,L}}{2}\right) + P_{cx}\left(H_c - \frac{d'_c}{2}\right) + \omega_{wy,R} H_{w,R}\left(L_L - \frac{d'_{b,L}}{2} + x_{wall,R}\right) \\ - \omega_{wy,L} H_{w,L}\left(-x_{wall,L} - L_L + \frac{d'_{b,L}}{2}\right) \end{array} \right]$$

[4-62]

$$R_{x,L} = \frac{1}{\left(H_c - \frac{d'_c}{2}\right)}\left[\begin{array}{l} R_{y,L}\left(L_L - \frac{d'_{b,L}}{2}\right) - \omega_{wy,L}H_{w,L}\left(-x_{wall,L}\right) - \omega_{wx,L}\left(H_cH_{w,L} - \frac{H_{w,L}d'_c}{2} - \frac{H^2_{w,L}}{2}\right) \\ -\frac{\omega_{rx,L}\left(H_c - H_{w,L}\right)\left(H_c - H_{w,L} - d'_c\right)}{2} - \frac{\omega_{ry,L}L^2_L}{2} \end{array}\right] \quad [4\text{-}63]$$

$$R_{x,R} = \frac{1}{\left(H_c - \frac{d'_c}{2}\right)}\left[\begin{array}{l} R_{y,R}\left(L_R - \frac{d'_{b,R}}{2}\right) - \omega_{wy,R}H_{w,R}\left(x_{wall,R}\right) - \omega_{wx,R}\left(H_cH_{w,R} - \frac{H_{w,R}d'_c}{2} - \frac{H^2_{w,R}}{2}\right) \\ -\frac{\omega_{rx,R}\left(H_c - H_{w,R}\right)\left(H_c - H_{w,R} - d'_c\right)}{2} - \frac{\omega_{ry,R}L^2_R}{2} \end{array}\right] \quad [4\text{-}64]$$

$$C_y = \omega_{wy,L}H_{w,L} + \omega_{ry,L}L_L - R_{y,L} \quad [4\text{-}65]$$

$$C_x = -\omega_{wx,L}H_{w,L} - \omega_{rx,L}\left(H_c - H_{w,L}\right) - R_{x,L} \quad [4\text{-}66]$$

6. ***Determine forces and moments and corresponding stresses on each section.*** Arches act as combined axial and flexural members. General free-body diagrams for both arch halves at sections both below and above the haunches are shown in **Figures 4.7 through 4.10**. The diagrams and corresponding equations are general for all cases of uniform loading with point loads applied at the crown. For other load cases, free-body diagrams and corresponding equations specific to the load case should be developed for the analysis.

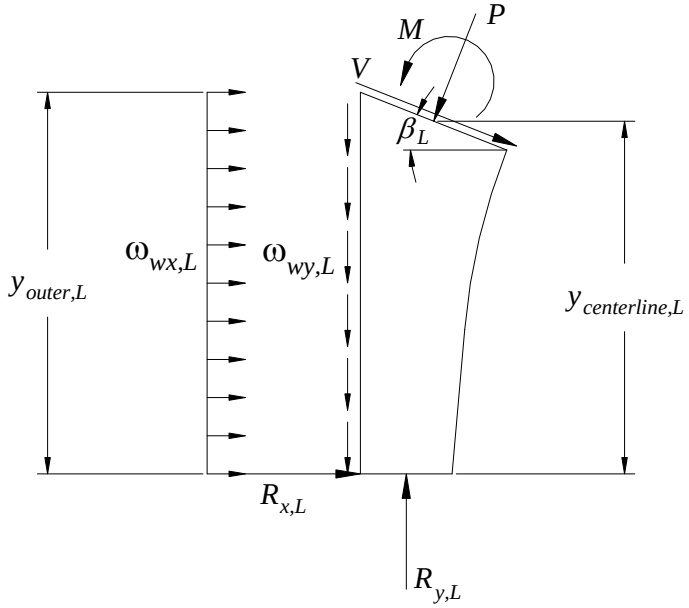

Figure 4.7. *Free body diagram of left arch half below the haunch.*

For the **left arch half** at any section **below the haunch**, the following equations were derived from the free-body diagram shown in **Figure 4.7**. For sections in the leg below the lower tangent point, the same equations apply with $\beta_L = \alpha_{leg,L}$.

$$M = R_{y,L}\left(x_{centerline,L} + L_L - \frac{d'_{b,L}}{2}\right) - R_{x,L}y_{centerline,L} - \omega_{wx,L}y_{outer,L}\left(y_{centerline,L} - \frac{y_{outer,L}}{2}\right) - \omega_{wy,L}y_{outer,L}\left(x_{centerline,L} - x_{wall,L}\right) \quad [4\text{-}67]$$

$$P = \sin\beta_L\left(R_{x,L} + \omega_{wx,L}y_{outer,L}\right) + \cos\beta_L\left(R_{y,L} - \omega_{wy,L}y_{outer,L}\right) \quad [4\text{-}68]$$

$$V = \frac{P\sin\beta_L - R_{x,L} - \omega_{wx,L}y_{outer,L}}{\cos\beta_L} \quad [4\text{-}69]$$

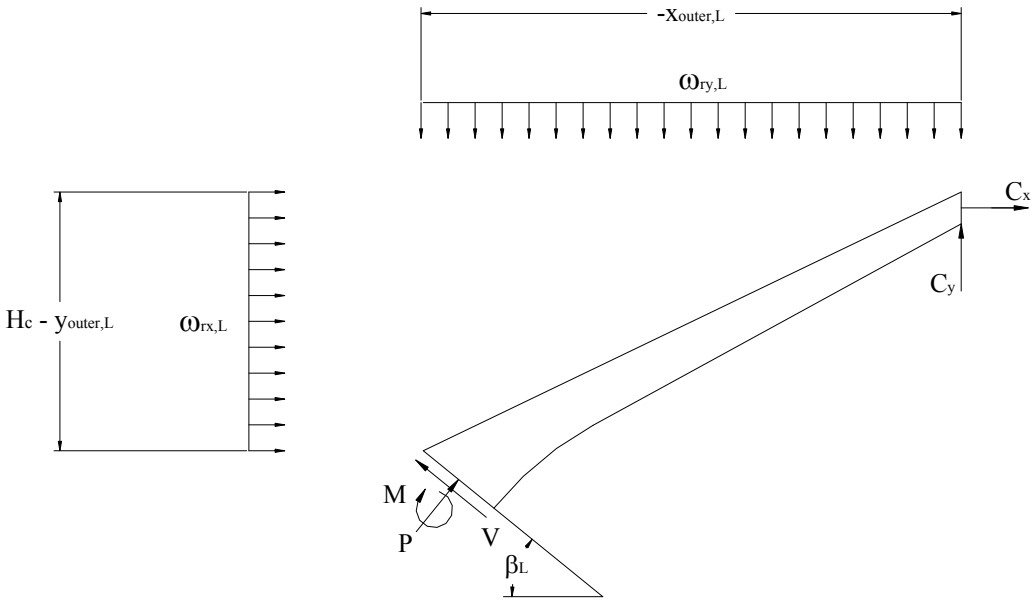

Figure 4.8. *Free body diagram of left arch half above the haunch.*

For the **left arch half** at any section **above the haunch**, the following equations were derived from the free-body diagram shown in **Figure 4.8**. For sections in the arm above the upper tangent point, the same equations apply with $\beta_L = 90^\circ - \phi_{b,L}$.

$$M = \omega_{ry,L}\left(x_{outer,L}\right)\left(\frac{x_{outer,L}}{2} - x_{centerline,L}\right) - C_y\left(x_{centerline,L}\right) - C_x\left(H_c - \frac{d_c'}{2} - y_{centerline,L}\right) - \omega_{rx,L}\left(H_c - y_{outer,L}\right)\left(\frac{H_c + y_{outer,L}}{2} - y_{centerline,L}\right) \quad [4\text{-}70]$$

$$P = \cos\beta\left[P_{y,L} - C_y - \omega_{ry,L}x_{outer,L}\right] - \sin\beta\left[P_{x,L} + C_x + \omega_{rx,L}\left(H_c - y_{outer,L}\right)\right] \quad [4\text{-}71]$$

$$V = \frac{-P\cos\beta_L - \omega_{ry,L}x_{outer,L} - C_y}{\sin\beta_L} \quad [4\text{-}72]$$

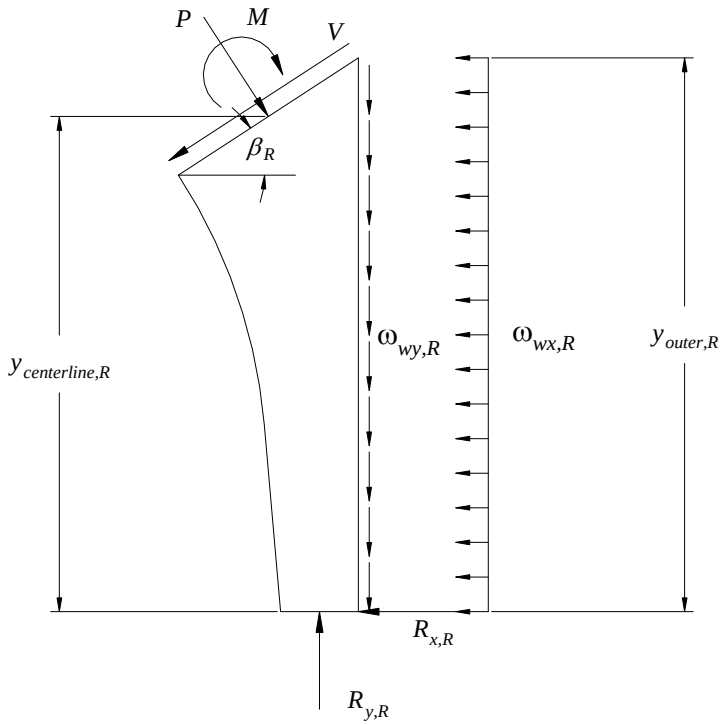

Figure 4.9. *Free body diagram of right arch half, below the haunch.*

For the **right arch half** at any section **below the haunch**, the following equations were derived from the free-body diagram shown in **Figure 4.9**. For sections in the leg below the lower tangent point, the same equations apply with $\beta_R = \alpha_{leg,R}$.

$$\begin{aligned} M = {} & R_{y,R}\left(L_R - \frac{d'_{b,R}}{2} - x_{centerline,R}\right) - R_{x,R}y_{centerline,R} \\ & - \omega_{wx,R}y_{outer,R}\left(y_{centerline,R} - \frac{y_{outer,R}}{2}\right) - \omega_{wy,R}y_{outer,R}\left(x_{wall,R} - x_{centerline,R}\right) \end{aligned} \quad [4\text{-}73]$$

$$P = \sin\beta_R\left(R_{x,R} + \omega_{wx,R}y_{outer,R}\right) + \cos\beta_R\left(R_{y,R} - \omega_{wy,R}y_{outer,R}\right) \quad [4\text{-}74]$$

$$V = \frac{P\sin\beta_R - R_{x,R} - \omega_{wx,R}y_{outer,R}}{\cos\beta_R} \quad [4\text{-}75]$$

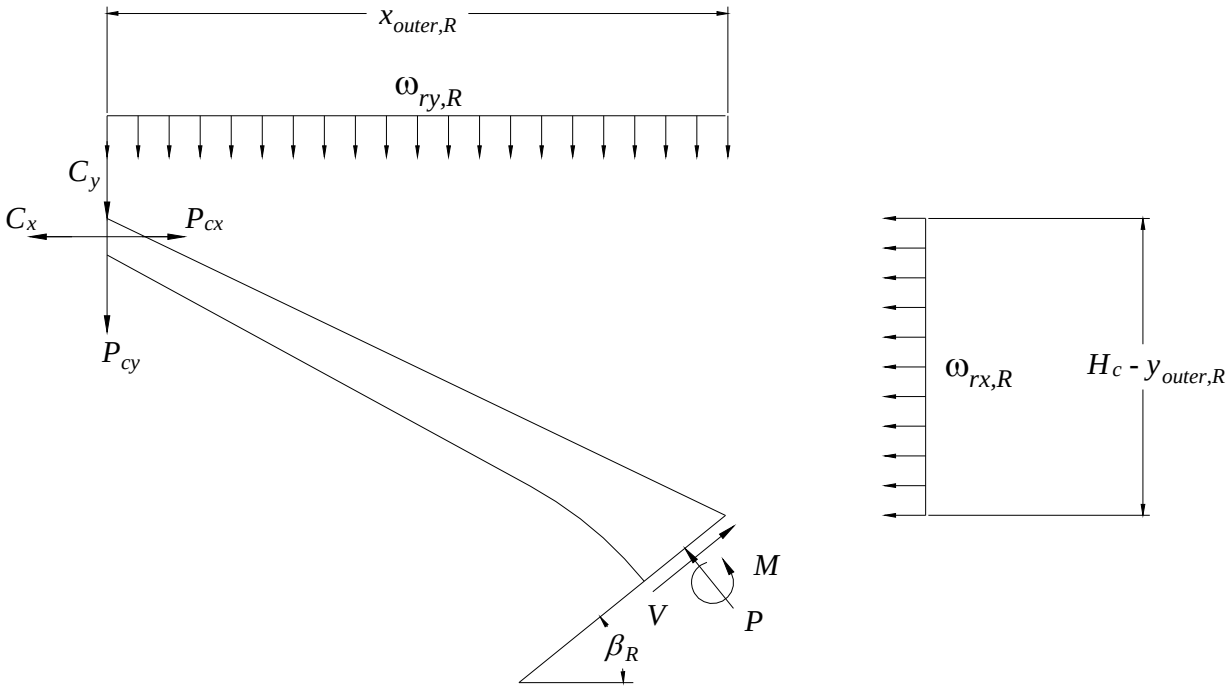

Figure 4.10. *Free body diagram for right arch half, above the haunch.*

For the **right arch half** at any section **above the haunch**, the following equations were derived from the free-body diagram shown in **Figure 4.10.** For sections in the arm above the upper tangent point, the same equations apply with $\beta_R = 90^\circ - \phi_{b,R}$.

$$M = P_{cx}\left(H_c - \frac{d_c'}{2} - y_{centerline,R}\right) - P_{cy}\left(x_{centerline,R}\right) - C_y\left(x_{centerline,R}\right)$$
$$- C_x\left(H_c - \frac{d_c'}{2} - y_{centerline,R}\right) - \omega_{ry,R}\left(x_{outer,R}\right)\left(x_{centerline,R} - \frac{x_{outer,R}}{2}\right) \qquad [4\text{-}76]$$
$$- \omega_{rx,R}\left(H_c - y_{outer,R}\right)\left(\frac{H_c + y_{outer,R}}{2} - y_{centerline,R}\right)$$

$$P = \cos\beta_R\left[P_{cy} + C_y + \omega_{ry,R}x_{outer,R}\right] - \sin\beta_R\left[P_{cx} - C_x - \omega_{rx,R}\left(H_c - y_{outer,R}\right)\right] \qquad [4\text{-}77]$$

$$V = \frac{P_{cy} - P\cos\beta_R + \omega_{ry,R}x_{outer,R} + C_y}{\sin\beta_R} \qquad [4\text{-}78]$$

7. ***Determine the adjusted design values (allowable stresses) for each section.*** Allowable stresses in compression, bending, and shear, must be determined for each of the sections

chosen for evaluation. Tabulated stresses should be adjusted by all appropriate adjustment factors. For tapered sections outside of the tangent points, where high-grade material on the face is removed, exposing lower grades toward the core, a reduction in the reference flexural stress is appropriate (Appendix A).

$$F'_{bx} = F_{bx} C_D C_M C_t \left(C_L \text{ or } C_V\right) C_I C_c \quad [4\text{-}79]$$

$$F'_{vx} = F_{vx} C_D C_M C_t \quad [4\text{-}80]$$

$$F'_c = F_c C_D C_M C_t C_P \quad [4\text{-}81]$$

$$F'_t = F_t C_D C_M C_t \quad [4\text{-}82]$$

$$F'_{rt} = F_{rt} C_D C_M C_t \quad [4\text{-}83]$$

$$F'_{rc} = F_{rc} C_D C_M C_t \quad [4\text{-}84]$$

$$E'_x = E_x C_M C_t \quad [4\text{-}85]$$

Out-of-plane buckling of arches should be considered between points of lateral support through application of the column stability factor, C_P. In-plane buckling of the straight segments of the arch should also be considered through application of the column stability factor, C_P. These segments should be analyzed as tapered columns modeling the large end as fixed and the small end as pinned for arch legs and modeling both ends as pinned for arch arms.

It is not necessary to evaluate in-plane buckling in the curved segment of Tudor arches, because secondary moments due to the eccentricity caused by buckling will generally be small compared to the bending moment due to the curved shape. Therefore, for in-plane buckling in the curved segment, the column stability factor is equal to unity ($C_P = 1.0$).

8. ***Calculate combined stresses on each section.*** Arches act as combined axial and flexural members, so stress interactions must be considered. The combined effect of axial compressive stresses and flexural stresses at each section must satisfy the inequality:

$$\left[\frac{f_c}{F_c'}\right]^2 + \left[\frac{f_{bx}}{F_{bx}'\left[1-\left(f_c/F_{cE}\right)\right]}\right] \le 1.0 \quad [4\text{-}86]$$

The following inequalities must be satisfied for sections stressed in combined bending and tension:

$$\frac{f_t}{F_t'} + \frac{f_{bx}}{F_{bx}^*} \le 1.0 \quad [4\text{-}87]$$

$$\frac{f_{bx} - f_t}{F_{bx}^{**}} \le 1.0 \quad [4\text{-}88]$$

The abrupt change in section at the haunch causes stress concentrations that can be accounted for by multiplying the bending stress calculated using the flexure formula by an empirical bending stress shape factor, K_θ. For the haunched section, this factor can be calculated using the following equation:

$$K_{\theta,haunch} = 1 + 2.7 \tan\left(\frac{180^\circ - \theta}{2}\right) = 1 + 2.7 \tan\left(\frac{90^\circ - \phi_t}{2}\right) \quad [4\text{-}89]$$

For sections between the haunch and the tangent points, it is permissible to estimate bending stress shape factors, $K_{\theta,leg}$ and $K_{\theta,arm}$, by interpolating between the value of $K_{\theta,haunch}$ at the haunch and a value of $1/C_I$ at the tangent point, using the angle, β, as the index value for interpolation:

$$K_{\theta,\,leg} = \left(\frac{\beta - \beta_{LT}}{\beta_{haunch} - \beta_{LT}}\right)\left(K_{\theta,haunch} - \frac{1}{C_I}\right) + \frac{1}{C_I} \qquad \text{for } \beta_{LT} \le \beta \le \beta_{haunch} \quad [4\text{-}90]$$

$$K_{\theta,\,arm} = \left(\frac{\beta_{UT} - \beta}{\beta_{UT} - \beta_{haunch}}\right)\left(K_{\theta,haunch} - \frac{1}{C_I}\right) + \frac{1}{C_I} \qquad \text{for } \beta_{haunch} \le \beta \le \beta_{UT} \quad [4\text{-}91]$$

If a detached haunch is used, two points of discontinuity will be created on the back face of the arch. At the lower point of discontinuity, the bending stress shape factor, K_θ, can be calculated using Equation [4-92]. At the upper point of discontinuity K_θ can be calculated using Equation [4-93].

$$K_{\theta,LD} = 1 + 2.7 \tan\left(\frac{\beta_{LD}}{2}\right) \quad [4\text{-}92]$$

$$K_{\theta,UD} = 1 + 2.7 \tan\left(\frac{90^\circ - \phi_t - \beta_{UD}}{2}\right) \quad [4\text{-}93]$$

For sections between the points of discontinuity and the tangent points, K_θ can be determined by interpolation using Equations [4-90] and [4-91], except with the appropriate angle through the point of discontinuity used in place of β_{haunch}. Interpolation between the two points of discontinuity can be used to calculate K_θ for intermediate sections or the larger value can be used.

9. *Evaluate radial stresses in the curved segment.* Loads that result in an increase in the radius of curvature cause radial tension stresses in the curved segment(s). Loads causing a decreased radius of curvature result in radial compression stresses. These stresses must satisfy the following inequality:

$$F_r' \ge f_r = K_r \frac{6M}{bd^2} \quad [4\text{-}94]$$

The radial stress shape factor at the haunch can be calculated as:

$$K_{r,haunch} = 0.29\left(\frac{d_c}{R_m}\right)^2 + 0.32\tan^{1.2}\left(\frac{180^\circ - \theta}{2}\right) \quad [4\text{-}95]$$

Linear interpolation between a value of $K_{r,haunch}$ at the haunch and a value of 0 at the tangent points can be used to estimate factors for the sections between the haunch and the tangent points.

For arches with detached haunches, K_r can be calculated for the section through the lower point of discontinuity using Equation [4-96] and can be calculated for the section through the upper point of discontinuity using Equation [4-97]. Interpolation can be used to estimate factors for the other sections between the tangent points.

$$K_{r,haunch} = 0.29\left(\frac{d_{LD}}{R_{m,LD}}\right)^2 + 0.32\tan^{1.2}\left(\frac{\beta_{LD}}{2}\right) \quad [4\text{-}96]$$

$$K_{r,UD} = 0.29\left(\frac{d_{UD}}{R_{m,UD}}\right)^2 + 0.32\tan^{1.2}\left(\frac{90^\circ - \phi_t - \beta_{UD}}{2}\right) \quad [4\text{-}97]$$

10. ***Use the principal of virtual work to calculate arch deflections.*** The deflections should be compared to any limits required for the design. In the absence of specified limits, the limits in **Table 1.1** are recommended for arch design.

10.1. *Calculate the reactions for a virtual load, P_1, applied downward at the peak.*

$$R_{y,L} = \frac{1}{\left(L_L - \frac{d'_{b,L}}{2} + L_R - \frac{d'_{b,R}}{2}\right)}\left[P_1\left(L_R - \frac{d'_{b,R}}{2}\right)\right] \quad [4\text{-}98]$$

$$R_{x,L} = \frac{1}{\left(H_c - \frac{d'_c}{2}\right)}\left[R_{y,L}\left(L_L - \frac{d'_{b,L}}{2}\right)\right] \quad [4\text{-}99]$$

$$R_{y,R} = \frac{1}{\left(L_L - \frac{d'_{b,L}}{2} + L_R - \frac{d'_{b,R}}{2}\right)}\left[P_1\left(L_L - \frac{d'_{b,L}}{2}\right)\right] \quad [4\text{-}100]$$

$$R_{x,R} = \frac{1}{\left(H_c - \frac{d'_c}{2}\right)}\left[R_{y,R}\left(L_R - \frac{d'_{b,R}}{2}\right)\right] \quad [4\text{-}101]$$

$$C_y = -R_{y,L} \quad [4\text{-}102]$$

$$C_x = -R_{x,L} \quad [4\text{-}103]$$

10.2. *Calculate the moment on selected sections caused by the virtual load, P_1.*

For the **left arch half** at any section **below the haunch**:

$$m_1 = R_{y,L}\left(x_{centerline,L} + L_L - \frac{d'_{b,L}}{2}\right) - R_{x,L}y_{centerline,L} \quad [4\text{-}104]$$

For the **left arch half** at any section **above the haunch**:

$$m_1 = -C_y x_{centerline,L} - C_x\left(H_c - \frac{d'_c}{2} - y_{centerline,L}\right) \quad [4\text{-}105]$$

For the **right arch half** at any section **below the haunch**:

$$m_1 = R_{y,R}\left(L_R - \frac{d'_{b,R}}{2} - x_{centerline,L}\right) - R_{x,R}y_{centerline,R} \quad [4\text{-}106]$$

For the **right arch half** at any section **above the haunch**:

$$m_1 = -C_y x_{centerline,R} - C_x\left(H_c - \frac{d'_c}{2} - y_{centerline,R}\right) - P_1\left(x_{centerline,R}\right) \quad [4\text{-}107]$$

10.3. *Calculate the vertical displacement at the peak for each load combination.*

$$\Delta_1 = \frac{1}{P_1}\sum\frac{Mm_1 s}{E'_x I} \quad [4\text{-}108]$$

10.4. *Calculate the reactions for a virtual load, P_2, applied rightward at the peak.*

$$R_{y,L} = \frac{1}{\left(L_L - \frac{d'_{b,L}}{2} + L_R - \frac{d'_{b,R}}{2}\right)}\left[-P_2\left(H_c - \frac{d'_c}{2}\right)\right] \quad [4\text{-}109]$$

$$R_{x,L} = \frac{1}{\left(H_c - \frac{d'_c}{2}\right)}\left[R_{y,L}\left(L_L - \frac{d'_{b,L}}{2}\right)\right] \quad [4\text{-}110]$$

$$R_{y,R} = \frac{1}{\left(L_L - \frac{d'_{b,L}}{2} + L_R - \frac{d'_{b,R}}{2}\right)}\left[P_2\left(H_c - \frac{d'_c}{2}\right)\right] \quad [4\text{-}111]$$

$$R_{x,R} = \frac{1}{\left(H_c - \frac{d'_c}{2}\right)}\left[R_{y,R}\left(L_R - \frac{d'_{b,R}}{2}\right)\right] \quad [4\text{-}112]$$

$$C_y = -R_{y,L} \quad [4\text{-}113]$$

$$C_x = -R_{x,L} \quad [4\text{-}114]$$

10.5. *Calculate the moment on selected sections caused by the virtual load, P_2.*

For the **left arch half** at any section **below the haunch**:

$$m_2 = R_{y,L}\left(x_{centerline,L} + L_L - \frac{d'_{b,L}}{2}\right) - R_{x,L}y_{centerline,L} \quad [4\text{-}115]$$

For the **left arch half** at any section **above the haunch**:

$$m_2 = -C_y x_{centerline,L} - C_x\left(H_c - \frac{d'_c}{2} - y_{centerline,L}\right) \quad [4\text{-}116]$$

For the **right arch half** at any section **below the haunch**:

$$m_2 = R_{y,R}\left(L_R - \frac{d'_{b,R}}{2} - x_{centerline,R}\right) - R_{x,R}y_{centerline,R} \quad [4\text{-}117]$$

For the **right arch half** at any section **above the haunch**:

$$m_2 = P_2\left(H_c - \frac{d'_c}{2} - y_{centerline,R}\right) - C_y x_{centerline,R} - C_x\left(H_c - \frac{d'_c}{2} - y_{centerline,R}\right) \quad [4\text{-}118]$$

10.6. *Calculate the horizontal displacement at the peak for each load combination.*

$$\Delta_2 = \frac{1}{P_2}\sum\frac{Mm_2 s}{E'_x I} \quad [4\text{-}119]$$

10.7. *Calculate the reactions for a virtual load, P_3, applied rightward at the haunch on the left arch half.*

$$R_{y,L} = \frac{-P_3 H_{w,L}}{\left(L_L - \frac{d'_{b,L}}{2} + L_R - \frac{d'_{b,R}}{2}\right)} \quad [4\text{-}120]$$

$$R_{x,L} = \frac{1}{\left(H_c - \frac{d'_c}{2}\right)}\left[R_{y,L}\left(L_L - \frac{d'_{b,L}}{2}\right) - P_3\left(H_c - \frac{d'_c}{2} - H_{w,L}\right)\right] \quad [4\text{-}121]$$

$$R_{y,R} = \frac{P_3 H_{w,L}}{\left(L_L - \frac{d'_{b,L}}{2} + L_R - \frac{d'_{b,R}}{2}\right)} \quad [4\text{-}122]$$

$$R_{x,R} = \frac{R_{y,R}\left(L_R - \frac{d'_{b,R}}{2}\right)}{\left(H_c - \frac{d'_c}{2}\right)} \quad [4\text{-}123]$$

$$C_y = R_{y,R} \quad [4\text{-}124]$$

$$C_x = -R_{x,R} \quad [4\text{-}125]$$

10.8. *Calculate the moment on selected sections caused by the virtual load, P_3.*

For the **left arch half** at any section **below the haunch**:

$$m_3 = R_{y,L}\left(x_{centerline,L} + L_L - \frac{d'_{b,L}}{2}\right) - R_{x,L} y_{centerline,L} \quad [4\text{-}126]$$

For the **left arch half** at any section **above the haunch**:

$$m_3 = C_y\left(-x_{centerline,L}\right) - C_x\left(H_c - \frac{d'_c}{2} - y_{centerline,L}\right) \quad [4\text{-}127]$$

For the **right arch half** at any section **below the haunch**:

$$m_3 = R_{y,R}\left(L_R - \frac{d'_{b,R}}{2} - x_{centerline,R}\right) - R_{x,R} y_{centerline,R} \quad [4\text{-}128]$$

For the **right arch half** at any section **above the haunch**:

$$m_3 = -C_y x_{centerline,R} - C_x\left(H_c - \frac{d'_c}{2} - y_{centerline,R}\right) \quad [4\text{-}129]$$

10.9. *Calculate the horizontal displacement at the left haunch for each load combination.*

$$\Delta_3 = \frac{1}{P_3}\sum \frac{M m_3 s}{E'_x I} \quad [4\text{-}130]$$

10.10. *Calculate the reactions for a virtual load, P_4, applied leftward at the haunch on the right arch half.*

$$R_{y,L} = \frac{P_4 H_{w,R}}{\left(L_L - \frac{d'_{b,L}}{2} + L_R - \frac{d'_{b,R}}{2} \right)} \quad [4\text{-}131]$$

$$R_{x,L} = \frac{R_{y,L}\left(L_L - \frac{d'_{b,L}}{2} \right)}{\left(H_c - \frac{d'_c}{2} \right)} \quad [4\text{-}132]$$

$$R_{y,R} = \frac{-P_4 H_{w,R}}{\left(L_L - \frac{d'_{b,L}}{2} + L_R - \frac{d'_{b,R}}{2} \right)} \quad [4\text{-}133]$$

$$R_{x,R} = \frac{1}{\left(H_c - \frac{d'_c}{2} \right)} \left[R_{y,R}\left(L_R - \frac{d'_{b,R}}{2} \right) - P_4 \left(H_c - \frac{d'_c}{2} - H_{w,R} \right) \right] \quad [4\text{-}134]$$

$$C_y = -R_{y,L} \quad [4\text{-}135]$$

$$C_x = -R_{x,L} \quad [4\text{-}136]$$

10.11. *Calculate the moment on selected sections caused by the virtual load, P_4.*

For the **left arch half** at any section **below the haunch**:

$$m_4 = R_{y,L}\left(L_L - \frac{d'_{b,L}}{2} + x_{centerline,L} \right) - R_{x,L} y_{centerline,L} \quad [4\text{-}137]$$

For the **left arch half** at any section **above the haunch**:

$$m_4 = C_y \left(-x_{centerline,L} \right) - C_x \left(H_c - \frac{d'_c}{2} - y_{centerline,L} \right) \quad [4\text{-}138]$$

For the **right arch half** at any section **below the haunch**:

$$m_4 = R_{y,R}\left(L_R - \frac{d'_{b,R}}{2} - x_{centerline,R} \right) - R_{x,R} y_{centerline,R} \quad [4\text{-}139]$$

For the **right arch half** at any section **above the haunch**:

$$m_4 = -C_y \left(x_{centerline,R} \right) - C_x \left(H_c - \frac{d'_c}{2} - y_{centerline,R} \right) \quad [4\text{-}140]$$

10.12. *Calculate the horizontal displacement at the right haunch for each load combination.*

$$\Delta_4 = \frac{1}{P_4}\sum \frac{Mm_4 s}{E'_x I} \qquad [4\text{-}141]$$

10.13. *Calculate the reactions for a virtual load, P_5, applied perpendicular to the arch arm at a point located between 50-60% of the distance from the upper tangent to the peak on the left arch half. (This is an estimation of the location of maximum deflection.)*

$$R_{y,L} = \frac{P_5 \cos\phi_{b,L}\left(L_R - \frac{d'_{b,R}}{2} - x_{P_5,centerline}\right) - P_5 \sin\phi_{b,L}\left(y_{P_5,centerline}\right)}{L_L - \frac{d'_{b,L}}{2} + L_R - \frac{d'_{b,R}}{2}} \qquad [4\text{-}142]$$

$$R_{y,R} = \frac{P_5 \cos\phi_{b,L}\left(L_L - \frac{d'_{b,L}}{2} + x_{P_5,centerline}\right) + P_5 \sin\phi_{b,L}\left(y_{P_5,centerline}\right)}{L_L - \frac{d'_{b,L}}{2} + L_R - \frac{d'_{b,R}}{2}} \qquad [4\text{-}143]$$

$$C_y = R_{y,R} \qquad [4\text{-}144]$$

$$C_x = \frac{-R_{y,R}\left(L_R - \frac{d'_{b,R}}{2}\right)}{H_c - \frac{d'_c}{2}} \qquad [4\text{-}145]$$

$$R_{x,L} = -P_5 \sin\phi_{b,L} - C_x \qquad [4\text{-}146]$$

$$R_{x,R} = -C_x \qquad [4\text{-}147]$$

10.14. *Calculate the moment on selected sections in the left arch half, between the upper tangent point and the peak, caused by the virtual load, P_5.*

For sections below the load point:

$$m_5 = R_{y,L}\left(L_L - \frac{d'_{b,L}}{2} + x_{centerline,L}\right) - R_{x,L}\left(y_{centerline,L}\right) \qquad [4\text{-}148]$$

For sections above the load point:

$$m_5 = -C_x\left(H_c - \frac{d'_c}{2} - y_{centerline,L}\right) - C_y x_{centerline,L} \qquad [4\text{-}149]$$

10.15. *Calculate the deflection at the selected point (relative to a line between the upper tangent and peak) for each load combination. Include only segments between upper tangent and peak.*

$$\Delta_5 = \frac{1}{P_5}\sum \frac{Mm_5 s}{E'_x I} \qquad [4\text{-}150]$$

10.16. *Calculate the reactions for a virtual load, P_6, applied perpendicular to the arch arm at a point located between 50-60% of the distance from the upper tangent to the peak on the right arch half. (This is an estimation of the location of maximum deflection.)*

$$R_{y,L} = \frac{P_6 \cos\phi_{b,R}\left(L_R - \frac{d'_{b,R}}{2} - x_{P_6,centerline}\right) + P_6 \sin\phi_{b,R}\left(y_{P_6,centerline}\right)}{L_L - \frac{d'_{b,L}}{2} + L_R - \frac{d'_{b,R}}{2}} \qquad [4\text{-}151]$$

$$R_{y,R} = \frac{P_6 \cos\phi_{b,R}\left(L_L - \frac{d'_{b,L}}{2} + x_{P_6,centerline}\right) - P_6 \sin\phi_{b,R}\left(y_{P_6,centerline}\right)}{L_L - \frac{d'_{b,L}}{2} + L_R - \frac{d'_{b,R}}{2}} \qquad [4\text{-}152]$$

$$C_y = -R_{y,L} = R_{y,R} - P_6 \cos\phi_{b,R} \qquad [4\text{-}153]$$

$$C_x = \frac{P_6 \cos\phi_{b,R}\left(x_{P_6,centerline}\right) - P_6 \sin\phi_{b,R}\left(y_{P_6,centerline}\right) - R_{y,R}\left(L_R - \frac{d'_{b,R}}{2}\right)}{H_c - \frac{d'_c}{2}} = \frac{-R_{y,L}\left(L_L - \frac{d'_{b,L}}{2}\right)}{H_c - \frac{d'_c}{2}} \qquad [4\text{-}154]$$

$$R_{x,L} = -C_x \qquad [4\text{-}155]$$

$$R_{x,R} = -P_6 \sin\phi_{b,R} - C_x \qquad [4\text{-}156]$$

10.17. *Calculate the moment on sections in the right arch half, between the upper tangent point and the peak, caused by the virtual load, P_6.*

For sections below the load point:

$$m_6 = R_{y,R}\left(L_R - \frac{d'_{b,R}}{2} - x_{centerline,R}\right) - R_{x,R}\left(y_{centerline,R}\right) \qquad [4\text{-}157]$$

For sections above the load point:

$$m_6 = -C_x\left(H_c - \frac{d'_c}{2} - y_{centerline,R}\right) - C_y\left(x_{centerline,R}\right) \qquad [4\text{-}158]$$

10.18. *Calculate the deflection at the selected point (relative to a line between the upper tangent and peak) for each load combination. Include only segments between upper tangent and peak.*

$$\Delta_6 = \frac{1}{P_6}\sum \frac{Mm_6 s}{E'_x I} \qquad [4\text{-}159]$$

11. ***Estimate deflections due to seasoning in service.*** The thickness of the laminations will change due to moisture content fluctuations in service. Typically, arches dry in service, resulting in shrinkage of the laminations. Shrinkage of the laminations results in the change in shape and displacement of the crown and haunches illustrated in Figures 4.11 and 4.12. As the lamination thickness becomes less, the angle η increases. The percentage change in angle η is approximately equal in magnitude to the percentage change in thickness of the laminations.

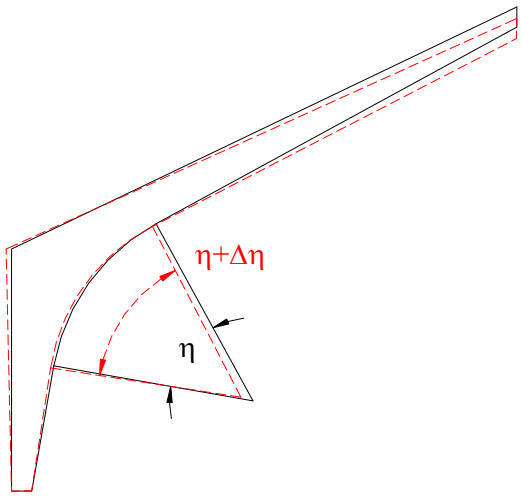

Figure 4.11. *Change in shape of arch half due to seasoning.*

11.1. *Estimate the expected change of angle, $\Delta\eta$, based on the expected equilibrium moisture content of the arches in service.* A 5% decrease in moisture content corresponds to 1% decrease in thickness and a 1% increase in angle η. Unless specified otherwise, the average moisture content at the time of manufacturing can be estimated as 12%.

$$\Delta\eta = -\frac{1}{5}\left(MC_{in-service} - 0.12\right)\eta \qquad [4\text{-}160]$$

11.2. *Calculate the length, a_L or a_R, of a line from the base to the crown for each arch half.* The length is calculated for the arch after the moisture content change using the law of cosines (**Figure 4.13**).

$$a_L = \sqrt{H_{w,L}^2 + \left(\frac{L_L}{\sin\left(90-\phi_{t,L}\right)}\right)^2 - 2H_{w,L}\left(\frac{L_L}{\sin\left(90-\phi_{t,L}\right)}\right)\cos\left(90+\phi_{t,L}-\Delta\eta_L\right)} \qquad [4\text{-}161]$$

$$a_R = \sqrt{H_{w,R}^2 + \left(\frac{L_R}{\sin\left(90-\phi_{t,R}\right)}\right)^2 - 2H_{w,R}\left(\frac{L_R}{\sin\left(90-\phi_{t,R}\right)}\right)\cos\left(90+\phi_{t,R}-\Delta\eta_R\right)} \qquad [4\text{-}162]$$

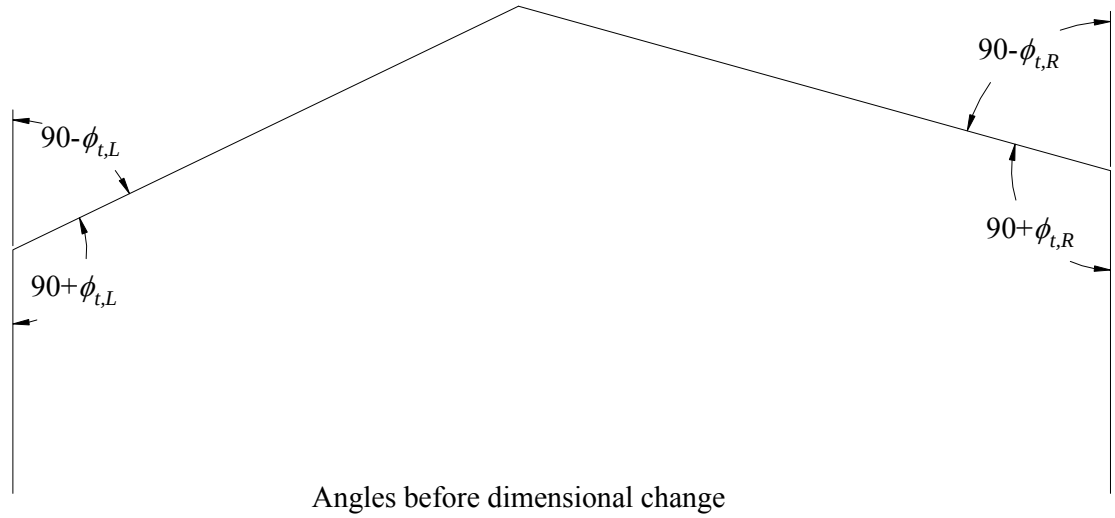

Angles before dimensional change

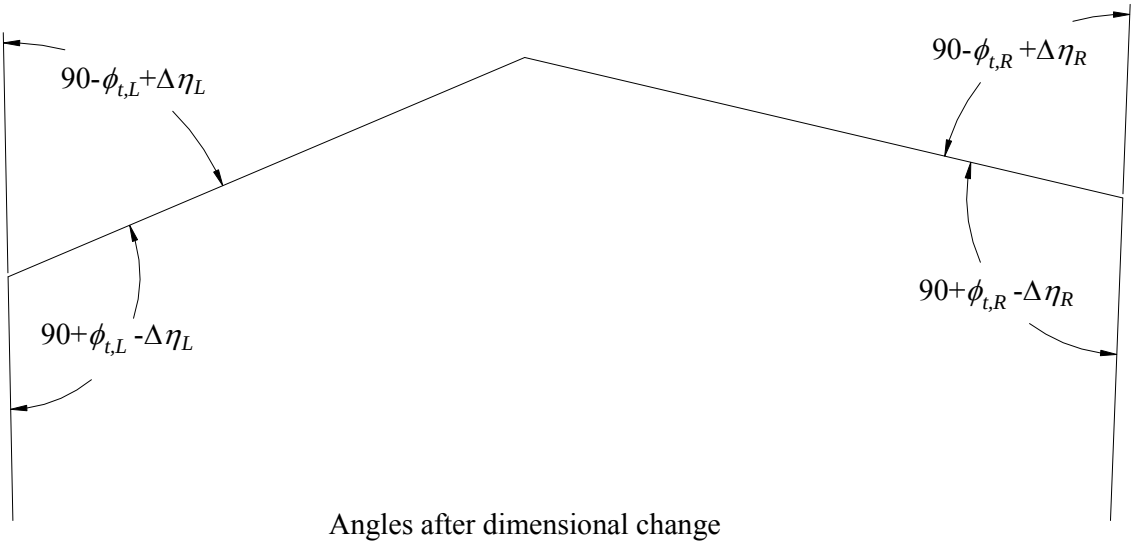

Angles after dimensional change

Figure 4.12. *Change in outside arch geometry due to moisture content change.*

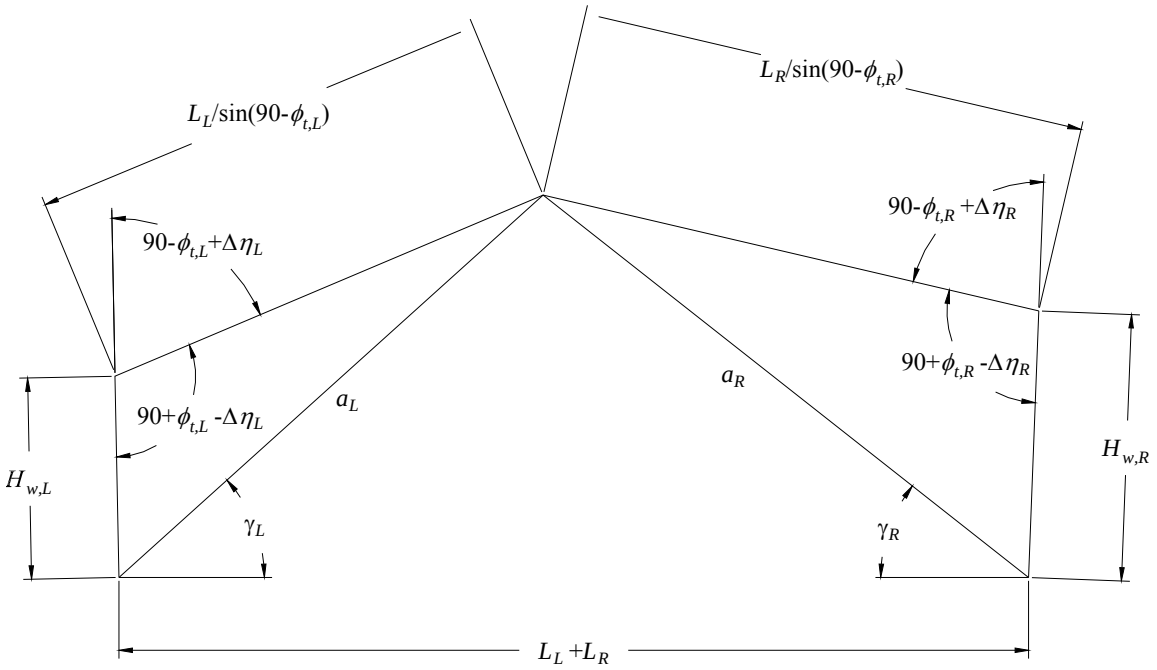

Figure 4.13. *Dimensions of seasoned arch for use in displacement calculations.*

11.3. *Calculate the angle, γ , between a horizontal line and the line from base to crown for each arch half* (**Figure 4.13**).

$$\gamma_L = \cos^{-1}\left[\frac{a_L^2 - a_R^2 + \left(L_L + L_R\right)^2}{2a_L\left(L_L + L_R\right)}\right] \quad [4\text{-}163]$$

$$\gamma_R = \cos^{-1}\left[\frac{a_R^2 - a_L^2 + \left(L_L + L_R\right)^2}{2a_R\left(L_L + L_R\right)}\right] \quad [4\text{-}164]$$

11.4. *Locate the coordinates of the crown,(x_c,y_c) after moisture content change.*

$$x_c = L_R - a_R\cos\gamma_R = a_L\cos\gamma_L - L_L \quad [4\text{-}165]$$

$$y_c = a_R\sin\gamma_R = a_L\sin\gamma_L \quad [4\text{-}166]$$

11.5. *Determine the displacement of the crown in each direction due to the change in moisture content.*

$$\Delta x_c = x_c \quad [4\text{-}167]$$

$$\Delta y_c = y_c - H_c \quad [4\text{-}168]$$

11.6. *Determine the angle of rotation, ψ , of each arch leg due to the change in moisture content* (**Figure 4.14**).

$$\xi_L = \sin^{-1}\left[\frac{L_L \sin\left(90+\phi_{t,L}-\Delta\eta_L\right)}{a_L \sin\left(90-\phi_{t,L}\right)}\right] \quad [4\text{-}169]$$

$$\xi_R = \sin^{-1}\left[\frac{L_R \sin\left(90+\phi_{t,R}-\Delta\eta_R\right)}{a_R \sin\left(90-\phi_{t,R}\right)}\right] \quad [4\text{-}170]$$

$$\psi_L = 90^\circ - \xi_L - \gamma_L \quad [4\text{-}171]$$

$$\psi_R = 90^\circ - \xi_R - \gamma_R \quad [4\text{-}172]$$

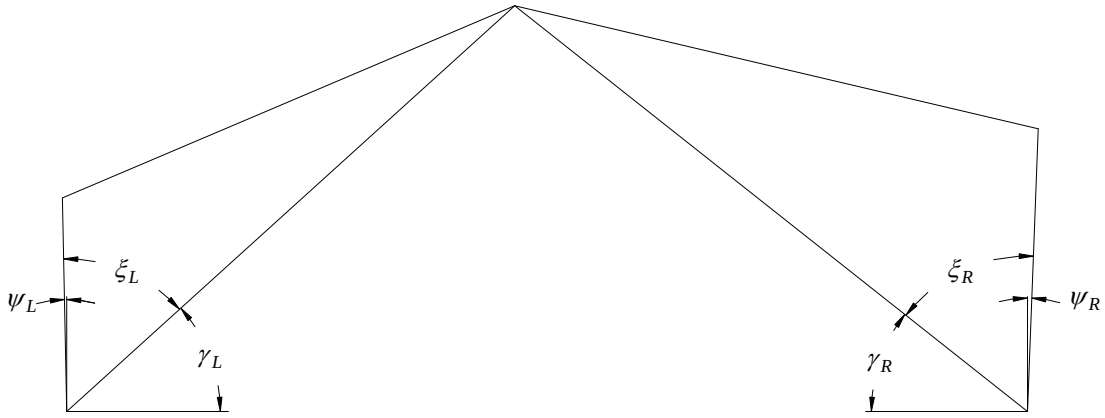

Figure 4.14. *Rotation of arch legs due to seasoning.*

11.7. *Determine the horizontal displacement of the haunches.* A negative value indicates outward displacement.

$$\Delta x_{haunch,L} = H_{w,L} \sin\psi_L \quad [4\text{-}173]$$

$$\Delta x_{haunch,R} = H_{w,R} \sin\psi_R \quad [4\text{-}174]$$

11. *Design and detail connections.* Shear plates are typically used to transfer the vertical reaction forces at the peak connection. Bolts with steel side plates are used to transfer tension forces between members at the peak. The base connection typically consists of a bearing seat to resist outward thrust, with a bolt to resist inward thrust and uplift.

Example 4-1: Design of Tudor Arch

Given: A building with outside dimension of 50 ft by 60 ft is to be constructed using Southern Pine Tudor arches spaced at 15 ft.

Preliminary design of the arches was performed in chapter 2. The trial geometry is shown in Figure E4.1.

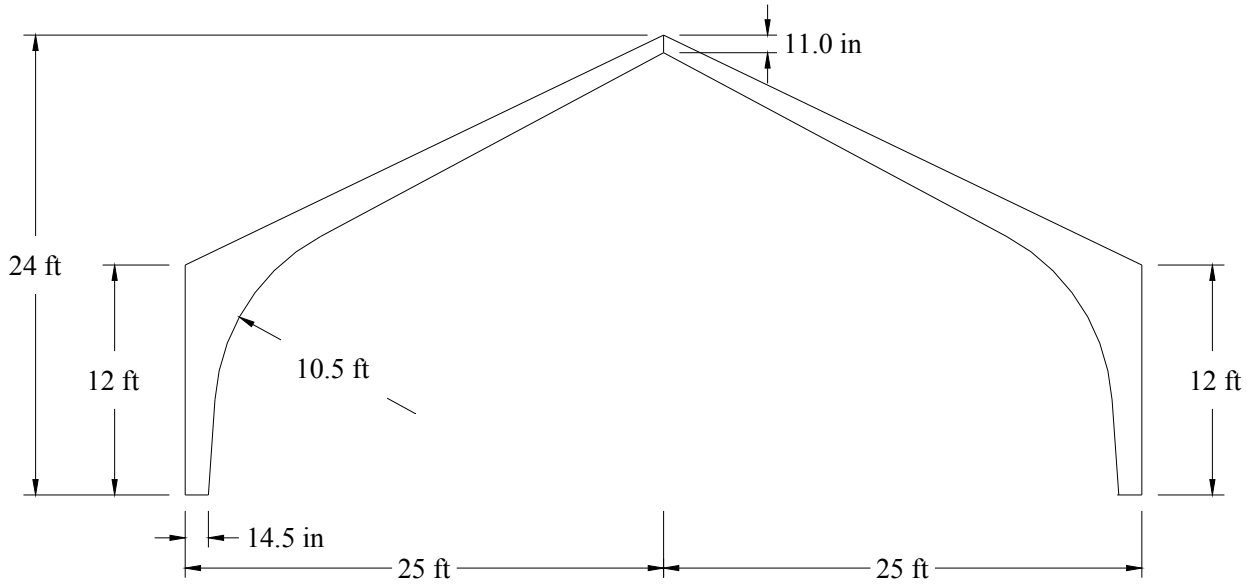

Figure E4.1. *Trial arch geometry with α_{arm} = 2.5° and α_{leg} = 4°.*

Parameters chosen for the trial arch geometry are as follows:

$b = 6.75$ in
$H_{w,L} = H_{w,R} = 144$ in $= 12$ ft
$H_c = 288$ in $= 24$ ft
$d'_{b,L} = d'_{b,R} = 14.5$ in
$d'_c = 11.0$ in
$R_L = R_R = 126$ in $= 10.5$ ft
$\alpha_{leg,L} = \alpha_{leg,R} = 4^\circ$
$\alpha_{arm,L} = \alpha_{arm,R} = 2.5^\circ$

The arch has continuous lateral bracing along the wall and roof.

The building has no shear walls at the ends, so the arches will be assumed to support all vertical and lateral loads acting parallel to the planes of the arches.

Loads: the loads have been determined as shown in Figures E4.2 through E4.5. The wall dead loads are assumed to act at the outer face of the arch.

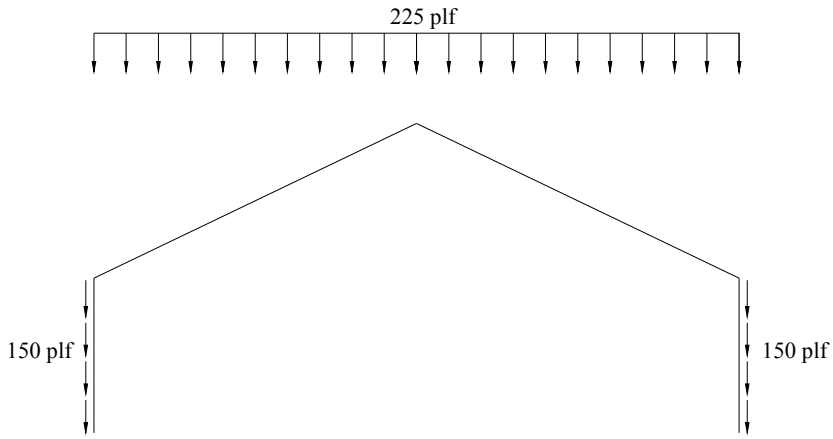

Figure E4.2. *Dead loads.*

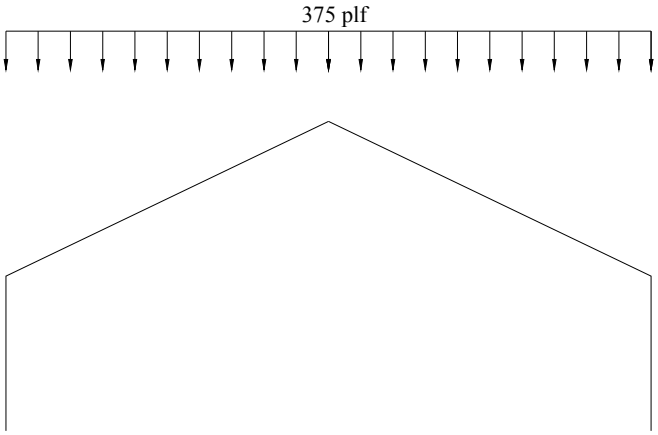

Figure E4.3. *Balanced snow load.*

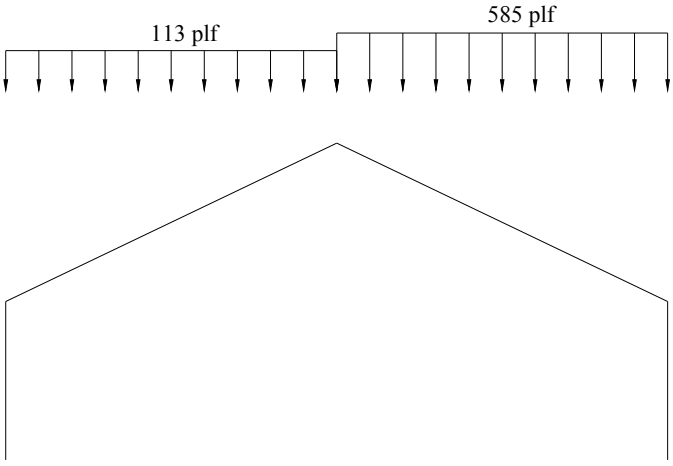

Figure E4.4. *Unbalanced snow load.*

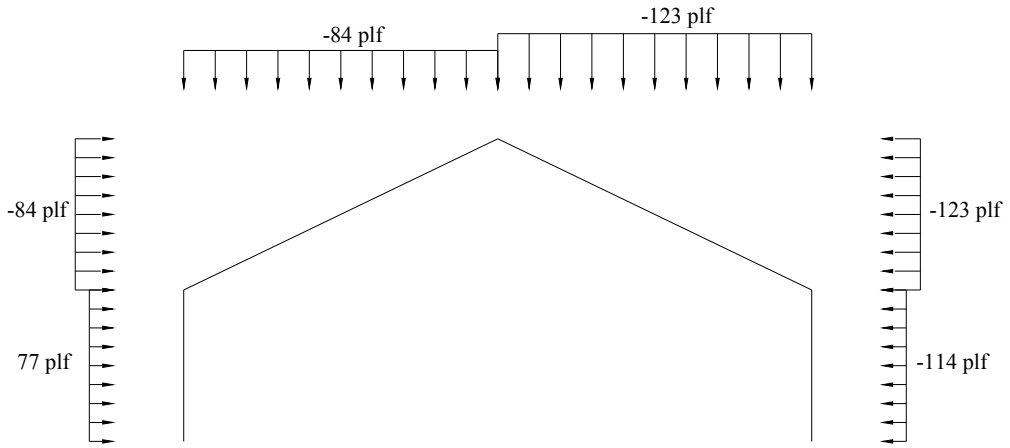

Figure E4.5. *Wind Load.*

Material Properties: $\mathbf{F_{bx}}^{+}_{\text{(at tangents)}} = 2000$ psi
$\mathbf{F_{bx}}^{+}_{\text{(at ends)}} = 1700$ psi
$\mathbf{F_c} = 1400$ psi
$\mathbf{E_x} = 1.6(10^6)$ psi
$\mathbf{F_{vx}} = 215$ psi
$\mathbf{F_{c\perp x}} = 650$ psi
$\mathbf{F_t} = 1000$ psi
$\mathbf{F_{bx}}^{-}_{\text{(d>85\% tangent depth)}} = F_{bx}^{+}$
$\mathbf{F_{bx}}^{-}_{\text{(d< 85\% tangent depth)}} = 1000$ psi
$\mathbf{E_{x\ min}} = 0.84(10^6)$ psi
$\mathbf{E_{y\ min}} = 0.84(10^6)$ psi
$\mathbf{F_{rt}} = 70$ psi
$\mathbf{F_{rc}} = 650$ psi

Wanted: Evaluate the trial geometry and re-design as appropriate. Determine the deflections of the arch at the haunch (horizontal), at the peak (vertical) and at a point slightly above the midway point between the upper tangent and the peak. Consider the following load combinations:

(1) D + S (balanced snow)
(2) D + S (unbalanced snow)
(3) D + 0.75W + 0.75S (balanced snow)
(4) 0.6D + W

In practice, additional load combinations may need to be considered.

Solution: Using a spreadsheet to perform the calculations, analysis of the arch designed in chapter 2 shows that the arch is adequate to support all of the considered load combinations. The reactions calculated based on the trial geometry are shown in **Table E4.1**. The combined bending and compression stress ratios for each of the load combinations are shown in **Table E4.2**. Shear stress ratios were less than 40% throughout the arch for all load combinations. Radial compression stresses ratios were less than 15% for all load combinations. Radial tension was developed in the windward arch half for the load combination **0.6D + W** with a stress ratio of 3%.

Table E4.1. *Reaction forces (lb) for selected load combinations.*

Load	$R_{y,L}$	$R_{x,L}$	C_y	C_x	$R_{y,R}$	$R_{x,R}$
D + S (balanced)	16800	7530	0	-7530	16800	7530
D + S (unbalanced)	13130	7210	-2880	-7210	19180	7210
D + 0.75S +0.75W	12360	4680	520	-4610	12670	6750
0.6D + W	1660	-550	690	640	2070	2210

Table E4.2. *Combined bending and compression stress ratios,* $\left(\frac{f_c}{F'_c}\right)^2 + \frac{f_{bx}}{F'_{bx}\left(1 - f_c/F_{cEx}\right)}$.

	Left Arch Half				Right Arch Half			
	Leg	**Lower Haunch**	**Upper Haunch**	**Arm**	**Arm**	**Upper Haunch**	**Lower Haunch**	**Leg**
D + S (balanced)	0.652	0.871	0.697	0.438	0.438	0.697	0.871	0.652
D + S (unbalanced)	0.631	0.849	0.805	0.670	0.810	0.555	0.817	0.617
D + 0.75S +0.75W	0.298	0.403	0.323	0.232	0.321	0.461	0.543	0.409
0.6D + W	0.022	0.025	0.023	0.041	0.279	0.175	0.162	0.126

Some observations from the spreadsheet output summarized in **Table E4.2** include:

1. The maximum combined stress ratio due to the load combination **D + S** (balanced snow) occurs at a section between the lower tangent and the haunch. The maximum combined flexural and compressive stresses were approximately 87% of the allowable combined stresses, indicating that the lower tangent point depth could be possibly be less.
2. The maximum combined stress ratio in any section above the haunch due to any load combination was less than 82%, indicating that the depth of the arm (away from the peak) could be reduced by decreasing the taper angle. Reducing the depth of the upper tangent point might also allow a reduction of depth at the lower tangent point. (The lower tangent point depth was increased to be within 10% of the upper tangent point depth).
3. The **D + S** (unbalanced snow on right side of roof) load combination produced the highest vertical reaction force at the crown connection (2870 lb). The **0.6D + W** load combination induced 640 lb of tension at the crown connection and a horizontal reaction of -550 lb at the left support. These values will be needed for connection design. No uplift occurred at the base.

Based on observations 1 and 2, the taper in the arm of the arch was reduced to 1.9 degrees, and the taper in the leg was reduced to 3.8 degrees, and the arch was reanalyzed. The redesigned arch would save an average of approximately 2 inches of depth along the length of arm and a small amount in the leg, resulting in a total savings of 4% of the volume of the original arch. The redesigned arch is illustrated in **Figure E4.6**.

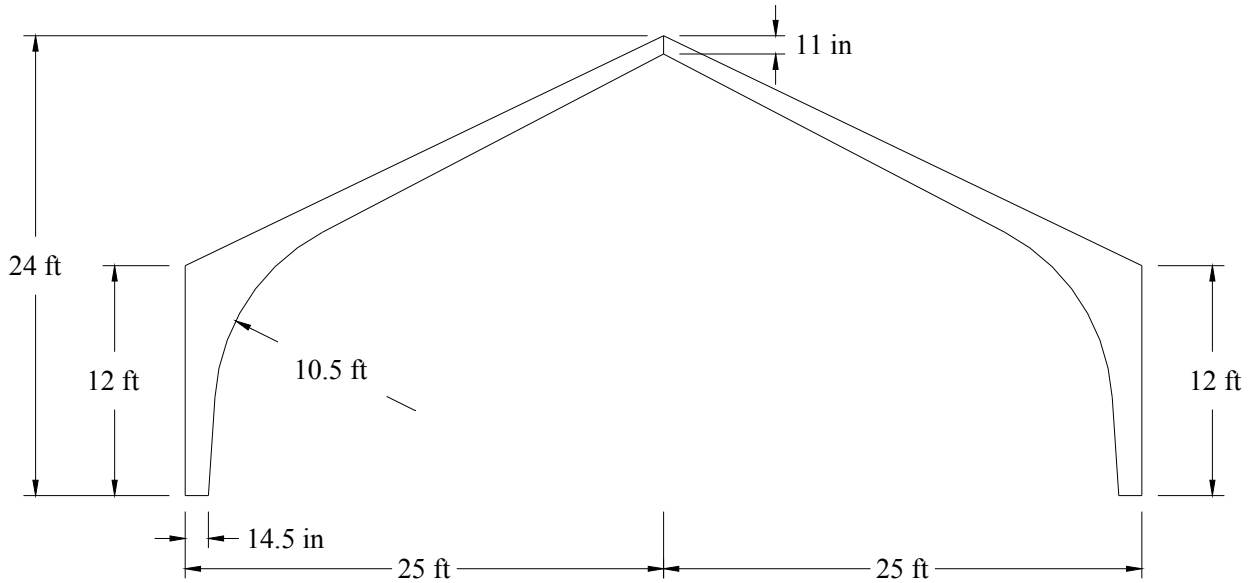

Figure E4.6. *Redesigned arch with α_{arm} = 1.9° and α_{leg} = 3.8°.*

Analysis of this arch using a spreadsheet to perform the calculations shows that the arch is adequate to support all of the considered load combinations. The reactions calculated based on the revised geometry are shown in **Table E4.3**. The combined stress ratios for each of the load combinations are shown in **Table E4.4**. As for the first trial geometry, the shear stresses and the radial stresses were small.

Table E4.3. *Reaction forces (lb) for selected load combinations.*

Load	$R_{y,L}$	$R_{x,L}$	C_y	C_x	$R_{y,R}$	$R_{x,R}$
D + S (balanced)	16800	7530	0	-7530	16800	7530
D + S (unbalanced)	13130	7210	-2880	-7210	19170	7210
D + 0.75S +0.75W	12360	4680	520	-4610	12670	6750
0.6D + W	1660	-550	690	640	2070	2210

Table E4.4. *Combined bending and compression stress ratios,* $\left(\frac{f_c}{F_c'}\right)^2 + \frac{f_{bx}}{F_{bx}'\left(1 - f_c/F_{cEx}\right)}$.

	Left Arch Half				Right Arch Half			
	Leg	**Lower Haunch**	**Upper Haunch**	**Arm**	**Arm**	**Upper Haunch**	**Lower Haunch**	**Leg**
D + S (balanced)	0.673	0.911	0.847	0.554	0.554	0.847	0.911	0.673
D + S (unbalanced)	0.651	0.888	1.000	0.766	0.881	0.658	0.856	0.637
D + 0.75S +0.75W	0.308	0.423	0.392	0.247	0.405	0.571	0.567	0.422
0.6D + W	0.022	0.025	0.029	0.047	0.326	0.221	0.168	0.129

Some observations from the spreadsheet output include:

1. The load combination **D + S** (unbalanced snow on right side of roof) resulted in a combined stress ratio of 100% in the upper haunch, indicating that the taper is optimal. The maximum combined stress ratio in the lower haunch was 91%, however, further experimentation with reduced taper or reduced base depth resulted in subtle changes in geometry which caused sections above the haunch to be overstressed.
2. The load combination **D + S** (unbalanced snow on right side of roof) produced the highest vertical reaction force at the crown connection (2880 lb). The **0.6D + W** load combination induced 640 lb of tension at the crown connection and a horizontal reaction of -540 lb at the left support. These values will be needed for connection design. No uplift occurred at the base.

Base Connection Design

The outward horizontal thrust at the bases will be resisted by a bearing seat connection. The required height of the back plate can be determined using the maximum horizontal force at the base:

$$\ell_b = \frac{R_x}{F'_{c\perp} b} = \frac{7530 \text{ lb}}{(650 \text{ psi})(6.75 \text{ in})} = 1.73 \text{ in}$$

A minimum height of 5 inches is typically specified.

The inward horizontal thrust at the base will be resisted by a bolt in double shear. The value will be taken from the NDS for the condition of a double shear connection with ¼ inch steel side plates. A 3/4 in. diameter bolt loaded perpendicular to the grain of the member has a reference design value of 2000 psi (NDS 2005). It can be shown by calculation that Mode III yielding governs the capacity of the bolt. Adjusting for duration of load gives a value of 3200 psi. This is more than adequate to resist the required 550 lb outward reaction caused by the **0.6D + W** load combination. The fastener is actually loaded at an angle of $(90° - \alpha_{leg}) = 86.2°$ to the grain. The capacity will be slightly higher than that under perpendicular to grain loading, but the difference is small and not worth calculating. A smaller bolt could have been used, but it is common practice to use ¾ in. or 1 in. bolts for arch connections.

Even though no uplift was calculated at the base of the arch, it is considered good practice to place the bolt a minimum distance of 7D from the end of the member. This will locate the bolt 5.25 inches above the base of the arch.

The height of the back plate will be selected as 7 in. Assuming 36 ksi steel (F_b = 24 ksi) and a ¼ in. positive tolerance on the seat width, the required thickness of the back plate can be calculated as follows (bearing plate is modeled as a beam with pinned ends and uniform load):

$$t = \sqrt{\frac{3Rb'}{4hF_b}} = \sqrt{\frac{3\left(7580 \text{ lb}\right)\left(6.75 \text{ in} + 0.25 \text{ in}\right)}{4\left(7 \text{ in}\right)\left(24000 \text{ psi}\right)}} = 0.49 \text{ in}$$

A 1/2 in. thick back plate will be required.

The member will have to be checked for the notch effect when the horizontal component of the base reaction is outward ($R_x < 1$). The shear force to be resisted at the base, perpendicular to the laminations, is calculated as:

$$V = -R_x \cos\alpha_{leg} \qquad \text{If no uplift is present } (R_y \geq 1)$$

$$V = -R_x \cos\alpha_{leg} - R_y \sin\alpha_{leg} \qquad \text{If uplift is present } (R_y < 1)$$

Therefore:

$$V = -R_x \cos\alpha_{leg} = -\left(-550 \text{ lb}\right)\cos\left(3.8°\right) = 548 \text{ lb}$$

Assuming the bolt is placed 6 in. from the outside face of the arch to minimize potential problems with shrinkage between bolt and bearing seat (Figure E4.7), the effective depth, d_e, and the total depth, d, of the section through the bolt hole can be calculated as:

$$d_e = \frac{x_h}{\cos\alpha_{leg}} = \frac{6 \text{ in}}{\cos\left(3.8°\right)} = 6.01 \text{ in}$$

$$d = d_e + \left(d_b' - x_h\right)\cos\alpha_{leg} + y_h \sin\alpha_{leg}$$

$$d = 6.01 \text{ in} + \left(14.5 \text{ in} - 6.0 \text{ in}\right)\cos\left(3.8°\right) + \left(5.25 \text{ in}\right)\sin\left(3.8°\right) = 14.8 \text{ in}$$

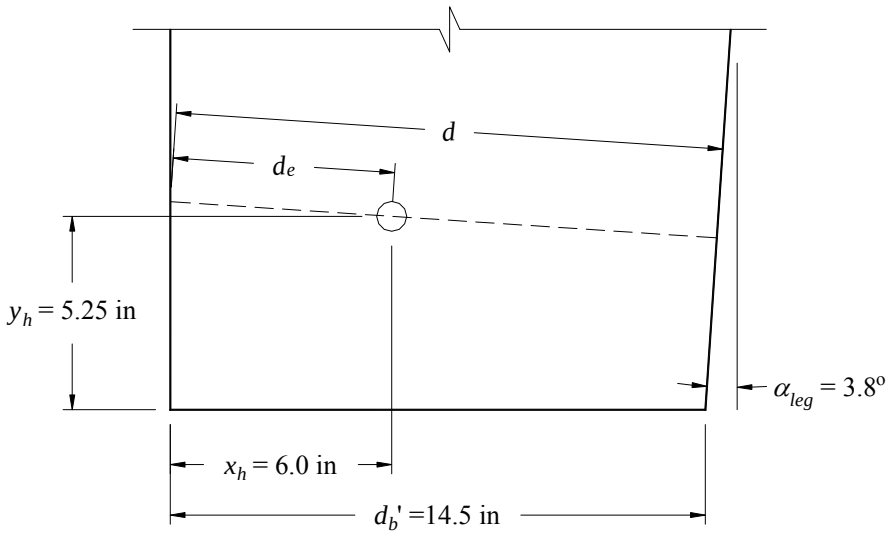

Figure E4.7. *Bolt placement and dimensions for notched shear calculation.*

The shear resistance of the member at the connection can be calculated as:

$$V_r' = \left[\frac{2}{3}F_{vx}' b d_e\right]\left[\frac{d_e}{d}\right]^2 = \left[\frac{2}{3}(215\text{ psi})(1.6)(6.75\text{ in})(6.01\text{ in})\right]\left[\frac{6.01\text{ in}}{14.8\text{ in}}\right]^2 = 1534\text{ lb}$$

The capacity of the member at the connection is adequate with the bolt placed 6 in. from the outside face (1534 lb > 548 lb).

One 3/4 in. bolt with ¼ in. steel side plates will be chosen for the connection. The connection will be detailed with the bolt positioned 5.25 inches from the base of the arch and 6 inches from the outside face.

Peak Connection Design

The shear forces at the peak will be transferred by two 4 in. shear plates as determined previously. Because the arm taper angle was changed from 2.5° to 1.9°, the angle of load to the grain will be increased, and the capacity of the connectors will be reduced and should be re-evaluated. The required spacing and edge distances will also be reduced, so the previously chosen spacing, edge distance, and geometry factor can be used conservatively.

$$\phi_t = \arctan\left(\frac{12\text{ ft}}{25\text{ ft}}\right) = 25.6°$$

$$\alpha_{arm} = 1.9°$$

$$90° - \phi_t - \alpha_{arm} = 90° - 25.6° - 1.9° = 62.5°$$

Hankinson's formula can be used to determine the reference capacity for a single shear plate loaded at an angle to the grain of $90° - \phi_t - \alpha_{arm}$.

$$N = \frac{PQ_{90}}{P\sin^2(90° - \phi_t - \alpha_{arm}) + Q_{90}\cos^2(90° - \phi_t - \alpha_{arm})}$$

$$N = \frac{(4360\text{ lb})(1824\text{ lb})}{(4360\text{ lb})\sin^2(62.5°) + (1824\text{ lb})\cos^2(62.5°)}$$

$$N = 2082\text{ lb}$$

The adjusted capacity (dry-use, normal temperatures, snow load) of the connection will be:

$$nN' = 2(NC_D C_\Delta C_g) = 2(2082\text{ lb})(1.15)(0.68)(1.0) = 3260\text{ lb} \geq 2950\text{ lb} \qquad \therefore \text{OK}$$

The shear capacity of the members at the crown must also be evaluated for the notch effect. The effective depth, perpendicular to the laminations, must be determined and the

shear capacity of the member determined. This shear capacity must be compared to the resultant shear force from the reaction forces at the crown. The depth of the notched member is calculated as:

$$d'_{c\,e} = d'_c - \mathrm{E} + \left(\frac{\text{inside groove diameter}}{2} \right)$$

$$d'_{c\,e} = 11.0 \text{ in} - 2.75 \text{ in} + \frac{3.62 \text{ in}}{2} = 10.1 \text{ in}$$

The effective depth measured perpendicular to the laminations is:

$$d_{c\,e} = \frac{d'_{c\,e} \cos \phi_t}{\cos\left(\alpha_{arm}\right)} = \frac{\left(10.1 \text{ in}\right)\cos\left(25.6^\circ\right)}{\cos\left(1.9^\circ\right)} = 9.1 \text{ in}$$

The depth of the full section measured perpendicular to the laminations is:

$$d_c = \frac{d'_c \cos \phi_t}{\cos\left(\alpha_{arm}\right)} = \frac{\left(11.0 \text{ in}\right)\cos\left(25.6^\circ\right)}{\cos\left(1.9^\circ\right)} = 9.9 \text{ in}$$

The member shear capacity at the connection is:

$$V'_r = \left[\frac{2}{3} F'_{vx} b d_{c\,e} \right] \left[\frac{d_{c\,e}}{d_c} \right]^2 = \left[\frac{2}{3} \left(215 \text{ psi}\right)\left(1.15\right)\left(6.75 \text{ in}\right)\left(9.1 \text{ in}\right) \right] \left[\frac{9.1 \text{ in}}{9.9 \text{ in}} \right]^2 = 8560 \text{ lb}$$

The shear force (perpendicular to the member) to be resisted by the member at the peak is calculated as:

$$V = C_y \cos \phi_b + C_x \sin \phi_b = \left(2880 \text{ lb}\right)\cos\left(25.6^\circ + 1.9^\circ\right) + \left(7210 \text{ lb}\right)\sin\left(25.6^\circ + 1.9^\circ\right) = 5880 \text{ lb}$$

Because $V'_r = 8560 \text{ lb} \geq V = 5880 \text{ lb}$, the notched shear capacity of the members at the trial crown connection is adequate.

The tension force of 640 lb will be transferred using bolts and ¼ in. steel side plates. A single 3/4 in. bolt has a reference capacity of 2000 lbs when loaded perpendicular to grain and 3480 lb when loaded parallel to grain. The capacity can be further increased by the load duration factor of 1.6. It is clear that a single 3/4 in. bolt on each arch half will be adequate to transfer the required tension force. A smaller bolt could have been used, but it is common practice to use ¾ in. or 1 in. bolts for arch connections.

The arch is adequate to resist all of the loads considered.

Deflections Due to Loads

The deflections should be checked against applicable limits. Applying the limits of Table 1.1, the following deflection limits can be determined (**Table E4.5**):

Table E4.5. *Deflection limits for arch example.*

	Haunch	Arms	Crown
With Brittle Finishes	$\frac{H_w}{120} = \frac{144 \text{ in}}{120} = 1.2 \text{ in}$	$\frac{\ell_{arm}}{360} = \frac{245 \text{ in}}{360} = 0.7 \text{ in}$	$\frac{L_L + L_R}{360} = \frac{600 \text{ in}}{360} = 1.7 \text{ in}$
With Flexible Finishes	$\frac{H_w}{60} = \frac{144 \text{ in}}{60} = 2.4 \text{ in}$	$\frac{\ell_{arm}}{180} = \frac{245 \text{ in}}{180} = 1.4 \text{ in}$	$\frac{L_L + L_R}{180} = \frac{600 \text{ in}}{180} = 3.3 \text{ in}$

Deflections due to the considered load combinations were estimated using the principle of virtual work and are shown in **Table E4.6**. (Calculated deflections are shown to nearest 0.01 in. to facilitate comparison with a spreadsheet developed by the reader, however, this level of precision is not justifiable for design. It is generally sufficient to estimate displacements to the nearest 0.1 in.)

Table E4.6. *Deflections (in.) for selected load combinations.*

Load	Δ_{cy}	Δ_{cx}	$\Delta_{arm,L}$	$\Delta_{arm,R}$	$\Delta_{x,L}$	$\Delta_{x,R}$
D + S (balanced)	0.72	0	0.31	0.31	-0.37	-0.37
D + S (unbalanced)	0.69	-0.85	-0.46	1.04	-1.26	0.54
D + 0.75S +0.75W	0.70	0.31	0.29	-0.09	-0.03	-0.69
0.6D + W	0.28	0.42	0.11	-0.40	0.29	-0.59

If the structure will be finished with flexible materials, the arch deflections will be within the acceptable limits. However, if the structure is finished with brittle materials, the deflection of the right arch arm under the unbalanced snow load exceeds the limit. Deflections at the crown and haunches can be decreased by increasing the size of the arch or through the use of a diaphragm and shear wall system as described in the next chapter. However, the use of a diaphragm and shear wall system will also cause a redistribution of moments in the arch. The change in moment distribution may increase or decrease the deflections in the arms.

Deflections Due to Seasoning

Additionally, deflections will be affected by seasoning of the arch in service. Assuming the arch will equilibrate to a moisture content of approximately 7%, the deflections due to seasoning can be estimated following the procedures of Section 11.

$$\Delta\eta_L = \Delta\eta_R = -\frac{1}{5}\left(MC_{in-service} - 0.12\right)\eta_L = -\frac{1}{5}\left(0.07 - 0.12\right)\left(58.7°\right) = 0.587°$$

$$a_R = a_L = \sqrt{H_{w,L}^2 + \left(\frac{L_L}{\sin\left(90° - \phi_{t,L}\right)}\right)^2 - 2H_{w,L}\left(\frac{L_L}{\sin\left(90° - \phi_{t,L}\right)}\right)\cos\left(90° + \phi_{t,L} - \Delta\eta_L\right)}$$

$$a_R = a_L = \sqrt{(144\text{ in})^2 + \left(\frac{300\text{ in}}{\sin\left(90° - 25.64°\right)}\right)^2 - 2(144\text{ in})\left(\frac{300\text{ in}}{\sin\left(90° - 25.64°\right)}\right)\cos\left(90° + 25.64° - 0.587°\right)}$$

$$a_R = a_L = 414.8\text{ in}$$

$$\gamma_R = \gamma_L = \cos^{-1}\left[\frac{a_L^2 - a_R^2 + \left(L_L + L_R\right)^2}{2a_L\left(L_L + L_R\right)}\right] = \cos^{-1}\left[\frac{(414.8\text{ in})^2 - (414.8\text{ in})^2 + (600\text{ in})^2}{2(414.8\text{ in})(600\text{ in})}\right]$$

$$\gamma_R = \gamma_L = 43.68°$$

$$x_c = a_L\cos\gamma_L - L_L$$

$$x_c = (414.8\text{ in})\cos(43.68°) - 300\text{ in} = 0$$

$$\Delta x_c = x_c = 0$$

$$y_c = a_L\sin\gamma_L = (414.8\text{ in})\sin 43.68° = 286.5\text{ in}$$

$$\Delta y_c = 286.5\text{ in} - 288\text{ in} = -1.5\text{ in} \qquad \text{(downward)}$$

$$\xi_R = \xi_L = \sin^{-1}\left[\frac{L_L\sin\left(90 + \phi_{t,L} - \Delta\eta_L\right)}{a_L\sin\left(90 - \phi_{t,L}\right)}\right]$$

$$\xi_R = \xi_L = \sin^{-1}\left[\frac{(300\text{ in})\sin\left(90° + 25.64° - 0.587°\right)}{(414.8\text{ in})\sin\left(90° - 25.64°\right)}\right] = 46.62°$$

$$\psi_R = \psi_L = 90° - \xi_L - \gamma_L = 90° - 46.62° - 43.68° = -0.30°$$

$$\Delta x_{haunch,R} = \Delta x_{haunch,L} = H_{w,L}\sin\psi_L = (144\text{ in})\sin(-0.30°) = -0.75\text{ in} \qquad \text{(outward)}$$

The designer will have to determine if the deflections due to seasoning are acceptable. If they are determined to be excessive, increasing the angles of taper in the arm and leg will reduce the angle η, leading to slight decreases in displacements. Placing additional restrictions on the moisture content of laminations used in the manufacture of the arch is an effective method that may be considered. However, the specification of lower lamination moisture contents may require additional time and expense for manufacturing.

Consideration should be given to specifying that the end walls be built with the peak at a lower elevation to accommodate the anticipated downward deflection of the arch crown due to seasoning, so the ridge of the structure does not appear to sag after the arches season.

Conclusion

This chapter presented equations for the design of Tudor arches. Arch geometry was established and free body diagrams were used to derive formulas for moment, shear, and axial force at any section in the arch under common load assumptions. Requirements and recommendations for analysis of stresses were given and a method of estimating displacements was presented. Efficient use of this information requires the development of computerized software or spreadsheets. Once created, however, the software or spreadsheets can be used to efficiently design Tudor arches.

Chapter 5
Arch-Diaphragm Interaction

Glulam arches are often used in conjunction with a diaphragm and shear walls to support the design loads on a structure. Diaphragm and shear wall systems are typically stiff relative to structural glued laminated timber arches, so the diaphragm acts as a partial support to the arch. The use of a diaphragm and shear walls can significantly reduce the overall deflection of an arch, resulting in structurally efficient design. The following additional steps can be followed to evaluate the effects of a diaphragm supporting the arch.

Nomenclature

A_c	cross sectional area of each diaphragm chord (in^2)
C_x	horizontal component of pin force at arch crown
C_y	vertical component of pin force at arch crown
D	dead load
E	modulus of elasticity of segment (psi)
E_c	modulus of elasticity of diaphragm chords (psi)
G_a	apparent diaphragm shear stiffness from nail slip and panel shear deformation (kip/in)
I	moment of inertia of segment (psi)
$K_{x,a}$	arch stiffness in the horizontal direction for load applied at peak (lb/in)
$K_{x,d}$	diaphragm stiffness in the horizontal direction (lb/in)
$K_{y,a}$	arch stiffness in the vertical direction for load applied at peak (lb/in)
$K_{y,d}$	diaphragm stiffness in the vertical direction (lb/in)
ℓ	length of diaphragm perpendicular to plane of arch (ft)
m_1	moment in segment caused by P_1 (in-lb)
m_2	moment in segment caused by P_2 (in-lb)
P_x	horizontal support load (positive rightward) (lb)
P_y	vertical support load (positive downward) (lb)
P_1	vertical unit load applied at the peak for virtual work calculation (lb)
P_2	horizontal unit load applied at the peak for virtual work calculation (lb)
$R_{x,L}$	horizontal reaction force at left base (lb)
$R_{x,R}$	horizontal reaction force at right base (lb)
$R_{y,L}$	vertical reaction force at left base (lb)
$R_{y,R}$	vertical reaction force at right base (lb)
S	snow load
s	segment length for virtual work calculation (in.)
s_a	tributary width for loads on arch (arch spacing) (ft)
u	distance from chord splice to nearest support (ft)

v	allowable unit shear in the diaphragm (lb/ft)
W	wind load
W_x	projected width of diaphragm parallel to direction of load (ft)
W_y	projected width of diaphragm in vertical direction (ft)
$\delta_{x,d}$	deflection of diaphragm in horizontal direction at the design shear (in.)
$\delta_{x,shearwall}$	horizontal displacement from deformation in the shear wall
$\delta_{y,d}$	deflection of diaphragm in vertical direction at induced unit shear (in.)
Δ_{1x}	deflection of the arch in the x-direction due to applied loads, assuming no diaphragm support
Δ_{1y}	deflection of the arch in the y-direction due to applied loads, assuming no diaphragm support
$\Delta_{arm,L}$	displacement of left arch arm
$\Delta_{arm,R}$	displacement of right arch arm
Δ_c	diaphragm chord splice slip at the induced unit shear, v, in diaphragm. This value can be estimated as 0.03 in. for tension chord splices and 0.005 in. for compression chord splices (APA Engineered Wood Handbook, 2002).
Δ_{cy}	vertical displacement at peak
Δ_{cx}	horizontal displacement at peak
Δ_x	horizontal displacement of peak (in.)
$\Delta_{x,L}$	horizontal displacement at left haunch
$\Delta_{x,R}$	horizontal displacement at right haunch
Δ_y	vertical displacement of peak (in.)
$\omega_{rx,L}$	horizontal distributed load on roof arm of left arch half (lb/in)
$\omega_{rx,R}$	horizontal distributed load on roof arm of right arch half (lb/in)
$\omega_{ry,L}$	vertical distributed load on roof arm of left arch half (lb/in)
$\omega_{ry,R}$	vertical distributed load on roof arm of right arch half (lb/in)
$\omega_{wx,L}$	horizontal distributed load on wall leg of left arch half (lb/in)
$\omega_{wx,R}$	horizontal distributed load on wall leg of right arch half (lb/in)
$\omega_{wy,L}$	vertical distributed load on wall leg of left arch half (lb/in)
$\omega_{wy,R}$	vertical distributed load on wall leg of right arch half (lb/in)

Procedure

The supporting effect of a diaphragm on a three-hinged arch can be modeled by linear spring elements attached to the peak of the arch (**Figure 5.1**). The diaphragm does not add any flexural stiffness to the individual arch members.

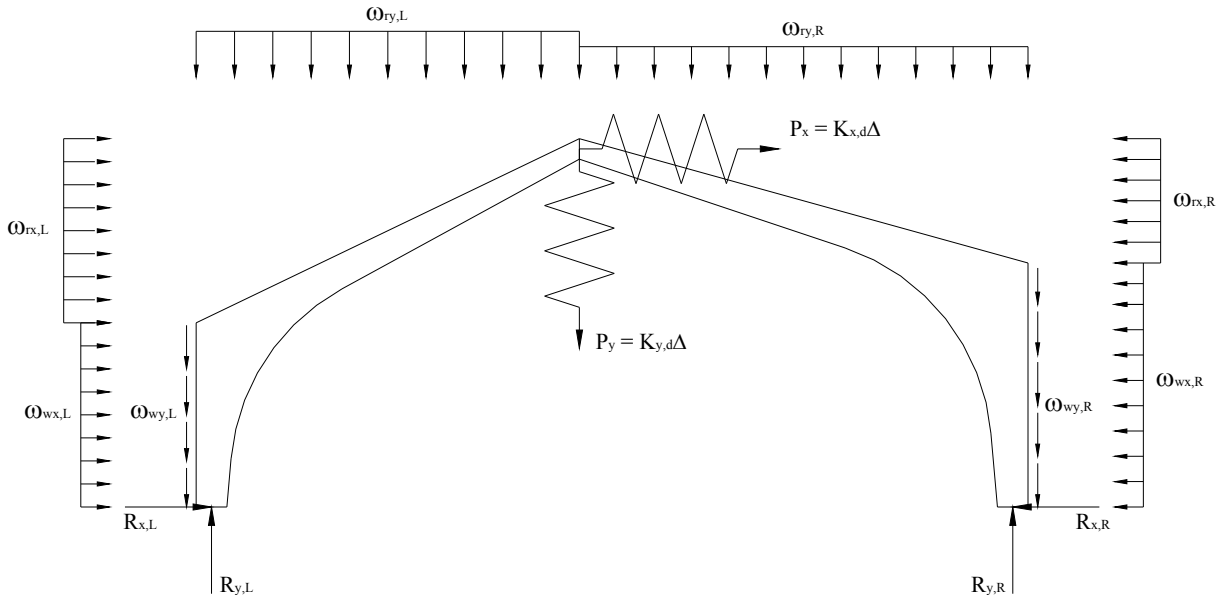

Figure 5.1. Spring model representing diaphragm support on arch.

The system is statically indeterminate, so the diaphragm must be designed, and a trial geometry for the arch must be chosen prior to determining the spring forces. Once the spring loads are determined for a given loading, the arch can be analyzed using the equations developed in the previous chapter.

The analysis is performed for an arch at the mid-span of the diaphragm, which will receive the least amount of support from the diaphragm and deflect the most. The spring forces on this arch can be determined using the following procedure:

1. *Design the roof diaphragm and shear walls to support all of the lateral roof loads and an estimated 5/8 of the lateral wall loads.* Although the arches will reduce the load on the diaphragm, the added design iterations and complexity necessary to determine the magnitude of the load reductions is generally not justified.

2. *Determine the stiffness of the diaphragm in each direction, $K_{x,d}$ and $K_{y,d}$* at the point of maximum deflection. For structural panel diaphragms the stiffness can be estimated as follows.

$$\delta_{x,d} = \frac{5v\ell^3}{8E_cA_cW_x} + \frac{0.25v\ell}{1000G_a} + \frac{\sum(u\Delta_c)}{2W_x} + \delta_{x,shearwall} \qquad [5\text{-}1]$$

$$K_{x,d} = \frac{2vW_xs_a}{\ell\delta_{x,d}} \qquad [5\text{-}2]$$

$$\delta_{y,d} = \frac{5v\ell^3}{8E_cA_cW_y} + \frac{0.25v\ell}{1000G_a} + \frac{\sum(u\Delta_c)}{2W_y} \qquad [5\text{-}3]$$

$$K_{y,d} = \frac{2\nu W_y s_a}{\ell \delta_{y,d}} \qquad [5\text{-}4]$$

3. *Calculate the stiffness of the arch, K_a, for point loads applied at the crown in each of the horizontal and vertical directions using virtual work.*

   Apply a virtual unit load, P_1, at the crown in the vertical direction. Calculate the vertical deflection at the peak and the corresponding stiffness of the arch. (For this analysis, the virtual load and the "real" load are equal).

$$P_1 \Delta_y = \sum \frac{m_1^2 s}{EI} \qquad [5\text{-}5]$$

$$K_{y,a} = \frac{P_1}{\Delta_y} \qquad [5\text{-}6]$$

   Apply a virtual unit load, P_2, at the crown in the horizontal direction. Calculate the horizontal deflection at the peak and the corresponding stiffness of the arch. (For this analysis, the virtual load and the "real" load are equal).

$$P_2 \Delta_x = \sum \frac{m_2^2 s}{EI} \qquad [5\text{-}7]$$

$$K_{x,a} = \frac{P_2}{\Delta_x} \qquad [5\text{-}8]$$

4. *Calculate the support forces from the diaphragm on the arch crown for each load combination.*

$$P_x = \frac{-\Delta_{1x} K_{x,a} K_{x,d}}{K_{x,a} + K_{x,d}} \qquad [5\text{-}9]$$

$$P_y = \frac{-\Delta_{1y} K_{y,a} K_{y,d}}{K_{y,a} + K_{y,d}} \qquad [5\text{-}10]$$

5. *Analyze the arch using the procedures of the previous chapter with the support forces determined in step 4 of this chapter applied at the crown of the arch in addition to all of the other loads. Support forces from the diaphragm will be different for each load combination.*

Example 5-1: Arch-Diaphragm Interaction

Given: The building from Example 4-1 will be modified to have shear walls at the ends and a structural panel diaphragm. The structural diaphragm (designed elsewhere) will consist of 7/16 OSB panels with 8d nails spaced at 6 inch intervals along all panel edges and 12 inches in the field of the panel. One 2 x 6 N2 SP chord will be used along each edge of the roof, and two 2 x 6 chords (or equivalent glulam) will be used at the ridgeline.

Wanted: Design the diaphragm and calculate its stiffness.
Determine the effect of the shearwall and diaphragm system on the arches from Example 3-1 using the same load combinations. Neglect the deflection of the shear walls.

Solution: From the Special Design Provisions for Wind and Seismic (AF&PA 2005), the following values can be obtained for the diaphragm:

$$v = 255\,\frac{\text{lb}}{\text{ft}}$$

$$G_a = 14.0\ \frac{\text{kip}}{\text{ft}}$$

The stiffness properties of each 2 x 6 chord are:

$$A_{2x6} = (1.5\text{ in})(5.5\text{ in}) = 8.25\text{ in}^2$$

$$E_c = 1.6(10^6)\text{ psi}$$

Assuming that chord splices will occur at every arch:

$$\sum(u\Delta_c) = (15\text{ ft} + 30\text{ ft} + 15\text{ ft})(0.03\text{ in}) + (0.005\text{ in})(15\text{ ft} + 30\text{ ft} + 15\text{ ft})(0.005\text{ in})$$

$$\sum(u\Delta_c) = 2.1\text{ ft-in.}$$

Determine diaphragm stiffness in the x-direction.

$$\delta_{x,d} = \frac{5v\ell^3}{8E_cA_cW_x} + \frac{0.25v\ell}{1000G_a} + \frac{\sum(u\Delta_c)}{2W_x} + \delta_{x,shearwall}$$

$$\delta_{x,d} = \frac{5(255)(60)^3}{8(1.6(10^6))(8.25)50} + \frac{0.25(255)(60)}{1000(14.0)} + \frac{2.1}{2(50)} + 0$$

$$\delta_{x,d} = (0.0522 + 0.273 + 0.021)\text{ in}$$

$$\delta_{x,d} = 0.346\text{ in}$$

$$K_{x,d} = \frac{2vW_xs_a}{\ell\delta_{x,d}} = \frac{2(255\text{ lb/ft})(50\text{ ft})(15\text{ ft})}{(60\text{ ft})(0.346\text{ in})} = 18.42(10^3)\ \frac{\text{lb}}{\text{in}}$$

Determine diaphragm stiffness in the y-direction.

$$\delta_{y,d} = \frac{5v\ell^3}{8E_cA_cW_y} + \frac{0.25v\ell}{1000G_a} + \frac{\sum(u\Delta_c)}{2W_y}$$

$$\delta_{y,d} = \frac{5(255)(60)^3}{8\left(1.6\left(10^6\right)\right)((2)8.25)12} + \frac{0.25(255)(60)}{1000(14.0)} + \frac{2.1}{2(12)} + 0$$

$$\delta_{y,d} = (0.1087 + 0.273 + 0.0875) \text{ in}$$

$$\delta_{y,d} = 0.469 \text{ in}$$

$$K_{y,d} = \frac{2vW_y s_a}{\ell\delta_{y,d}} = \frac{2(255 \text{ lb/ft})(12 \text{ ft})(15 \text{ ft})}{(60 \text{ ft})(0.469 \text{ in})} = 3.26\left(10^3\right) \frac{\text{lb}}{\text{in}}$$

Determine stiffness of the arch in x and y directions for point loading at the crown

Using a spreadsheet to apply the principle of virtual work, the stiffness of the arch in the x- and y-directions is determined to be:

$$K_{y,a} = 4970 \frac{\text{lb}}{\text{in}}$$

$$K_{x,a} = 5340 \frac{\text{lb}}{\text{in}}$$

Calculate the support forces on the arch for each load combination

$$P_y = \frac{-\Delta_{1y}K_{y,a}K_{y,d}}{K_{y,a} + K_{y,d}} = \frac{-\Delta_{1y}(4970 \text{ lb/in})(3260 \text{ lb/in})}{4970 \text{ lb/in} + 3260 \text{ lb/in}} = (1969 \text{ lb/in})(-\Delta_{1y})$$

$$P_x = \frac{-\Delta_{1x}K_{x,a}K_{x,d}}{K_{x,a} + K_{x,d}} = \frac{-\Delta_{1x}(5340 \text{ lb/in})(18420 \text{ lb/in})}{5340 \text{ lb/in} + 18420 \text{ lb/in}} = (4140 \text{ lb/in})(-\Delta_{1x})$$

Table E5.1. *Calculation of support forces.*

Load	Δ_{1y} (in)	Δ_{1x} (in)	P_y (lb)	P_x (lb)
D + S (balanced)	0.72	0	-1418	0
D + S (unbalanced)	0.69	-0.85	-1360	3520
D + 0.75S +0.75W	0.70	0.31	-1370	-1290
0.6D + W	0.28	0.42	-560	-1720

With the support forces determined, the arch is reanalyzed according to the procedures of Chapter 4

Table E5.2. *Reaction forces (lb) for arch with diaphragm support.*

Load	$R_{y,L}$	$R_{x,L}$	C_y	C_x	$R_{y,R}$	$R_{x,R}$
D + S (balanced)	16090	6800	710	-6800	16090	6800
D + S (unbalanced)	10750	4740	-500	-4740	20190	8260
D + 0.75S +0.75W	12300	4610	580	-4550	11360	5390
0.6D + W	2210	20.0	140	64.0	960	1060

Table E5.3. *Deflections (in.) for selected load combinations.*

Load	Δ_{cy}	Δ_{cx}	$\Delta_{arm,L}$	$\Delta_{arm,R}$	$\Delta_{x,L}$	$\Delta_{x,R}$
D + S (balanced)	0.44	0	0.46	0.46	-0.22	-0.22
D + S (unbalanced)	0.42	-0.19	0.06	0.82	-0.42	-0.01
D + 0.75S +0.75W	0.42	0.07	0.30	0.19	-0.14	-0.29
0.6D + W	0.17	0.09	-0.01	-0.16	0.01	-0.19

Table E5.4. *Combined bending and compression stress ratios,* $\left(\frac{f_c}{F_c'}\right)^2 + \frac{f_{bx}}{F_{bx}'\left(1 - f_c/F_{cEx}\right)}$.

	Left Arch Half				**Right Arch Half**			
	Leg	**Lower Haunch**	**Upper Haunch**	**Arm**	**Arm**	**Upper Haunch**	**Lower Haunch**	**Leg**
D + S (balanced)	0.606	0.819	0.726	0.513	0.513	0.726	0.819	0.606
D + S (unbalanced)	0.425	0.578	0.570	0.386	0.789	0.828	0.988	0.734
D + 0.75S +0.75W	0.304	0.417	0.385	0.251	0.257	0.401	0.444	0.333
0.6D + W	0.015	0.029	0.046	0.033	0.126	0.074	0.065	0.054

Some comparisons can be made with the design from the previous chapter where identical arches were used, but shear walls and a diaphragm were not used:

1. The combined flexural and compressive stresses due to the load combination **D + S** (balanced snow) decreased in sections below the haunch, but increased in sections above the haunch.
2. For the load combination **D + S** (unbalanced snow on right side of roof), the diaphragm support caused reductions in stress ratios on the left arch half, but the maximum stress ratios through the haunch of the right arch half increased as a result of the diaphragm support. The combined stress ratio increased from 86% to 99% in sections between the lower tangent and haunch of the right arch half.
3. The tension at the crown connection due to the **0.6D + W** load combination was reduced to 64 lb (as compared to 640 lb without the diaphragm support). The horizontal base reaction, $R_{x,L}$, is no longer negative, so no forces will be transferred through the bolt at the base.

Conclusion

This chapter has presented a model for consideration of system effects between a Tudor arch and a roof diaphragm. In the example provided, the arch deflected much less than the same arch without diaphragm support. In general, the deflections and stresses were reduced by the use of the diaphragm and shear walls in conjunction with the arches. In some sections, however, the stresses increased when the diaphragm support was present. The deformed shape of the arch changed due to the support forces at the peak. Therefore, it may not be conservative in all cases to size the arch as a single member, then use it in conjunction with a diaphragm and shear wall system. The complete system should be modeled as accurately as possible for the analysis of the arch members.

Chapter 6
Seismic Design

The design of structures to resist seismic loads is somewhat different than design for wind and gravity loads. Ductility of the structure becomes an important consideration. Yielding mechanisms in the vertical components (walls and frames) of the structure reduce the loads transmitted to the rest of the structure. Simplified methods have been developed to account for the non-linear inelastic yielding of the structure while using elastic analysis. These methods require the use of seismic coefficients specific to the structural system. In seismic-critical zones, special detailing may be required to ensure ductile yielding can occur.

Glulam arches can be used to resist seismic forces alone or in conjunction with a shearwall/diaphragm system. This chapter will present information for designing the arch as the primary lateral force resisting system. When used in conjunction with shearwalls and a diaphragm, the lower seismic design coefficients for the arch or shearwalls should be used. The model presented in Chapter 4 can be used to analyze the interaction of the two systems.

Nomenclature

b	width
C/D	ratio of fastener capacity to demand
C_d	deflection amplification factor
C_d	penetration factor
C_{eg}	end grain factor
C_M	wet service factor
C_{st}	metal side plate factor
C_t	temperature factor
C_x	horizontal component of pin force at arch crown
C_y	vertical component of pin force at arch crown
D	dead load
d	depth
d_e	effective depth
d_t/b	ratio of tangent point depth to width
f_c	compression stress from applied loads
F_c^*	partially adjusted compression stress
F'_{vx}	allowable shear stress
h_w	wall height
I	importance factor
K_F	format conversion factor
n	number of fasteners
P_r	parallel to grain reference rivet capacity

Q_E	lateral seismic load effect
Q_r Q_r	perpendicular to grain reference rivet capacity
R	response modification factor
R_x	horizontal reaction force at base
$R_{x,L}$	horizontal reaction force at left base
$R_{x,R}$	horizontal reaction force at right base
R_y	vertical reaction force base
$R_{y,L}$	vertical reaction force at left base
$R_{y,R}$	vertical reaction force at right base
S	snow load
S_{DS}	design spectral response acceleration parameter
v	distributed seismic shear
V	seismic base shear
V_r'	shear resistance of member at connection
W	effective seismic weight of structure
x_h	horizontal distance from back of arch to bolt hole at base connection
y_h	vertical distance from floor to bolt hole at base connection
Z	reference lateral design value for a single fastener
α_{leg}	leg taper angle
Δ	allowable horizontal displacement (drift)
$\Delta_{x,L}$	horizontal displacement of left arch half at haunch
$\Delta_{x,R}$	horizontal displacement of right arch half at haunch
λ	time effect factor
ϕ_z	LRFD resistance factor for fasteners
ρ	reliability factor for redundancy
ω	distributed seismic weight of structure
Ω	overstrength factor

Seismic Coefficients

Two sets of seismic coefficients have been established for glulam arch systems. One set of values is limited to zones of low seismic hazard (seismic categories A, B, and C) and requires no special detailing. The other set of coefficients is required for zones of high seismic hazard (seismic categories D, E, and F) and requires special detailing to increase the likelihood of ductile yield mechanisms. The seismic design coefficients for each system are shown in Table 5.1.

Table 6.1. *Seismic Design Coefficients for Glulam Arches.*

Seismic Force Resisting System	R	Ω	C_d
1. Special glulam arch	2.5	2.5	2.5
2. Glulam arch not specifically detailed for seismic resistance - limited to seismic design categories A, B and C	2.0	2.5	2.0

Detailing Requirements

For timber structures, ductility is obtained through fastener yielding and localized wood crushing mechanisms at connections. Failure of the timber members themselves generally produces undesirable brittle failure mechanisms. For the s*pecial glulam arch* system, the detailing requirements discussed below provide additional assurance that the timber components of the arch system will not fail prematurely before yielding can occur at the base of the arch. This is achieved by sizing the member to resist the over-strength load combinations of ASCE 7 or ensuring that the members have more capacity than required to develop the nominal strength of the base connection. To promote yielding, the fastener(s) at the base are designed to resist the seismic loads without considering the over-strength load combinations.

The following provisions are taken from a paper titled "Special Requirements for Seismic Design of Structural Glued Laminated Timber (Glulam) Arch Members and Their Connections in Three-hinge Arch Systems" in Part 3 of the 2009 *NEHRP National Earthquake Hazard Reduction Program Recommended Seismic Provisions for New Buildings and Other Structures* (FEMA P750).

> *Glulam arch systems* shall comply with recommended detailing in *AITC 104-2003 Typical Construction Details*, requirements of the *2005 National Design Specification® for Wood Construction* (*NDS®*) including Appendix E, *ASCE 7-05 Minimum Design Loads for Buildings and Other Structures*, and the applicable building code.
>
> Arch members and arch member connections shall be in accordance with the requirements of the *2005 NDS* including Appendix E Local Stresses in Fastener Groups.
>
> In addition, s*pecial glulam arch* systems shall be in accordance with the Sections 6.1 through 6.7.
>
> 6.1 Connection requirements
> Connections that are part of the *special glulam arch* seismic force resisting system shall be in accordance with requirements of *NDS* Chapter 10 for Mechanical Connections and additional requirements of this Section.
>
> 6.1.1 Arch Base: Arch base connections shall utilize a steel shoe assembly in accordance with *AITC 104 Typical Construction Details*. Timber rivets or dowel-type fasteners such as thru-bolts or lag screws shall attach the arch to the shoe.

Dowel-type fasteners shall be chosen such that the expected yield mode is Mode III or Mode IV as defined in *NDS*. Timber rivet connections shall be designed to ensure that the expected strength limit state is characterized by rivet capacity.

6.1.2 Arch Peak: Connection of the arch at the peak shall utilize shear plates, bolts, steel dowels, or metal side plates or combination thereof in accordance with *AITC 104 Typical Construction Details.*

6.2 Nominal connection capacity

The nominal capacity of a connection shall be determined in accordance with the following:

a. For dowel type fasteners: n x $Z(K_F)(\lambda)(C_M)(C_t)(C_{eg})$ where n is the number of fasteners, Z is the reference lateral design value for a single fastener, and K_F, λ, C_M, C_t, and C_{eg} are adjustment factors specified in *NDS* for format conversion, time effect, wet service, temperature and end grain, respectively.

b. For timber rivets: (P_r or Q_r) x $(K_F)(\lambda)(C_M)(C_t)(C_{st})$ where P_r is parallel to grain reference rivet capacity, Q_r is perpendicular to grain reference rivet capacity, and K_F, λ, C_M, C_t, and C_{st} are adjustment factors specified in *NDS* for format conversion, time effect, wet service, temperature and metal side plate, respectively.

c. For split ring and shear plate connectors: n x P x $(K_F)(\lambda)(C_M)(C_t)(C_d)(C_{st})$ or n x Q x $(K_F)(\lambda)(C_M)(C_t)(C_d)$ where n is the number of fasteners, P is the reference design value parallel to grain for a single split ring connector unit or shear plate unit, Q is the reference design value perpendicular to grain for a single split ring connector unit or shear plate unit and K_F, λ, C_M, C_t, C_d and C_{st} are adjustment factors specified in *NDS* for format conversion, time effect, wet service, temperature, penetration and metal side plate, respectively.

6.3 Member requirements

Arch members that are part of the *special glulam arch* seismic force resisting system shall meet requirements of NDS and requirements of this Section.

6.3.1 Slenderness: The ratio of tangent point depth to breadth (d_t/b) shall not exceed 6, based on actual dimensions, when one edge of the arch is braced by decking fastened directly to the arch, or braced at frequent intervals as by girts or roof purlins. When such lateral bracing is not present, d_t/b shall not exceed 5.

6.3.2 End grain bearing: At the arch base, end grain bearing shall be on a metal plate with sufficient strength and stiffness to distribute the applied load. At

moment splices, end grain bearing shall be on a metal plate when $f_c > (0.75)(F_c^*)$ as required in accordance with NDS 3.10.1.3.

6.3.3 Compression perpendicular to grain: Compression perpendicular to grain, induced at the arch base, shall be by a metal plate with sufficient strength and stiffness to distribute the applied load.

6.4 Member resistance

6.4.1 Moment, Tension, Compression, and Shear: The arch member shall be designed to resist moment, tension, compression, shear, and applicable combinations of these induced by seismic forces determined in accordance with load combinations of Section 12.4.3.2 of *ASCE 7* (load combinations with over-strength) but need not exceed forces resulting from strength at connections determined in accordance with Section 6.4.2 (a).

6.4.2 Member Resistance at Connections: The member shall be designed for limit states of net section tension rupture, row tear-out, group tear-out as defined in *NDS* Appendix E, and shear in accordance with *NDS* 3.4.3.3 due to the seismic forces as determined by the lesser of:

a. The nominal connection capacity determined in accordance with Section 6.2 for LRFD, or the nominal connection capacity determined in accordance with Section 6.2 divided by 1.35 for ASD.
b. The required capacity resulting from load combinations of Section 12.4.3.2 of *ASCE 7* (load combinations with over-strength).

6.5 Transfer of forces to the arch members
The diaphragm, members and connections shall be sized to transfer of out-of-plane wall and roof forces into the arch.

6.6 End fixity
In accordance with assumed pinned behavior of a 3-hing arch, determination of reaction and arch member forces is based on assumed idealized pin behavior at the arch peak and base. Actual detailing may introduce partial moment fixity at reactions, and consideration shall be given to the effect of such fixity on member and connection response.

6.7 Arch Moment Splice
Arch moment splices shall utilize a metal bearing plate (when required), metal side plates, shear plates, bolts, steel dowels, timber rivets or combination thereof in accordance with *AITC 104 Typical Construction Details*. Design forces for determining the size and number of fasteners shall be based on load combinations of Section 12.4.3.2 of ASCE 7 (load combinations with over-strength) but need not exceed the member design force based on forces resulting from strength at connections (see Section 6.4.1 and 6.4.2 (a)).

Drift Limits

In addition to the capacity checks and detailing as required above, arches must be stiff enough to avoid excessive lateral displacement (drift) under seismic loads. The applicable drift limits are adapted from ASCE 7-05 and depend on the Seismic Use Group as shown in table 6.2.

Table 6.2. *Allowable drift at haunch of Tudor arch.*

Occupancy Category	I or II	III	IV
Allowable Drift	$0.020\,h_w$	$0.015\,h_w$	$0.010\,h_w$

These drift limits are calibrated based on LRFD loads and must therefore be calculated using the LRFD seismic load combinations. However, the stresses in the arch do not need to be checked using the LRFD load combinations when performing an ASD analysis.

Seismic Load Distribution

A Tudor arch resists lateral and vertical loads (in the plane of the arch) primarily through bending. As such, the distribution of the loads throughout the arch has a significant effect on the deflected shape and on the stress distribution in the arch. It is, therefore, not appropriate to concentrate the seismic mass of the structure at a single location for the analysis; the load (mass) should be distributed as it occurs along the length of the arch.

Procedure

Generally speaking, the seismic analysis is done after the arch has been designed and proportioned to meet other design criteria. The arch is then analyzed to determine if it meets the seismic design criteria. The following steps are applied to analyze the arch.

1. Design the arch and connections to resist all loads and deformations other than seismic.
2. Apply the seismic load combinations without over-strength factors and verify that the fasteners at the base connection are adequate to resist the applied loads and are designed to yield in a ductile failure mode (Mode III or Mode IV for bolts, rivet failure for timber rivets).
3. Determine the ratio of capacity/demand of the connection (C/D).
4. Satisfy one of the following options. (If the demand on the fastener is zero under the seismic loads, option b. must be followed.):
    a. Amplify all forces on the arch by multiplying by (C/D)*(1/ϕ_z) and verify that the combined member stress ratios do not exceed 1.0 and that member failure modes at connections (row and group tear-out, notched shear, etc.) do not occur. (This provision ensures that the member capacity is higher than the nominal connection capacity).
    b. Apply the seismic load combinations with over-strength factors (ASCE 7-05, Section 12.4.3.2) and verify that the combined member stresses do not exceed

1.0 and that member failure modes at connections (row and group tear-out, notched shear, etc.) do not occur.

5. Apply the LRFD seismic load combinations (without the redundancy factor, ρ) and check drift against the applicable limits.

Example 6-1: Seismic Analysis of Tudor Arch

The Equivalent Lateral Force Procedure will be used to analyze the arch from Example 4-1 for seismic loads.

Given: S_{DS}=1.0. The building is classified in occupancy category III (I=1.25) and is located in seismic design category D. Snow load is not required to be considered as part of the mass of the structure for determining lateral seismic loads. The system has sufficient redundancy for the reliability factor to be taken as ρ = 1.0.

Wanted: Analyze the arch under seismic loading.

Solution: Using the Equivalent Lateral Force procedure, the seismic base shear is given by:

$$V = \frac{IS_{DS}W}{R}$$

The total shear forces on the structure must result in this base shear, which is caused by the mass of the structure subject to seismic acceleration. For analysis of the tudor arch system, the weight of the structures is distributed as it occurs in the structure and the lateral distributed loads on the arch are determined by:

$$\nu = \frac{IS_{DS}\omega}{R}$$

Because the building is classified as occupancy category III, the importance factor is 1.25. For seismic design category D, R = 2.5 and special detailing is required. The design acceleration coefficient was given as S_{DS} = 1.0 in the problem statement. Because the snow load is not included in the seismic mass, ω is simply the distributed dead weight of the structure.

$$\nu = \frac{1.25(1.0)\omega_D}{2.5} = 0.5\omega_D$$

Therefore, the lateral seismic loads (Q_E) are calculated as 50% of the vertical dead load and are distributed as shown in **Figure E6.1**.

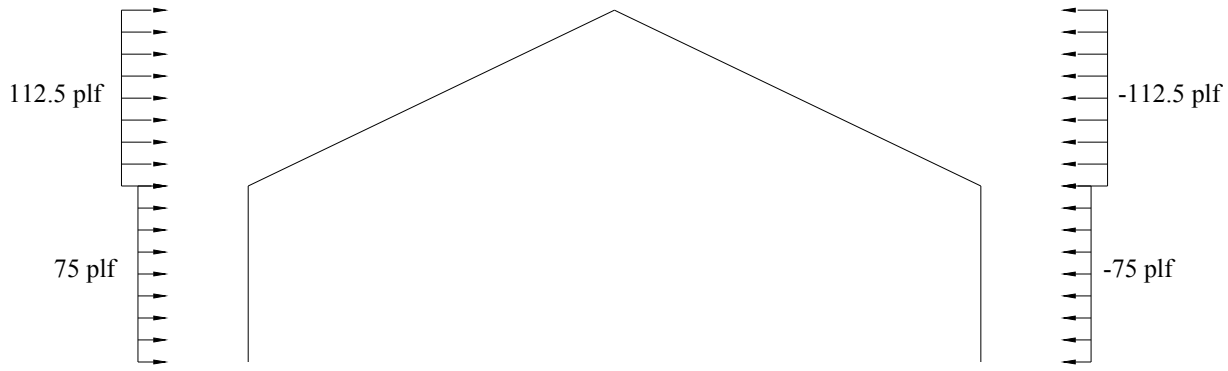

Figure E6.1 Lateral Seismic Loads (load from left).

The bolted connection at the base must be adequate to support the following load combinations from ASCE 7-05, Section 12.4.2.3 and be designed for Mode III or IV yield mechanisms.

$$\left(1.0+0.14S_{DS}\right)D+0.7\rho Q_E$$
$$\left(1.0+0.105S_{DS}\right)D+0.525\rho Q_E+0.75S$$
$$\left(0.6-0.14S_{DS}\right)D+0.7\rho Q_E$$

Reaction forces for these load combinations are shown in **Table E6.1**.

Table E6.1. *Reaction forces (lb) for arch subject to seismic load combinations.*

Load Combination	$R_{y,L}$	$R_{x,L}$	C_y	C_x	$R_{y,R}$	$R_{x,R}$
$(1.0+0.14S_{DS})D+0.7\rho Q_E$	7610	1610	850	-3190	9320	4760
$(1.0+0.105S_{DS})D+0.525\rho Q_E+0.75S$	14600	5460	640	-6640	15880	7820
$(0.6-0.14S_{DS})D+0.7\rho Q_E$	2560	-290	850	-1290	4270	2860

From Example 4-1, a ¾ in. bolt was used at the base. Its capacity was determined to be 3200 lb. The demand on this bolt under the seismic load combinations is 290 lb. The ratio of capacity to demand is C/D = 3200/290 = 11.0.

The arch members and the peak connection must be adequate to resist the overstrength load combinations from ASCE 7-05, Section 12.4.3.2 or be adequate to resist the seismic loads amplified by a factor of $(C/D)*(1/\phi_z)=11.0/0.65 = 16.9$. Because the seismic loading places very low demand on the fastener relative to its capacity, it will be more efficient to ensure that the arch is adequate to resist the overstrength load combinations from ASCE 7-05, 12.4.3.2.

The overstrength load combinations from ASCE 7-05, 12.4.3.2 are as follows:

$$\left(1.0+0.14S_{DS}\right)D+0.7\Omega Q_E$$
$$\left(1.0+0.105S_{DS}\right)D+0.525\Omega Q_E+0.75S$$
$$\left(0.6-0.14S_{DS}\right)D+0.7\Omega Q_E$$

The reactions calculated for the overstrength load combinations are shown in **Table E6.2**.

Table E6.2. *Reaction forces (lb) for seismic load combinations with overstrength factor.*

Load Combination	$R_{y,L}$	$R_{x,L}$	C_y	C_x	$R_{y,R}$	$R_{x,R}$
$(1.0+0.14S_{DS})D+0.7\Omega Q_E$	6330	-750	2130	-3190	10590	7130
$(1.0+0.105S_{DS})D+0.525\Omega Q_E+0.75S$	13640	3690	1600	-6640	16830	9600
$(0.6-0.14S_{DS})D+0.7\Omega Q_E$	1290	-2650	2130	-1290	5550	5220

Analysis of this arch using a spreadsheet to perform the calculations shows that the arch is adequate to support all of the considered overstrength load combinations (Table E6.3).

Table E6.3. *Combined stress ratios for seismic overstrength load combinations.*

	Left Arch Half				**Right Arch Half**			
	Leg	**Lower Haunch**	**Upper Haunch**	**Arm**	**Arm**	**Upper Haunch**	**Lower Haunch**	**Leg**
$(1.0+0.14S_{DS})D+0.7\Omega Q_E$	0.033	0.037	0.209	0.424	0.641	0.694	0.597	0.444
$(1.0+0.105S_{DS})D+0.525\Omega Q_E+0.75S$	0.247	0.340	0.250	0.493	0.644	0.861	0.815	0.605
$(0.6-0.14S_{DS})D+0.7\Omega Q_E$	0.154	0.203	0.342	0.362	0.662	0.542	0.429	0.321

The analysis indicates that no uplift occurs at the base of the arch. No tension forces are transferred between arch halves at the peak of the arch. The shear plate connection at the peak of the arch must be sufficient to transfer 2130 lb. The base of the arch must be detailed to transfer 2650 lb from the bolt to the member considering the notch effect.

Base Connection

The shear force to be resisted at the base of the arch, perpendicular to the laminations, is calculated as:

$V=-R_x\cos\alpha_{leg}$ If no uplift is present ($R_y \geq 1$)

$V=-R_x\cos\alpha_{leg}-R_y\sin\alpha_{leg}$ If uplift is present ($R_y < 1$)

Therefore:

$$V=-R_x\cos\alpha_{leg}=-\left(-2650\text{ lb}\right)\cos\left(3.8°\right)=2640\text{ lb}$$

In Example 4-1, the capacity of the member to resist the shear from the bolt was determined to be 1534 lb with the bolt placed 6 inches from the bearing face. This is not sufficient to resist the required seismic shear load of 2640 lb. Moving the bolt toward the inside face of the arch (away from the bearing seat) will reduce the notch effect and increase the member's capacity to resist the shear force.

Assuming the bolt is placed 8 in. from the outside face of the arch (Figure E6.2) to minimize potential problems with shrinkage between bolt and bearing seat, the effective depth, d_e, and the total depth, d, of the section through the bolt hole can be calculated as:

$$d_e = \frac{x_h}{\cos \alpha_{leg}} = \frac{8 \text{ in}}{\cos(3.8°)} = 8.02 \text{ in}$$

$$d = d_e + (d_b' - x_h)\cos \alpha_{leg} + y_h \sin \alpha_{leg}$$
$$d = 8.02 \text{ in} + (14.5 \text{ in} - 8.0 \text{ in})\cos(3.8°) + (5.25 \text{ in})\sin(3.8°) = 14.9 \text{ in}$$

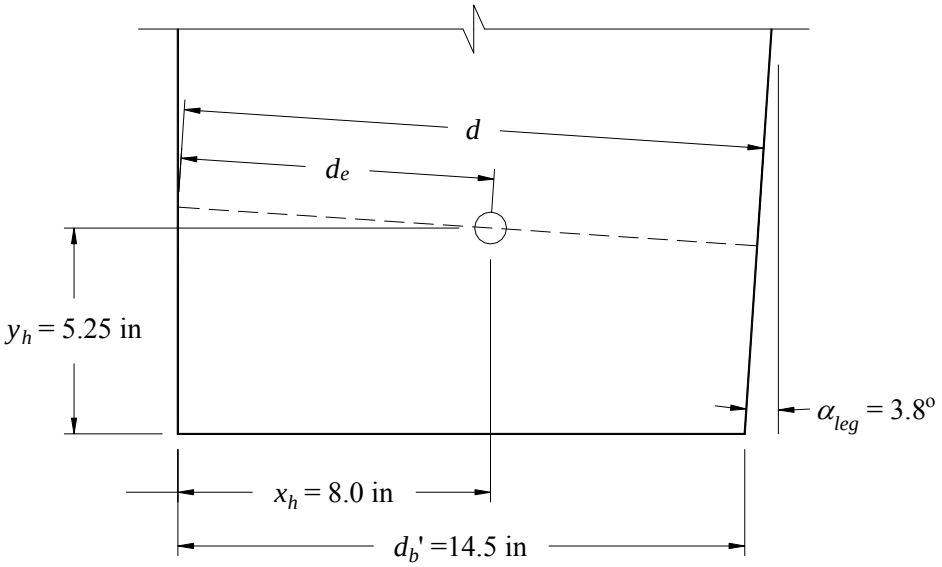

Figure E6.2. *Bolt placement and dimensions for revised base connection.*

The shear resistance of the member at the connection can be calculated as:

$$V_r' = \left[\frac{2}{3} F_{vx}' b d_e\right]\left[\frac{d_e}{d}\right]^2 = \left[\frac{2}{3}(215 \text{ psi})(1.6)(6.75 \text{ in})(8.02 \text{ in})\right]\left[\frac{8.02 \text{ in}}{14.9 \text{ in}}\right]^2 = 3600 \text{ lb}$$

The capacity of the member at the connection is adequate with the bolt placed 8 in. from the bearing seat (3600 lb > 2640 lb). It is important to note, however, that placing the bolt a long distance from the bearing seat is not recommended, because a split can form as the member shrinks (see AITC 104). If possible, the bolt should be placed within 6 inches of the bearing seat, or further detailing must be considered. In this case, the hole in the timber member will be oversized by 1/8 in. (instead of the standard 1/16 in.

oversize) to accommodate additional shrinkage. The hole in the steel plate will be oversized by a standard 1/16 in.

Peak Connection

In Example 4-1, the adjusted capacity of the two 4 in. shear plates was determined to be 3220 lb for snow load, and the notched member shear capacity of the member at the peak was calculated as 8,000 lb for snow load. For seismic load duration, the resistances will be 1.6/1.15 = 1.39 times higher resulting in capacities of 4480 lb for the connectors and 11,130 lb for the members. Therefore, the peak connection is adequate to transfer the 2130 lb of shear from the overstrength load combinations.

Displacement (Story Drift)

In addition to evaluation of the stresses on the arch, a calculation of story drift is typically required. For the case of arches in a structure classified in Occupancy Category III, the displacement at the top of the wall must be limited to no more than 1.5% of the wall height (**Table 5.2**). The allowable drift is calculated as:

$$\Delta \le 0.015 h_w = 0.015(144 \text{ in}) = 2.16 \text{ in}$$

The LRFD load combinations should be used when calculating displacements for comparison with this drift limit. The results of the calculations are shown in **Table E6.4**.

Table E6.4. *Displacements (in.) at haunches under LRFD seismic load combinations.*

Load Combination	$\Delta_{x,L}$	$\Delta_{x,R}$
$(1.2+0.2S_{DS})D+Q_E+0.2S$	0.59 in.	-1.09 in.
$(0.9-0.2S_{DS})D+Q_E$	0.74 in.	-0.94 in.

The displacements of the haunches are well below the prescribed limit of 2.16 in.

The arch is adequate to resist the seismic loads.

Conclusion

This chapter presented requirements and procedures for the analysis of tudor arches as the primary seismic resisting system. In general, seismic analysis is performed as a design check after the arches are designed for all other requirements. In seismic zones D, E, and F, special detailing is required to minimize the occurrence of brittle failures. In addition to stress assessments, the arches must be sufficiently stiff to prevent excessive displacement under seismic forces. These concepts were illustrated with an example problem.

Chapter 7
Specifying Arch Geometry

Once the design has been completed, the requirements must be communicated from the designer to the laminated timber manufacturer. The arch geometry, species and grade, and any special lay-up requirements must be specified. This chapter illustrates the parameters that should be specified to communicate the required arch geometry to the manufacturer in a clear, succinct manner. The parameters specified in this chapter correspond to the lay-out procedure illustrated in Appendix B.

The dimensions illustrated in **Figure 7.1** should be communicated to the laminated timber manufacturer. Dimensions d_1 and d_2 are measured perpendicular to the outside of the arch at the tangent points.

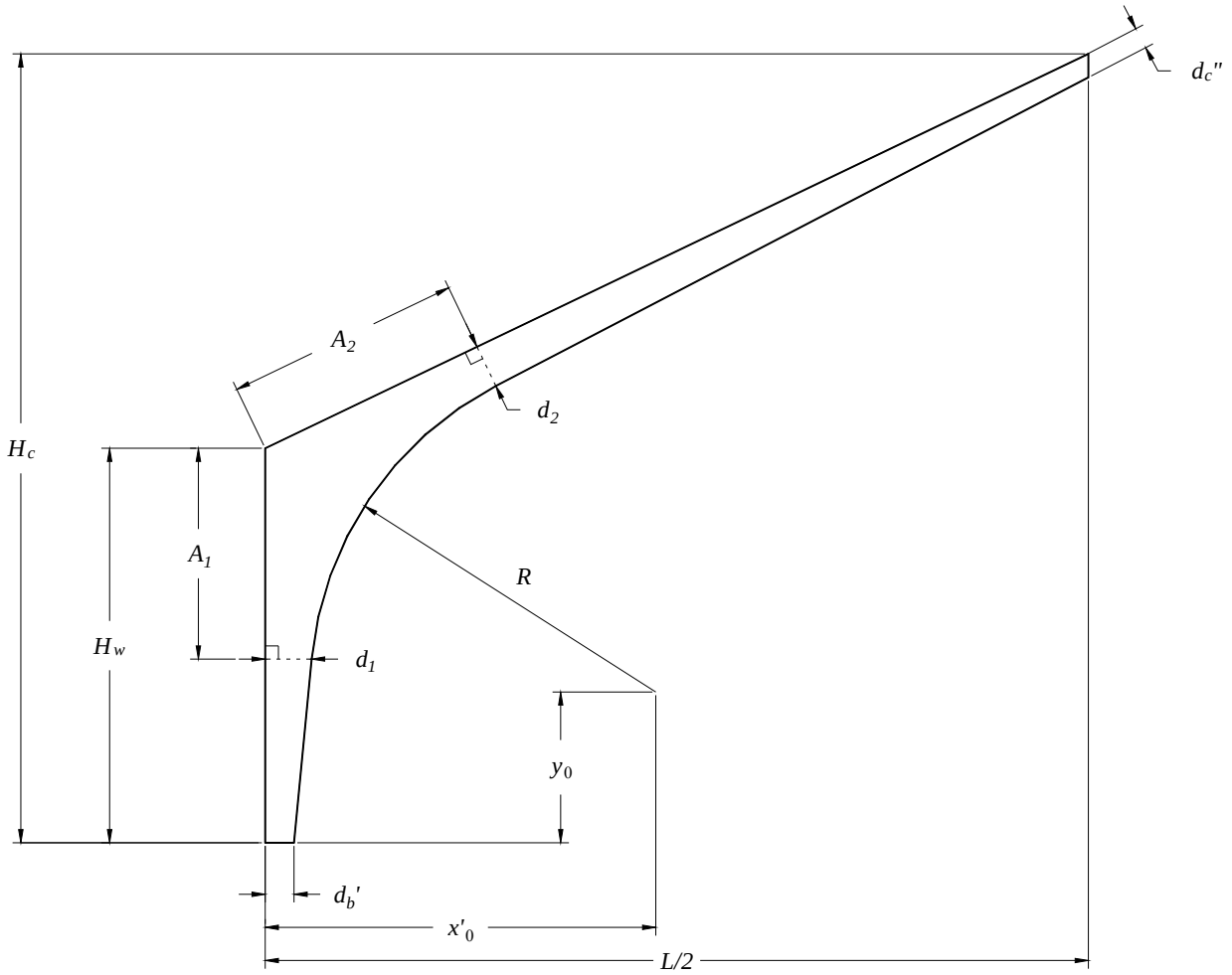

Figure 7.1. *Parameters required for Tudor arch specification (only left half shown for clarity).*

Dimensions d_1 and d_2 and their corresponding locations A_1 and A_2 can be calculated with the following equations:

$$A_1 = H_{w,L} - y_{LT,L} \quad [7\text{-}1]$$

$$d_1 = d_{LT,L} \cos \alpha_{leg,L} \quad [7\text{-}2]$$

$$A_2 = \frac{\left(x_{UT,L} - d_{UT,L} \cos \alpha_{arm,L}\right) \sin \phi_{t,L} + L_L}{\cos \phi_{t,L}} \quad [7\text{-}3]$$

$$d_2 = d_{UT,L} \cos \alpha_{arm,L} \quad [7\text{-}4]$$

The center of curvature can be located with the following equations:

$$x_0' = L_L - x_{0,L} \quad [7\text{-}5]$$

$$y_0 = y_{0,L} \quad [7\text{-}6]$$

The depth at the crown, measured perpendicular to the roof is calculated as:

$$d_c'' = d_c \frac{\cos \phi_{b,L}}{\cos \phi_{t,L}} \quad [7\text{-}7]$$

Appendix A

Arch Lay-up

A standard arch lay-up is divided into 7 zones as shown in **Figure A1**. The zones are numbered starting from the inside face of the arch.

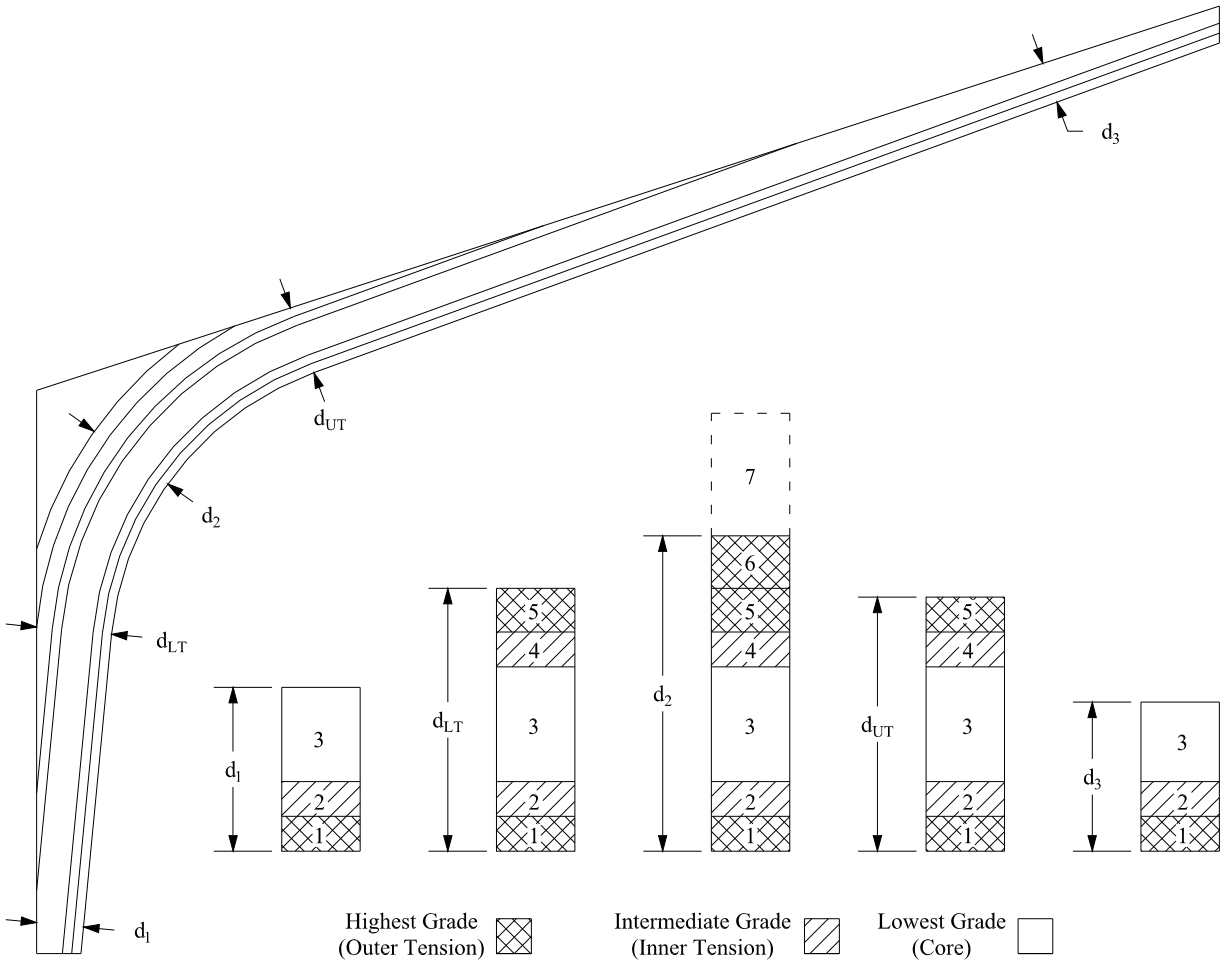

Figure A1. *Requirements for a standard arch lay-up.*

Grade Requirements by Zone

Zones 1, 5, and 6 require the highest grade of laminations in the lay-up corresponding to the tabulated outer tension zone requirements in AITC 117.

Zones 2 and 4 use the 2nd highest grade of laminations in the lay-up, corresponding to the tabulated inner tension zone requirements in AITC 117.

Zones 3 and 7 use the lowest grade of laminations permitted in the lay-up, corresponding to the core zone grade tabulated in AITC 117.

Zone Thicknesses

The thicknesses of zones 1 and 2 are determined based on the lay-up requirements from AITC 117 and the total depth at the lower tangent point (d_{LT}) or at the upper tangent point (d_{UT}), whichever is greater.

Zones 4 and 5 are required to be as thick or thicker than zones 2 and 1, respectively, at all sections between the upper and lower tangent points.

Zone 6 is required to be sufficiently thick to ensure that depth d_2 is a minimum of 1.2 times the larger of d_{LT} or d_{UT}.

Zones 4, 5, and 6, are permitted to taper off along the outer face of the arch as shown.

Effect of Taper on Reference Design Values

For tapered arches, the taper sawn on the outside faces of the arch will result in the removal of high grade material, necessitating consideration in design. The flexural design value and modulus of elasticity are both affected by the removal of high grade material.

Tapered Face in Flexural Compression

Where the tapered face is stressed in compression and high grade material is removed, reduced design values can be obtained from AITC 117-2004, Table A3. These reduced reference design values are permitted to be applied to the end section of the arch, and linear interpolation (between the reduced reference design value at the end section and the full reference value at the nearest tangent point) is used to assign positive flexural design values for intermediate sections.

Tapered Face in Flexural Tension

Where the tapered face is stressed in tension and the core zone is exposed, it is recommended that the flexural reference stress be reduced by 50%. For sections where part of the tension zones are removed, but the core zone is not exposed, the reference design value for negative flexure can be set equal to the reduced positive design value at the same section. The depth of the tension zone can be conservatively estimated as 15% of the tangent point depth for most combinations, so the 50% reduction should generally be applied to sections shallower than 85% of the tangent point depth.

Modulus of Elasticity

Because a significant portion of the arch will generally have core-grade laminations on the outer face, a reduced modulus of elasticity is recommended for the entire arch. The reduced moduli from AITC 117-2004, Table A3 are sufficient for arch design.

Alternate Arch Lay-ups

The standard arch lay-up is generally the most economical method of manufacturing an arch. It uses high-strength material sparingly, placing lower grade material where stresses are typically lower. Reductions in reference design values in segments where high-grade material is removed by tapering generally have minimal impact on the design of the arch. However, there may be cases where the designer requires full design values at all sections of the arch. For these cases, the designer should specify the appropriate uniform-grade lay-up from AITC 117, Table A2 or require that the tension zone requirements are maintained along the full length of the arch. Either of these options may increase the cost of the arch, depending on the grades of lumber involved.

Appendix B

Arch Lay-out

One method of laying out a tudor arch using the parameters specified in Chapter 7 is presented here. Four basic steps are used to establish the arch geometry. All depths are measured perpendicular to the outside of the arch to facilitate lay-out using a tool such as a carpenter's square.

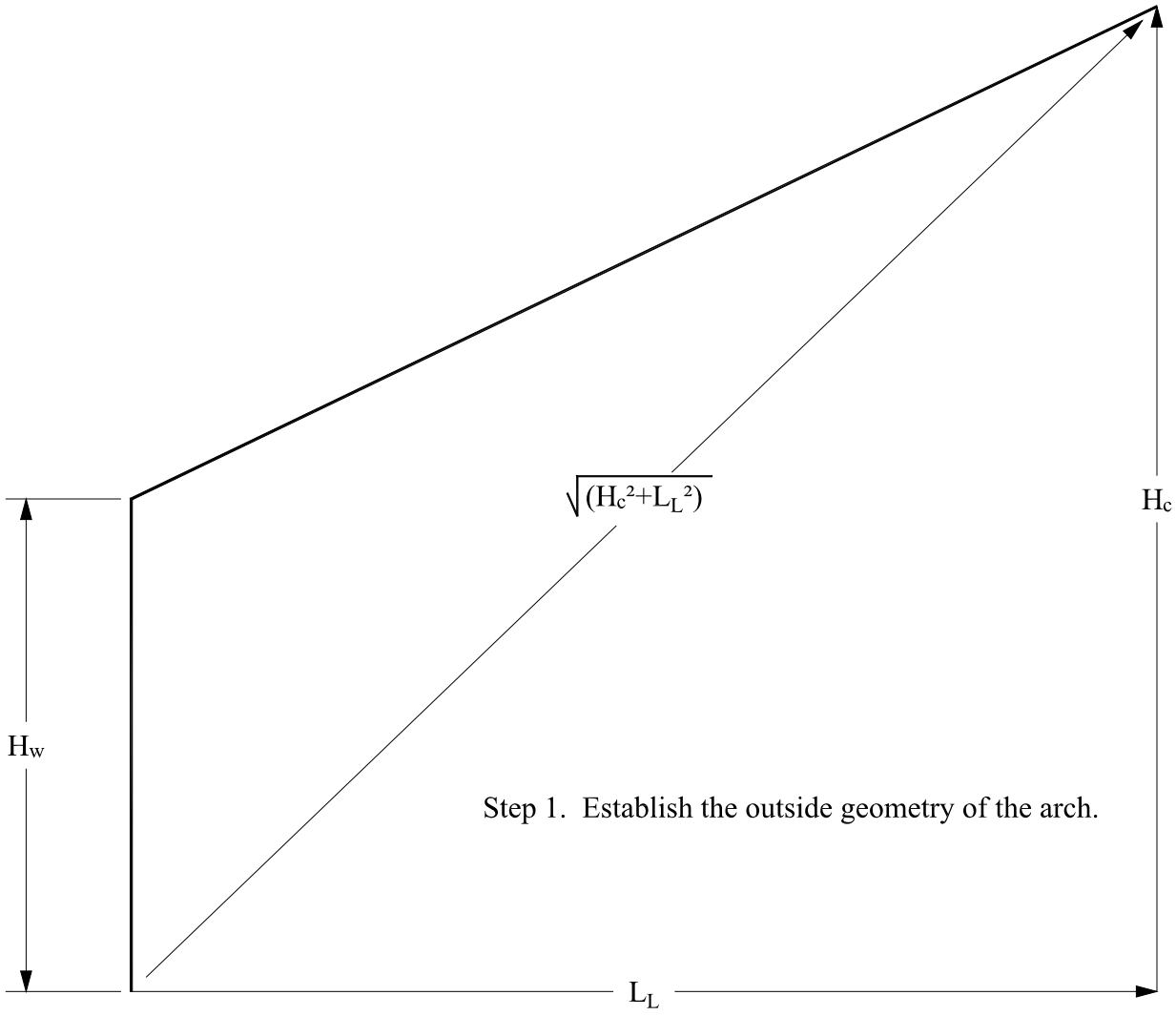

Step 1. Establish the outside geometry of the arch.

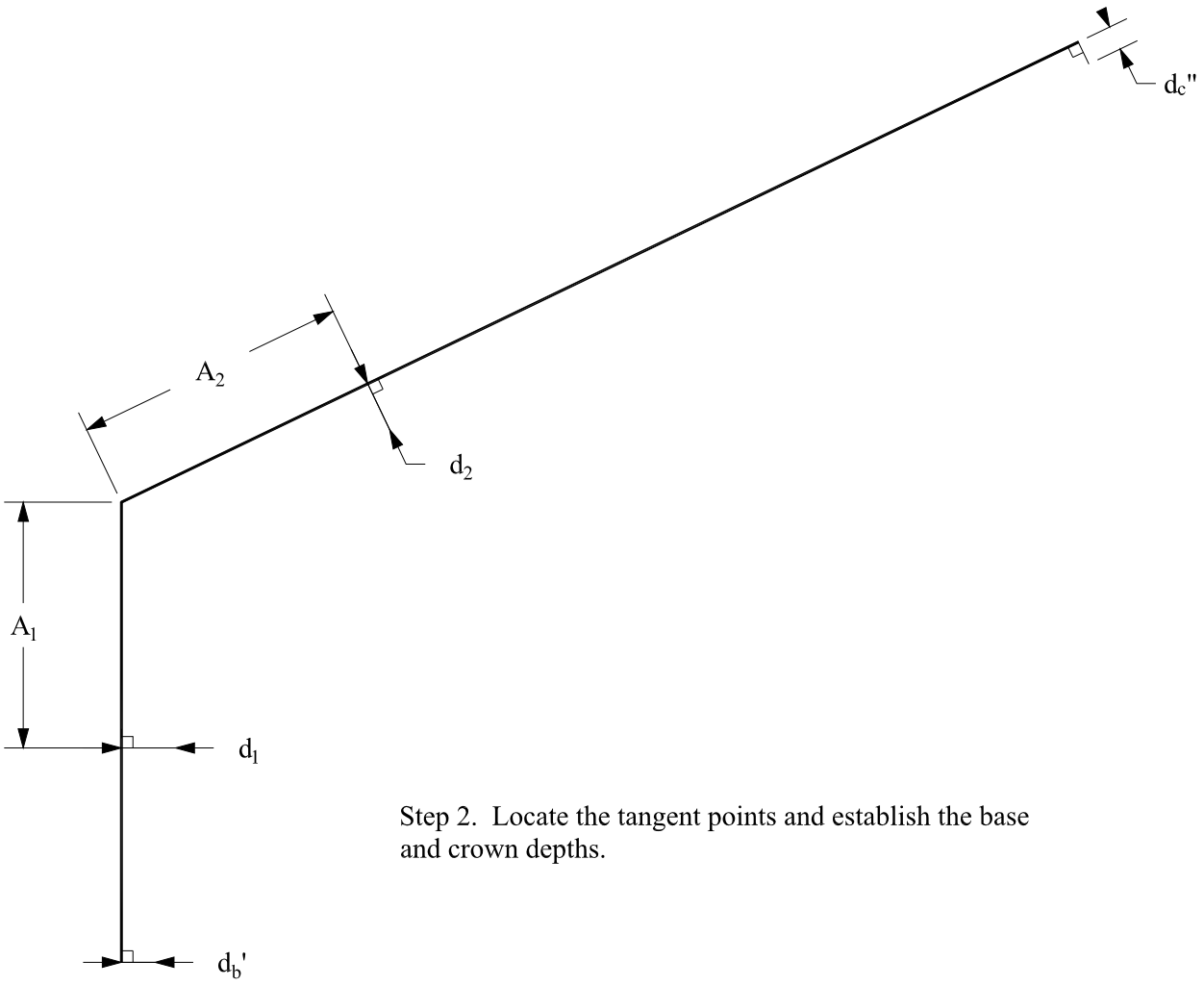

Step 2. Locate the tangent points and establish the base and crown depths.

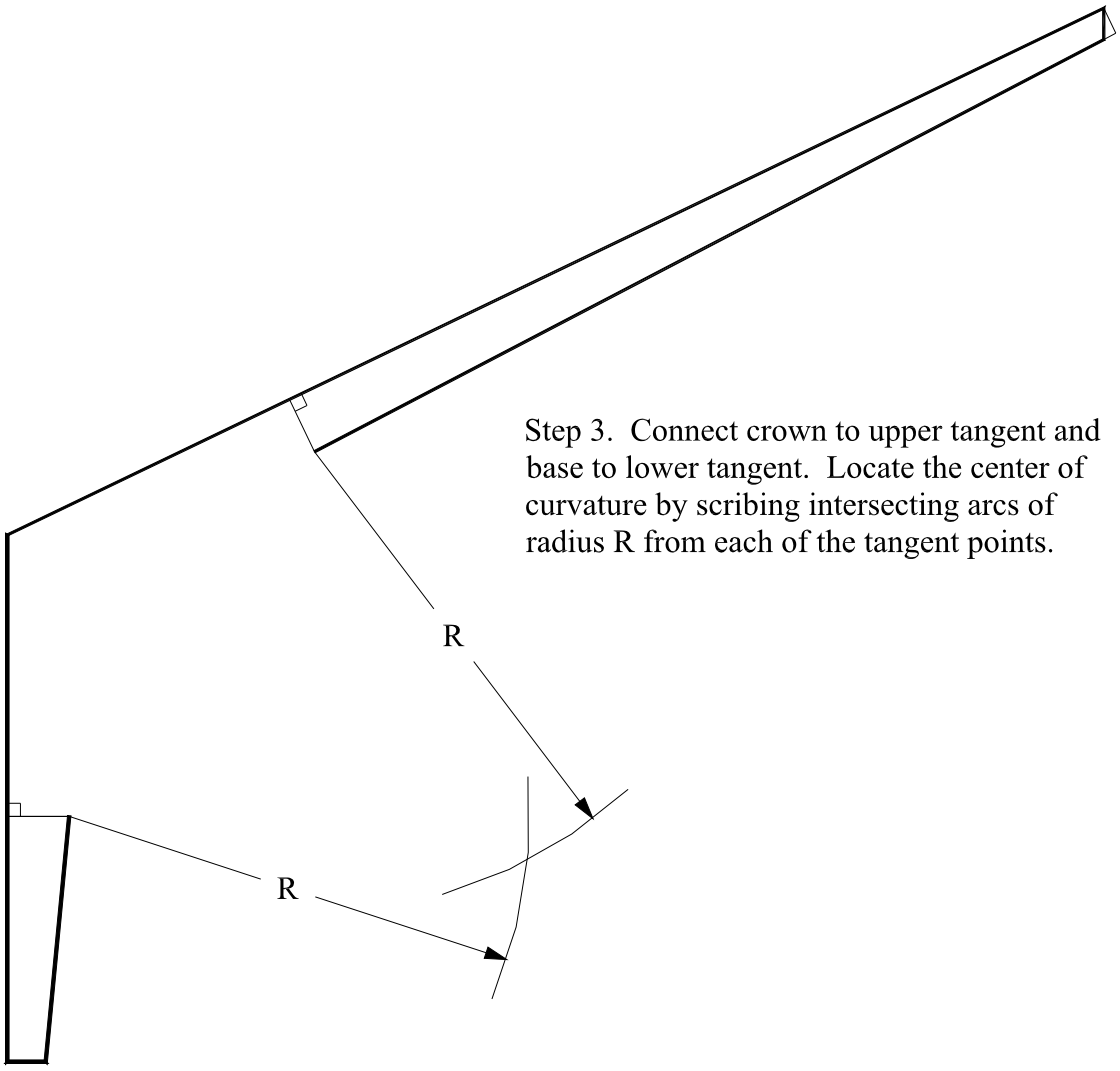

Step 3. Connect crown to upper tangent and base to lower tangent. Locate the center of curvature by scribing intersecting arcs of radius R from each of the tangent points.

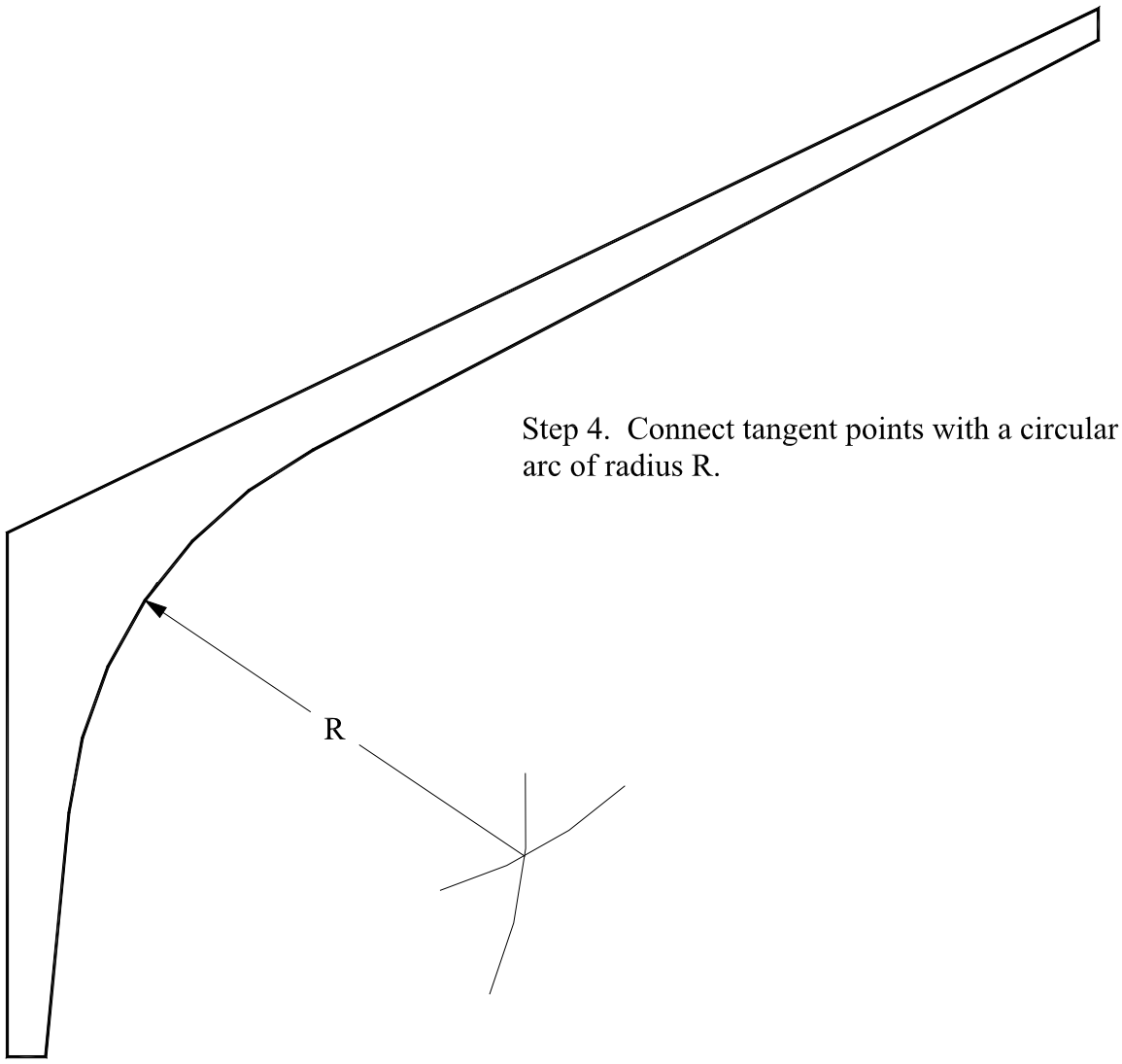

Step 4. Connect tangent points with a circular arc of radius R.

American Institute of Timber Construction

7012 South Revere Parkway • Suite 140 • Centennial, CO 80112
Phone: 303/792-9559 Fax: 303/792-0669 http://www.aitc-glulam.org

THE SYMBOL OF QUALITY IN ENGINEERED TIMBER